

CARNEGIE MELLON UNIVERSITY
CARNEGIE INSTITUTE OF TECHNOLOGY

THESIS

SUBMITTED IN PARTIAL FULFILMENT OF THE
REQUIREMENTS FOR THE DEGREE OF
DOCTOR OF PHILOSOPHY

Title: A Decentralized Approach to Reducing the Social Costs of
Cascading Failures

Presented by: Paul Hines

Accepted by: the Department of Engineering and Public Policy

Major Professor Date

Department Head Date

Approved by the college council:

Dean Date

A Decentralized Approach to Reducing the Social Costs of Cascading Failures

Paul Hines

A thesis submitted in partial fulfillment of the requirements

for the degree of Doctor of Philosophy

Carnegie Mellon University

Carnegie Institute of Technology

Department of Engineering and Public Policy

©Copyright, 2007, Paul Hines. All rights reserved.

A Decentralized Approach to Reducing the Social Costs of Cascading Failures

A thesis submitted in partial fulfillment of the requirements
for the degree of Doctor of Philosophy

Carnegie Mellon University
Carnegie Institute of Technology
Department of Engineering and Public Policy

August, 2007

Thesis committee: Sarosh Talukdar (chair),
Jay Apt, Bruce Krogh, Granger Morgan and Le Tang

©Copyright, 2007, Paul Hines. All rights reserved.

for Vanessa

*“Glorify the LORD with me;
let us exalt his name together.”*

Ps. 34:3 (NIV)

and Forest

*“They will be called oaks of righteousness,
a planting of the LORD for the display of his splendor.”*

Isaiah 61:3 (NIV)

Contents

	iii
List of Figures	ix
List of Tables	xi
Acknowledgments	xiii
Abstract	xv
Notation and terminology	xvii
Chapter 1. Introduction	1
1.1. Optimal Operations	5
1.2. Solving the OOP via Distributed Model Predictive Control	11
1.3. Multi-agent systems	12
1.4. Related Literature	15
1.5. Related Policy Problems	23
1.6. Thesis structure	23
Chapter 2. Blackouts	25
2.1. The impact and social costs of large blackouts	26
2.2. Related research results	27
2.3. Data	28
2.4. Power-Laws	31

2.5.	Time trends in the blackout data	34
2.6.	Estimating the expected cost of large blackouts	36
2.7.	Explanations for the lack of improvement	41
2.8.	Conclusions	43
Chapter 3.	Operations	45
3.1.	An Architecture for the Optimal Operation of Power Networks	46
3.2.	The Optimal Stress Mitigation Problem for Power Networks	49
3.3.	Results	66
3.4.	Discussion	70
Chapter 4.	Cooperation	71
4.1.	The cooperative agent problem	72
4.2.	Cooperation in the decentralized solution of the SMP	77
4.3.	Cooperation results	80
4.4.	Discussion	81
Chapter 5.	Decomposition	83
5.1.	Decomposition method	85
5.2.	Adaptation to power networks	96
5.3.	Properties of the network operations problem	99
5.4.	Discussion	111
Chapter 6.	Verification	113
6.1.	Simulated network data	114
6.2.	Power system simulation	115
6.3.	Simulation Method 1: Sequential code	119
6.4.	Simulation method 2: Parallel code	120
6.5.	Discussion	124
Chapter 7.	Conclusions	127

7.1. Technical contributions	128
7.2. Implementation and policy challenges	131
7.3. Future work	132
Bibliography	137
Bibliography	137
Appendix A. Blackout data	145
Appendix B. IEEE 300 bus network data	155

List of Figures

2.1	The number of blackouts by year in the full data set	31
2.2	The power-law relationship between blackout size and frequency	33
2.3	The relative impact of large blackouts in several size ranges	35
2.4	The average number of blackouts by month	36
2.5	The number of blackouts for 1984-2006 with size in customers	37
2.6	The number of blackouts for 1984-2006 with size in MW	38
2.7	The annual impact of large blackouts for 1984-2006	39
3.1	A depiction of the proposed power system operations architecture	48
3.2	Branch current derivatives in phasor form	57
3.3	Illustration of the stress cost (penalty) function for current magnitudes	65
3.4	An illustration of the test case for examples in Chapter 3 (case300-1-1)	67
3.5	The time domain results of test 6, as shown in table 3.4	68
5.1	An illustration of agent n and its neighborhoods/sub-models within the network	89
5.2	A timeline of agent actions	94
5.3	Sparsity pattern of the LP constraints	97
5.4	Time series trajectory for case300-1-1, test 2	102
5.5	Time series plot showing the amount of data exchange required by the agent algorithm for the 300 bus system	103
5.6	Illustration of the simple resistor circuit used for testing network structures	107

5.7 The structure of 5 example networks	108
5.8 Changes in relative sensitivity with changes in distance between two variables	109
5.9 The percent of all node pairs whose magnitude is at least as large as the threshold S	110
6.1 A depiction of case300-10-3	116
6.2 The CDF of simulated blackout sizes for all 100 test cases	119
6.3 Simulated blackout sizes for the “simple” cooperation method	121
6.4 Simulated blackout sizes for the “negotiate” cooperation method	122
6.5 Communication burden for 8 versions of the agent control method	123
6.6 The cost difference between the “no control” and agent-based control test cases	124
6.7 Results from the simulation of case300-2-5 on a parallel computer cluster	125
B.1 One-line diagram of the IEEE 300 bus network [1]	156
B.2 Graph of the IEEE 300 bus network with bus numbers	157

List of Tables

0.1 Mathematical notation	xvii
0.1 Mathematical notation	xviii
0.1 Mathematical notation	xix
0.1 Mathematical notation	xx
0.2 Acronyms and abbreviations	xx
0.2 Acronyms and abbreviations	xxi
0.2 Acronyms and abbreviations	xxii
1.1 Some notable cascading failures in North America and Europe	4
2.1 Power-law fit statistics	32
2.2 Results from statistical tests on the blackout data	37
3.1 Time horizons for power network operations and MPC applicability	49
3.2 Control variables that could be included in the stress mitigation problem	59
3.3 Typical input parameters for the SMP experiments	66
3.4 Results that show the effects of changes to some of the parameters in this model	69
3.5 Detailed control actions from case300-1-1, test 3	69
4.1 Results that show the difference between cooperation methods 1 and 2	80
4.2 The average number of buses that can be reached by crossing no more than r branches for several power networks	81
5.1 Computational requirements for case300-1-1, test 2 with perfect information	98

5.2 Test results that show the effects of changes to various parameters in the agent MPC problems	100
5.3 Detailed agent control actions from case300-1-1, test 3	101
5.4 Descriptive statistics for the 6 example networks tested in Chapter 4	111

Acknowledgments

This work is the result of invaluable support, feedback and assistance from many, some of whom are acknowledged below.

Firstly, I would like to thank my advisor, Sarosh Talukdar, for fascinating ideas and challenging questions that have contributed enormously to the quality of my research, and have made me a better engineer. Thanks are also due the others on my thesis committee: Granger Morgan, Jay Apt, Bruce Krogh and Le Tang, for their valuable questions and suggestions. In particular I would like to thank Granger Morgan for facilitating the interdisciplinary study of engineering and policy problems and for helpful advice along the way and Jay Apt for making the Carnegie Mellon Electricity Industry Center a great place for electricity research and for his work on the blackout data analysis in Chapter 2. Thank you also to Marija Ilic for her contributions to my education and research.

This work was supported in part by ABB Corporate Research in Raleigh, North Carolina, the Alfred P. Sloan Foundation and the Electric Power Research Institute under grants to the Carnegie Mellon Electricity Industry Center. Le Tang and Xiaoming Feng at ABB deserve particular mention for their efforts to facilitate the financial support of this work and for providing valuable feedback during the development of these ideas.

Many thanks also go to my fellow students in the Engineering and Public Policy department, who make EPP the best place in the world to do a Ph.D. Particular credit is due to Pavan Racherla, Seth Blumsack, Sean McCoy, Elisabeth Gilmore, Mary Schoen, Stacia Thomas, Sarah Ryker, Costa Samaras and Dalia Patiño-Echeverri

(among others), firstly for their friendship, but also for stimulating intellectual conversations and feedback along the way.

Finally, I want to thank my family for supporting me along the road to completing this work. My parents, Don and Myrna Hines, have supported my education in innumerable ways and challenged me to work well for the glory of the LORD. My grandparents, Forrest and Glenna Hines, continue to encourage me and allow us restful visits to beautiful Tacoma. Most importantly, I want to thank my amazing wife Vanessa, for her encouragement, patience and volunteer editorial work. Thank you and I love you.

Abstract

Large cascading failures in electrical power networks come with enormous social costs. These can be direct financial costs, such as the loss of refrigerated foods in grocery stores, or more indirect social costs, such as the traffic congestion that results from the failure of traffic signals. While engineers and policy makers have made numerous technical and organizational changes to reduce the frequency and impact of large cascading failures, the existing data, as described in Chapter 2 of this work, indicate that the overall frequency and impact of large electrical blackouts in the United States are not decreasing. Motivated by the cascading failure problem, this thesis describes a new method for Distributed Model Predictive Control and a power systems application. The central goal of the method, when applied to power systems, is to reduce the social costs of cascading failures by making small, targeted reductions in load and generation and changes to generator voltage set points. Unlike some existing schemes that operate from centrally located control centers, the method is operated by software agents located at substations distributed throughout the power network. The resulting multi-agent control system is a new approach to decentralized control, combining Distributed Model Predictive Control and Reciprocal Altruism.

Experimental results indicate that this scheme can in fact decrease the average size, and thus social costs, of cascading failures. Over 100 randomly generated disturbances to a model of the IEEE 300 bus test network, the method resulted in nearly an order of magnitude decrease in average event size (measured in cost) relative to cascading failure simulations without remedial control actions. Additionally, the communication requirements for the method are measured, and found to be within the bandwidth capabilities of current communications technology (on the order of

100kB/second). Experiments on several resistor networks with varying structures, including a random graph, a scale-free network and a power grid indicate that the effectiveness of decentralized control schemes, like the method proposed here, is a function of the structure of the network that is to be controlled.

Notation and terminology

Table 0.1 defines most of the mathematical notation used in this document. In most cases the notation is also defined in context. In general, I stick to mathematical convention with italic symbols representing scalars (x) and bold symbols (\mathbf{x} or \mathbf{X}) indicate a matrix or vector. Matrices are generally written as bold capital letters (\mathbf{A}) and vectors are written as bold lower-case letters (\mathbf{x}), except where convention in the power systems literature is to do otherwise. For example, \mathbf{V} represents the vector of complex bus voltages and not a matrix. Sets are generally represented by italic capital letters (M). In many cases I use a set as a subscript to indicate the subset of a vector's elements. For example, \mathbf{V}_M refers to the sub-vector of \mathbf{V} that gives the voltages at buses in the set M .

In a number of places the text refers to objects within graphs or networks. In the graph theory literature it is common to refer to the elements of a network as vertexes and edges. In most of this text I refer to graph components as nodes and links or, where the text refers specifically to power networks, buses and branches. The terms may be mixed somewhat, but the intention should be clear from context.

In addition, Table 0.2 defines most of the abbreviations and acronyms used in this text.

Table 0.1: Mathematical notation

<i>Symbol(s)</i>	<i>Description</i>
j	The complex number ($j = \sqrt{-1}$). In some cases j is used as an index/subscript variable (x_j).
i	Frequently used as an index/subscript variable

Table 0.1: Mathematical notation

<i>Symbol(s)</i>	<i>Description</i>
A, B, C	Matrices associated with the dynamic constraints for an MPC problem
t_k	The actual time at step k along a time horizon.
$\mathbf{U} = [\mathbf{u}_0 \cdots \mathbf{u}_K]$	A matrix of control variables
$\mathbf{X} = [\mathbf{x}_0 \cdots \mathbf{x}_K]$	A matrix of state variables. In some cases x is used as a temporary or generic variable, but this should be clear from context.
$\mathbf{Y} = [\mathbf{y}_0 \cdots \mathbf{y}_K]$	A matrix of stress/output variables. In some cases y is used as a temporary or generic variable, but this should be clear from context.
$\mathbf{E} = [\mathbf{e}_0 \cdots \mathbf{e}_K]$	A matrix of exogenous variables.
$\mathbf{Z} = [\mathbf{z}_0 \cdots \mathbf{z}_K]$	A matrix of network variables (the combination of u,x,y above)
ρ^k	A discount factor for step k in an MPC problem.
$\mathbf{g}(\dots) = 0$	A set of constraint functions.
$\nabla_{\mathbf{x}}g(\dots)$	The gradient of function g with respect to the vector \mathbf{x} .
S	A set variable used in Chapter 4 to describe the model reduction procedure.
\mathbf{S}, s_{ij}	A sensitivity matrix used only in section 5.3, where s_{ij} is the sensitivity of state variable i to changes in control variable j .
\mathcal{L}	A Lagrangian function used to obtain optimality conditions
\mathbf{Y}_{BUS}	The system admittance matrix for a power system. Context should help to differentiate from \mathbf{Y} above.
\mathbf{Z}_{BUS}	The inverse of the \mathbf{Y}_{BUS} matrix. $\mathbf{Z}_{BUS} = \mathbf{Y}_{BUS}^{-1}$
$y_{ij} = g_{ij} + jb_{ij}$	The real and imaginary portions of the \mathbf{Y}_{BUS} matrix
n_V	The number of buses (voltages, V) in the network

Table 0.1: Mathematical notation

<i>Symbol(s)</i>	<i>Description</i>
n_I	The number of branches (currents, I) in the network
N_n, M_n, R_n	Sets of variables that belong to agent n . N_n is agent n 's local variables. M_N is the set of local neighbor variables. R_n is the set of extended neighbor variables.
Υ_n	The union of an agent's neighborhoods s.t. $\Upsilon_n = N_n \cup M_n \cup R_n$.
Φ_n	The set of agents that agent n chooses to exchange data with during the "negotiation" cooperation method.
$w(n, m), \mathbf{W}(n, M)$	A message (or set of messages) passed between agent n and agent m (or set of agents M).
$x^{[n]}$	The (generic) variable x according to agent n .
\mathbf{D}, d_{ij}	A matrix of node-to-node distances for a network, where d_{ij} is the distance between nodes i and j .
r_l, r_e	The graph radius of an agent's local and extended neighborhood
$C(\dots)$	A cost function
$V(\dots)$	A value function (not to be confused with the voltage vector \mathbf{V})
$\mathbf{V} = \mathbf{V} \odot e^{j\theta}$	A vector of complex voltages at each bus in the network, with phase angles θ and magnitudes $ \mathbf{V} $
$\mathbf{I}, \mathbf{I} $	A vector of complex branch currents and magnitudes
\mathbf{I}_{BUS}	A vector of complex current injections into each bus (sum of all injections for all sources and sinks)
$\mathbf{S}_D = \mathbf{P}_D + j\mathbf{Q}_D$	Real and reactive power consumption at buses that include loads. In this context D is the set of buses that include loads.
$\mathbf{S}_G = \mathbf{P}_G + j\mathbf{Q}_G$	Real and reactive power output at generator buses. In this context G is the set of buses that include generators.
$ V_G $	Voltage magnitude set points at generator buses.

Table 0.1: Mathematical notation

<i>Symbol(s)</i>	<i>Description</i>
\mathbf{o}_k, o_{ik}	An over-current memory variable such that o_{ik} is the cumulative overcurrent on branch i at time t_k
$\mathbf{z} = \mathbf{x} \odot \mathbf{y}$	Indicates that \mathbf{z} is the element-by-element product of vectors \mathbf{x} and \mathbf{y} ($z_i = x_i y_i, \forall i$)
$x \in (a, b]$	Indicates that x is in the continuous range bounded by a and b , including b , but not a
$x \in \{0, 1, \dots, X\}$	Indicates that x can be equal to any of the values in the discrete set specified
$\Delta x_k = x_{k+1} - x_k$	Indicates a change in x at time t_k
x_{\min}, x_{\max}	Minimum and maximum values or limits on x
α_V, α_I	Stress variable increase/decrease rates

Table 0.2: Acronyms and abbreviations

<i>Acronym</i>	<i>Definition</i>
ACP	Agent Control Problem
ALM	Augmented Lagrangian Method
BPA	Bonneville Power Administration
CGE	Computable General Equilibrium
cust.	Customers.
DAWG	(NERC) Disturbance Analysis Working Group
DMPC	Distributed Model Predictive Control
DOE	US Department of Energy
EIA	US DOE Energy Information Agency
EPRI	Electric Power Research Institute

Table 0.2: Acronyms and abbreviations

<i>Acronym</i>	<i>Definition</i>
eq.	Equation
ERO	Electricity Reliability Organization
FAA	US Federal Aviation Administration
FERC	US Federal Energy Regulatory Commission
Gen.	Generator
HVDC	High Voltages Direct Current
ISO	Independent System Operator
LP	Linear Program / Programming
LSMP	Linear Stress Mitigation Problem
LTI	Linear Time Invariant
LTV	Linear Time Varying
MGI	US DOE Modern Grid Initiative
MPC	Model Predictive Control
MPI	Message Passing Interface
NERC	North American Electric Reliability Corporation
NYPP	New York Power Pool
OOP	Optimal Operations Problem
OPF	Optimal Power Flow
pers.	Persons
PJM	Pennsylvania Jersey Maryland (an ISO in the US)
PMU	Phasor Measurement Unit
PSLF	Positive Sequence Load Flow (power analysis software)
RAS	Remedial Action Scheme
RHC	Receding Horizon Control
RTO	Regional Transmission Organization

Table 0.2: Acronyms and abbreviations

<i>Acronym</i>	<i>Definition</i>
SMP	Stress Mitigation Problem
SO	System Operator
SPID	Strategic Power Infrastructure Defense
SPS	Special Protection Scheme
SPS	Special Protection Scheme
TLR	Transmission Loading Relief
UFLS	Under Frequency Load Shedding
US	United States (of America)
UTCE	Union for the Coordination of Transmission in Europe

CHAPTER 1

Introduction

On August 14, 2003 a fairly small set of human and mechanical failures in the Midwestern United States initiated a sequence of events that ended with the interruption of electrical service to approximately 50,000,000 people in eight US states and one Canadian province [2]. As public transportation and traffic lights ceased to operate, hundreds of thousands were left to walk miles to reach their homes. Six weeks later a single over-heated transmission line contacted a tree in Switzerland, initiating a sequence of events that interrupted electricity service to almost all of Italy's 57,000,000 residents and a significant portion of the Swiss population [3]. Thirty thousand passengers were left stranded in 110 trains, and several deaths occurred as lighting and traffic signals failed.

In both of these power system failures, post-mortem analyses indicate that a small set of carefully selected control actions would have vastly reduced the size of the resulting blackouts. According to US and Canadian officials who studied the North American event, "this blackout could have been prevented" [2]. While completely preventing a blackout would have been difficult in the later stages of the sequence, a small amount of load reduction in the Cleveland-Akron area after the trip of the "Eastlake 5" power plant could have greatly reduced the size and impact of the blackout. In the Italian case, operators in Italy realized that imports from France and Switzerland needed to be reduced in order to prevent a large blackout. Italian and Swiss operators agreed to reduce their transfers by 6500 MW and began to implement these actions about 20 minutes after the initial failure. Unfortunately, before these changes could fully take effect, the system exceeded its ability to withstand the stress

of the situation (high currents and low voltages), and a rapid sequence of failures began.

These two events illustrate two important points regarding the control of cascading failures in complex networks. First, given a network that has become stressed due to an initial set of disturbances, there generally exists a fairly small set of control actions that could restore the system to a relatively normal state. Second, the choice of a good time horizon or schedule for implementing control actions is at least as important as the choice of good actions. In the Italian case, operators apparently negotiated a good set of control actions to take (reduce transfers through load and generation reduction) but did not implement them along a good time horizon; their actions came too late to prevent a massive blackout. In other words the chosen set of actions was nearly optimal, but the time horizon upon which the actions were taken was perilously sub-optimal.

The large European and North American blackouts of 2003 have gained much attention due to their size and impact, but moderately sized cascading failures are surprisingly common. Even after excluding hurricanes, earthquakes, ice storms, tornadoes, and supply shortages, the US experiences about 12 large (at least 300 MW or 50,000 customers), transmission-level, blackouts per year (see Chapter 2). While it is difficult to know exactly how many of these fit in the “cascading failure” category, many of the event records indicate that some demand interruption resulted from cascading relay operations. In the cascading failure cases, like the Italian and North American events, the consequences could be dramatically less costly if operators consistently choose and implement appropriate control actions over an appropriate time horizon. According to a recent NERC (the North American Electric Reliability Council) report:

System operators have been at the center of every blackout investigation since the 1965 Northeast blackout, which was the catalyst for the formation of NERC. In almost every instance, had system

operators taken appropriate actions, these blackouts would not have occurred. [4]

Many in the electricity industry have offered many explanations for the relatively frequent and costly failure of the electricity delivery system (operators inclusive) including poor operator training, insufficient investment in network infrastructure, inappropriate incentives for utilities to manage reliability, and a lack of system-wide planning.

While these explanations have some merit, at the core of the problem is the fact that electricity delivery systems (including human operators) frequently react to stress sub-optimally. The current mechanisms by which human operators and mechanical devices observe the network, calculate and negotiate control plans and implement decisions, result in actions that are exceedingly slow, suffer from reliability problems inherent with centralized decision making and provide little to no chance for optimal results. This is particularly true when the discrete and continuous dynamics of the network require precisely calculated and coordinated actions over short time horizons (seconds to minutes). As evidence, table 1.1 lists eight notable cascading failures in North America and Europe showing the initial event that triggered the failure and some remedial actions that would likely have reduced the size and consequences of the ensuing blackout. During all of the post-blackout investigations of these events, it became clear that the systems involved reacted sub-optimally to the initial events. If networks could react to stress more optimally in real time, the consequences of such events could be dramatically reduced.

Problems associated with sub-optimal operations, such as cascading failures, are not unique to electricity networks. Other complex networks undergo massive failures when the agents who control the network act sub-optimally with respect to the system as a whole. Cascading failures are particularly common when such networks occasionally undergo extreme stress. Automobile traffic networks provide an illustrative example. When a traffic accident occurs and snarls traffic on a major artery, it is often

Table 1.1: Some notable cascading failures in North America and Europe. The far right column shows remedial actions that would likely have substantially reduced the social costs associated with the event.

<i>Date</i>	<i>Location</i>	<i>Size</i>	<i>Causes and outcomes</i>	<i>Remedial actions that could have reduced costs</i>
9-Nov-1965	Northeast US	30,000,000 pers. 20,000 MW	A relay on lines from Niagara Falls to Toronto was set too low and tripped, triggering a cascade throughout the region. The event led to the creation of NYPP and NERC.	Immediate reduction of load in Toronto and generation at Niagara would likely have reduced the consequences [5, 6].
13-July-1977	Northeast US	9,000,000 pers.	Three transmission lines opened due to lightning, resulting in the loss of generation in NY. Con Edison system separated from grid within 30 min. Led to widespread use of UFELS relays.	Shed load and/or increase gen. in the NYPP area after the initial generation loss [7].
29-Feb-1984	Western US	3,160,000 cust.	Transmission line fault in OR initiated cascading failure. Controlled separation scheme did not operate as intended.	UFELS relays reduced the consequences of the event after separation. Quickly reducing N-S flows may have prevented the separation [8].
13-Mar-1989	Hydro Quebec, Northeast US	19,400 MW	Solar flare caused 5 735kV transmission lines to trip, initiating a cascading failure.	Quickly reduce HQ area demand by 9000 MW[8].
10-Aug-1996	Western US	7,500,000 cust.	500kV line sagged into a tree. The line and one parallel to it tripped, initiating a cascade.	Reduce flows on the CA-OR intertie within 5 min. of initial events. Increase reactive power in North along Columbia R. [9, 10].
14-Aug-2003	Northeast US, Canada	50,000,000 pers. 57,669 MW	Transmission cables in OH contacted trees, initiating a cascading failure.	Load reduction, and/or reactive power voltage support near Cleveland would have dramatically reduced the size of the event [2].
<i>Recent European Events</i>				
28-Sept-2003	Italy, France, Switzerland	57,000,000 pers.	Transmission line contacted tree, initiating a cascade, resulting in lost service to most Italian customers, and some of Italy, Switzerland.	After initial event, operators reduced imports by 300 MW. Imports should have been reduced by much more [11, 3].
4-Nov-2006	Germany, France	15,000,000 cust.	Operators disconnected a double circuit line over the Ems River to allow a ship to pass, triggering a cascading failure, splitting European grid into 3 regions.	30 min. after initial event E.ON operators implemented incorrect remedial switching actions. Reducing flow on the Landesbergen-Wehrendorf line, would have reduced blackout size [12].

1. INTRODUCTION

the case that alternate routes exist that could maintain a reasonable level of traffic flow. Unfortunately it is also often true that the agents (drivers in this case) who must decide which roads to take have insufficient planning and information-exchange capabilities and motivations, resulting in an artery that remains congested for hours after the accident is cleared. Internet communication networks, financial markets, biological systems, and nuclear power plants are among the many networked systems that at least occasionally suffer from globally sub-optimal responses to stressed conditions.

1.1. Optimal Operations

Motivated by large cascading failures in power networks, this thesis provides organizations responsible for the control of large networks with improved tools for real-time operations. Most engineered networks exist to facilitate the provision of some service. Electricity networks facilitate the flow of energy to customers. Water systems facilitate the flow of potable water to homes. The Internet exists to facilitate the flow of information. In all of these networks, flows are governed by physical laws. A plan for operating the network must consider these physical constraints. In systems where the dynamics are important, operators must use these physical laws to predict the future effects of a decision stream and choose actions that are appropriate to both current and future conditions. In other words, the optimal operation of a network involves facilitating the provision of a service over a time horizon, while considering the dynamical nature of the network.

What follows is a formal definition of the Optimal Operations Problem (OOP), which is the starting point for the methods and results in this thesis. The OOP can be used to describe any control problem with the following properties:

- (1) Given the trajectory of state and control variables over a finite, discrete time horizon, one can evaluate the performance of the network by a computable, scalar benefit or cost function.

- (2) Given the current state of the network, a trajectory of control (decision) variables over the time horizon and perfect information about any random variables in the network (disturbances or other uncertainties), one can compute the trajectory of state variables using a set of computable predictive functions (eq. 1.2).
- (3) The control variables can be represented by box constraints as shown in 1.3.¹

The time horizon for the OOP is a discrete infinite sequence of time steps beginning with the current time (t_0). $\mathbf{X} = [\mathbf{x}_0 \ \mathbf{x}_1 \ \dots \ \mathbf{x}_K]$ represents the stream of state variables that result from a stream of control actions ($\mathbf{U} = [\mathbf{u}_0 \ \mathbf{u}_1 \ \dots \ \mathbf{u}_K]$). $\mathbf{E} = [e_0 \ e_1 \ \dots \ e_K]$ is a stream of exogenous events and variables that affect the network over the time horizon. To simplify the notation somewhat, \mathbf{z}_k is used to represent the combined vector of all of the problem's endogenous variables (not including \mathbf{e}_k) for time t_k . With these definitions, the goals and constraints for optimal operations are as follows:

$$(1.1) \quad \text{OOP} \quad \underset{\mathbf{U}}{\text{Maximize}} \quad V(\mathbf{X}) - C(\mathbf{U})$$

$$(1.2) \quad \text{Subject to} \quad \mathbf{g}(\mathbf{z}_k, \mathbf{z}_{k+1}, \mathbf{e}_k) = \mathbf{0}, \forall k$$

$$(1.3) \quad \mathbf{u}_{\min}(\mathbf{u}_{k-1}) \leq \mathbf{u}_k \leq \mathbf{u}_{\max}(\mathbf{u}_{k-1}), \forall k$$

In this formulation² $V(\mathbf{X})$ is a function that evaluates the value of the services provided by the network over the time horizon, and $C(\mathbf{U})$ is a function that gives the costs associated with providing those services. Thus the objective is to maximize the net benefit (social welfare) of the service being provided by the network, though the results given in this thesis should be valid for any scalar-valued objective function. In

¹In Chapter 3 one additional assumption is added: that the exogenous variables (\mathbf{e}_k , disturbances, demand, etc.) do not change over the time horizon. In other words, \mathbf{e}_0 is known and $\mathbf{e}_{k+1} = \mathbf{e}_k, \forall k \geq 0$.

²Note that there are no inequality constraints on \mathbf{x} . In general constraints on state variables are either fundamental to the nature of the variable (such as a magnitude variable that cannot be less than zero) such that a good predictor function \mathbf{g} will not map from a feasible state to an infeasible one, or are actually soft constraints in that the consequences of exceeding the bound depend upon the extent to which the bound was exceeded.

the case of a power network $V(\mathbf{X})$ gives the social benefit associated with electricity services, and $C(\mathbf{U})$ gives the cost of generating and distributing the power needed to provide that service. The equality constraint $\mathbf{g}(\dots) = \mathbf{0}$ represents the equations that govern the dynamics of the network, and the final constraint in OOP defines the feasible control space for each time step (t_k). Given this formulation, the role of a network operator (or a set of operators) is to choose a stream of actions (\mathbf{U}) that results in a stream of services (\mathbf{X}) that maximize the net value of the services provided by the network, given restrictions imposed by the dynamics of the network. Thus the output of OOP is a stream of decisions that, when applied to the physical network, produces a dynamic stream of services—in the case of a power network, a stream of electrical energy delivered to consumers.

For most large network systems, the task of calculating and implementing \mathbf{U} is the joint responsibility of many actors—human, computerized and mechanical. Rarely does a single actor, or agent, have the ability to measure or control the state of the entire network. This is certainly true for electrical power networks, where in the US Eastern Interconnection alone, there are more than 100 control areas and more than 100,000 substations each of which contains ten or hundreds of control and measurement devices.

When the agents responsible for a network make good decisions with respect to the goals of that network, choosing actions that are nearly optimal with respect to OOP, the result is a relatively efficient and reliable stream of services. Unfortunately, when the services provided by the network are an important part of urban life, as is the case with electricity, a small set of errors in the decision stream (\mathbf{U}) can have enormous social consequences. Large cascading failures are one case where a small set of poor decisions result in enormous social costs. Sub-optimal decisions with respect to the global operations problem can have massive social consequences.

While the OOP is general, it has several properties that make it a useful starting point for this work. Firstly, it has an objective that at least closely aligns with

the purpose of the network. Secondly, the constraints do not add any unnecessary restrictions on the decision space. Avoiding unnecessary restrictions on the decision space is valuable because expanding the feasible region of a problem often reveals superior solutions. Restricting the decision space can eliminate good solutions. For this reason, the OOP does not restrict the decision space to a single snapshot in time, allowing for flexibility in the timing of control actions. Finally, the OOP explicitly accounts for system dynamics, allowing for decision streams that are appropriate to the dynamics of the system. These advantages are discussed in more detail below.

1.1.1. Objective function. The choice of a good objective function, or set of objective functions, is vital to the development of a good problem formulation. Without a good problem formulation it is nearly impossible to obtain good solutions. This objective function in this case was chosen to align with the purpose of engineered networks—to facilitate the maximum value of services provided, minus the cost of providing that service. In other words, to maximize social welfare.³

It is important to note that this objective is written from the perspective of a global social welfare maximizer. While this may not be exactly the objectives employed by a profit-maximizing entity managing a power network, it is the role of the policy maker to define rules that encourage such entities to operate from this perspective. Certainly a well-regulated large Regional Transmission Operator (RTO) or Independent System Operator (ISO) would operate with a similar objective function. Because this thesis is written from a policy perspective, it will start from the social welfare maximization perspective.

Note also that the objective of the OOP can be any real valued, computable, scalar function; the objective does not need to be social welfare maximization. Even within the context of power systems, there are other objectives that are not explicitly

³In the economics literature, a social welfare function is one that ranks preferences for social outcomes. Particularly in the field of regulatory economics, the general social welfare function is written as consumer benefit minus supplier costs.

represented by this objective. For example, it does not explicitly model environmental goals. Since the test case for this thesis (cascading failures in electrical power networks) is generally on short time horizons, other costs and benefits are likely to be small in magnitude relative to the control costs and the value of services. Even if this were not the case externalities, such as social costs associated with pollution, could be Incorporated into $C(U)$ or $V(X)$ with little difficulty.

1.1.2. Increased decision spaces. The OOP was written in a fairly general form, in part, to avoid eliminating good solutions that could be eliminated by unnecessary restrictions on the decision space. Because larger decision spaces can expose superior solutions, we can improve the quality of the solution—and with respect to OOP, operations—by adding variables into a problem formulation and avoiding unnecessary restrictions on the decision space. The results in Chapter 3 illustrate this result. In a power network there are many variables that could be included in the operations problem. These include continuous variables such as generator outputs, the set points for controllable reactive power resources, FACTS device set points and energy prices. Additionally many discrete variables can influence the solution of this type of problem. Among the potentially useful discrete variables are circuit breaker statuses and transformer tap positions. The results included in this thesis focus on the use of continuous variables, though future work will look at the potential for the use of discrete variables.

1.1.3. Increasing decision spaces in time (dynamic decision making). In addition to allowing for an expanded decision space through the addition of control variables, the extension of problems over a time horizon results in similarly improved decision streams. For example, by extending the decision space in time, an operator can choose between taking an action now or delaying until later when more information is available. In this way, the decision maker acts iteratively, which is

tremendously valuable when the model used to approximate $\mathbf{g}(\dots) = \mathbf{0}$ gives a less-than-perfect approximation of the system dynamics. Chapter 3 provides an example of the benefits associated with expanding the decision spaces in time.

1.1.4. The OOP and Model Predictive Control. If the network problem in question has continuous and discrete variables and a computable set of non-linear dynamic equations, the OOP is a mixed integer non-linear, model predictive control (MPC) problem. If the problem could be solved efficiently from a central location by a single operator, the standard MPC implementation procedure, enumerated below, would be employed to solve this problem.

- (1) Measure the state of the network and update the state vector for the current time, \mathbf{x}_0 .
- (2) Calculate a set of control actions for the chosen time horizon: $\mathbf{u}_0, \mathbf{u}_1, \dots, \mathbf{u}_K$.
- (3) Implement the decision for t_0 (implement \mathbf{u}_0).
- (4) Advance the time horizon given the step size (Δt): $t_0 = t_0 + \Delta t$.
- (5) When the current time approaches t_0 (to within the time required to calculate and implement a new control vector), repeat from (1).

The unit commitment problem, commonly employed by power system operators, provides evidence of the value associated with this type of rolling horizon problem. The unit commitment problem, which can be considered a subset of the OOP, though with long time horizons (hours to days rather than seconds to minutes), seeks to minimize dispatch costs by repeatedly creating a plan for starting and stopping generators over a time horizon and then implementing the result for the first time period in the horizon. In a system containing generators with significant start-up and shutdown costs and constraints, the mixed integer, time-horizon approach employed in the unit commitment dispatch solution process results in vastly reduced costs relative to standard economic dispatch methods [13].

1.2. Solving the OOP via Distributed Model Predictive Control

For large network problems it is often impractical, or even impossible, to implement MPC control in a timely fashion from a central location. With a centrally managed control system, the time required to collect state data and implement solutions for large network problems can be prohibitively large. Indeed, nearly four years after the Aug. 14, 2003 North American blackout, the state of the US Eastern Interconnect on that afternoon remains substantially unknown. Centrally operated systems can also be vulnerable to failures at the central facility. Decentralized solutions however have a number of advantages, including robustness to failures and reduced communication delays (see Chapter 5 for a more thorough discussion of decentralized control). In order to take advantage of these benefits, this work builds on the methods described in [14] and [15] to design a new approach to decomposing decision and control processes into sub-problems that can be solved by a network of autonomous software agents. The general form of this decomposition scheme has the following properties (see Chapter 4 for a detailed description of the method). Firstly, the global decision (\mathbf{u}) and state (\mathbf{x}) vectors are separated into geographically disjoint components. Defining $\mathbf{z} = [\mathbf{u}^T \quad \mathbf{x}^T]^T$, and N_n (or just N , when the agent number is clear from context) to be the subset of all variables in \mathbf{z} that can be directly measured or controlled from agent- n 's location, this decomposition has the following properties:

- the subsets for each agent- n ($\mathbf{z}_N = [\mathbf{u}_N^T \quad \mathbf{x}_N^T]^T$) combine to form the complete control and state vectors:

$$z_S = z, S = \bigcup_{\forall n} N_n$$

- the subsets (N_n) do not overlap ($N_a \cap N_b = \emptyset, a \neq b$);
- agent n can locally control only the variables in \mathbf{u}_N ;
- agent n can locally measure only the variables in \mathbf{x}_N ;

- each agent makes its decisions with a fairly high degree of autonomy—i.e. they do not need to ask permission to choose and implement actions according to the information available and the preferences of the agent.

Secondly, the agents maintain overlapping sets of network models by constantly exchanging information with their neighbors, and occasionally exchanging information with centrally located operators. The agent models have the following properties:

- a local model that contains control and state variables that are “owned by” a small set of “local neighbors”—for agent n this set will be referred to as M_n ;
- an extended model that contains control and state variables that overlap with a set of “extended neighbors”—for agent n this set will be referred to as R_n ;
- an extremely simple model of the remainder of the network, which can be updated via occasional (not more than weekly) communications with a centrally located operator.

Finally, each agent uses its network models to solve a problem that approximates the global OOP as accurately as possible given communication and computational constraints. The agents cooperate with their neighbors to achieve improved results and implement only the portion for local variables \mathbf{u}_N .

1.3. Multi-agent systems

“Agent” is a term often used in recent academic literature but not often defined. Roughly, agent definitions come in two types—structural definitions that describe the components of an agent and behavioral definitions that describe an agent’s actions. Following the definitions given in [16], in this text “agent” refers structurally, to “a network of sensors, decision-makers and actuators” or behaviorally, to “a mapping from an in-space (all the things the agent can sense) to an out-space (all the things the agent can affect).” Within a network of sensors, decision-makers and actuators (an agent) there exists a control flow and a data flow. The control flow is the mechanism

by which control decisions are implemented. Data flow is the mechanism by which data moves among elements of the network. This definition is recursive in that one agent can be composed of many sub-agents. For example a firm is often thought of as a unified agent in the economic literature, but firms are typically composed of many employees, who are also agents.

It is common to identify and categorize agents by their properties. Arguably the most important property of agents is autonomy. “An agent is autonomous to the extent that it can act independently, that is, to the extent that it is unsupervised.”[16]⁴ Autonomy is thus a continuous measure, as some agents are more autonomous than others. A prisoner, for example, has substantially less ability to choose his activities than a non-incarcerated individual. It is common to refer to an agent with a substantial degree of autonomy as an “autonomous agent.”

Another property of agents is cognition, or the ability to map information to decisions. Cognition is similarly a continuous measure. A thermostat is frequently discussed as an agent, since it maps information (temperature) to decisions (heat on/heat off), but it would measure low on the cognition scale due to the simplicity of its decision-making process. Agents with sophisticated cognitive abilities are often referred to as “intelligent agents.” Thomas Aquinas, in *Summa Theologica*, argues that cognitive agents (*cognoscentia*) “differ from those that do not know in the fact that the nonknowers possess their own form only, while the knower is adapted from its origin to possess also the form of another thing, in the sense that the species of the known thing may be present in the knower” [18]. Cognition is the ability to capture (possess) information about other things (species). Aquinas differentiates between plants, which do not know of other beings, and animals, which do have a sense of the other. In [19] Lesser defines an intelligent (software) agent as, an object that will “typically operate according to a set of preferences or objectives, which it uses

⁴In [17], Wooldridge defines autonomy as the ability to “operate without the direct intervention of humans or others, and have some kind of control over their actions and internal state.” Other definitions exist as well, but the sense of being free to choose and take action apart from supervision is common to most.

to choose among various actions given different environmental and social conditions, rather than simple rules that precisely specify its cognitive mapping.”

Many, if not most, agents also have some sort of social ability—an ability to interact with other agents within an environment. Social interactions can take a variety of forms. Ants, for example, exchange information primarily through the product of their work, and by depositing pheromones on their environment [20]. Computer-based agents generally exchange information through digital communication channels, either via direct point-to-point communications or through some sort of blackboard system.

Agents rarely exist in isolation. A collection of agents that exist within the same environment is known as a multi-agent system.⁵ Multi-agent systems generally fall into one of three broad categories: biological systems that exist in nature, engineered systems of electrical and/or mechanical agents, and hybrid systems of biological and non-biological agents. The design of a multi-agent system to simulate a biological system in a computer model is often known as “agent-based modeling” and is commonly used in economics as an alternative to micro-economic, or Computable General Equilibrium (CGE) models. A multi-agent system that has been engineered to complete a task is commonly known as an agent-based control system. This thesis focuses on the design of an agent-based control system to mitigate the costs of cascading failures.

Within most multi-agent systems, agents cooperate to some extent. In this thesis cooperation refers the ways in which agents help one another to meet their goals. In many cases cooperation involves the transfer of useful information. There are two primary mechanisms of inter-agent information transfers: message passing and message posting. In message passing, agents send information directly to other agents. In message posting, messages are sent to a common space from which other agents can collect information. The agent-based control systems described here uses message

⁵Given that an agent is a bundle of sensors, decision-makers, and actuators, a multi-agent system is itself an agent.

passing for the exchange of information. The content of this message passing is described in chapters 4 and 5.

There are many types and degrees of cooperation. On the non-cooperative extreme is pure competition, in which agents operate with non-coincident local objective functions. If information transfers occur among competitive agents, they are generally unintentional (theft) or are not intended to be useful (a lie). A private company will not typically share strategy information with its competitors, as such an exchange could give the receiving company a market advantage. On the cooperative extreme is a case in which agents operate according to perfectly commensurate objective functions and share useful information freely with one another. Each member of a string quartet, for example, acts with the same goal of producing an agreed musical result and each member has nearly complete information about the four musical parts being played. Between these two extremes sits a form of cooperation known as “reciprocal altruism,” in which agents agree to share some goals with their neighbors.[21] The multi-agent system described here is based upon the reciprocal altruism concept. The control-agents agree to (are designed to) work with similar objective functions. The result is agents that may choose locally costly actions in order to maximize global utility.

1.4. Related Literature

The research described here draws from and builds upon concepts from a variety of disciplines, including complex systems, model predictive control, multi-agent systems, and a number of research areas within the electrical power systems literature. The following is a brief review of relevant literature in these fields, focusing on the literature that is particularly related to electrical power systems and the research results contained in this thesis.

1.4.1. Complex systems, networks and cascading failures. According to [22], a system is complex if its “properties are not fully explained by an understanding

of its component parts.” Properties commonly found in complex systems include phase transitions, cascading failures and power-law probability distributions. For example, [23] explains the existence of power-law probability distributions (1/f noise) that occur in many systems with the principle of self-organized criticality (SOC). In the SOC model, systems self-organize to a point of near collapse, experience a cascading failure, and then gradually return to the point of critically. This model has been related to the properties of many systems including electrical power networks [24] (see Chapter 2 for a more detailed discussion of this model). Relatedly, [25] provides evidence that power networks experience phase transitions.

An important branch of complex systems is the study of network structure. Until recently, random graph theory [26] was the network structure of choice for the study of interacting systems. More recently, the small world network model [27], which is characterized by links that span across large sections of an otherwise fairly regular network, has provided insight into numerous social and biological systems. As a sub-class of the small-world network, the “scale free” network [28] and the role of preferential attachment in the evolution of complex networks have provided substantial insight into the nature of several real-world networks such as the World-Wide Web and some cellular networks. While the structure of power networks differs substantially from these standard network models, much can be learned by relating simple graph models to the structure of actual power networks (see [29]). Chapter 3 shows how the structure of a network affects the extent to which decentralized control is feasible within that network.

1.4.2. Model predictive control. Model predictive control (MPC) techniques integrate the reliability benefits of closed-loop control and the predictive benefits of feed-forward control. An MPC controller uses an explicitly coded model of the process to simultaneously choose control actions and predict their effects over a given time horizon. The result is a sequence of control actions for the entire time horizon. If u_k represents a vector of control actions for time period $t_k \in \{t_o, t_1, \dots, t_K\}$, this output

sequence is $\{u_0, u_1, \dots, u_K\}$. The controller then implements the control actions for the current time period (u_0), advances the time horizon, takes additional measurements, and repeats the process. Due to the use of repeatedly shifting time horizons, MPC is sometimes also referred to as Receding Horizon Control (RHC). Since the controller uses an optimization algorithm rather than a closed form control law, MPC controllers can naturally handle complex inequality constraints and discrete variables. The use of optimization algorithms also allows the controller to explicitly account for the costs and benefits associated with control actions rather than aiming a set of variables at the origin. This feature makes MPC methods quite appropriate for problems where cost is an important factor in decisions (eg. industrial plant control). The disadvantages of the MPC approach include the fact that mathematical programming methods used to solve for the control trajectory can require substantial time between discrete control steps, and that it is generally more difficult to prove the stability of a given MPC controller. As the speed of computing resources increases, the first problem becomes increasingly minor, and an increasing set of methods exist to ensure the stability of MPC controllers (see e.g., [30]). While MPC is a fairly new technology, treatments are available in textbook [31] and tutorial [32] formats. MPC has found wide acceptance in the chemical industry [33, 31], where the method's ability to handle complex plant models have resulted in significant economic and process gains.

Recently, several authors have adapted MPC to decentralized control problems. Camponogara et. al [34] describe an approach to cooperative, distributed MPC, and illustrate the method by using it to synchronize a small network of pendulums and machines in small power networks. Similarly, Keviczky et. al [35] describe a decentralized RHC approach that has been applied to paper process control [36] and the formation flight of autonomous aircraft [37]. A method for ensuring the stability in decentralized MPC is discussed in [38].

A few recent papers focus on the application of MPC to power systems problems. Hiskins and Gong [39] describe an MPC algorithm that incrementally reduces load,

assuming that load can be reduced as a continuous variable, to prevent voltage collapse. The algorithm is similar to the Stress Mitigation Problem (SMP) described in Chapter 3 with the main difference being that the SMP is not specific to the voltage collapse problem and focuses more precisely on minimizing the social costs associated with control actions. The algorithm described in [40] uses MPC to control the trajectory of a power network toward a pre-defined path. For example, one of the control objectives in [40] is to, “minimize the absolute value of reactive power production of all generators.” This approach differs substantially from the OOP approach, in that the control goal is significantly different than the actual goal of the network—that of reliably delivering energy to customers. Finally, Larsson [41] describes an MPC-like algorithm for enhanced dynamic stability through load shedding. All three methods are designed to operate from a centrally located facility that has complete information about the network. The decentralized algorithm described here is thus a new approach to MPC in power networks.

1.4.3. Multi-agent cooperation. Successful cooperation among agents, whether human or mechanical, is not a trivial task. Agents with incomplete information and conflicting objectives can work in ways that are detrimental to the whole [42]. Even when agents’ objectives are congruent, information exchange can prove costly. Nevertheless, cooperation is necessary in order to obtain good results to problems that are inherently large, decentralized, and complex.

The literature on cooperation among biological agents is well developed. The theory and practice for cooperation among human agents within organizations is mature. Cooperation among non-human animals has also been studied extensively (see e.g., [20]). In biological systems cooperative methods can be quite effective for solving complex problems though not without costs. Cooperation among biological agents is difficult largely due to the tendency of biological agents to think and act according to rather myopic objective functions.

The theory and practice of cooperation among non-biological agents is less mature, but rapidly developing. Talukdar et al. [43] show that asynchronous teams of agents can cooperatively solve difficult optimization problems such that solution quality increases nearly linearly with team size. This approach is most effective when applied to offline problems where time is not critical. Modi et al. [44] present a method for solving constraint satisfaction problems using cooperative agents, but again, this method was applied to problems where time is not particularly critical. Some literature has resulted from efforts to design teams of robots that can compete in soccer [45], though the actions of such teams are generally far from optimal. Similarly, some cooperative methods exist for controlling groups of autonomous vehicles in real time [46, 47, 48]. The ability of such systems to react to external disturbances is limited and the problems that face autonomous vehicles are substantially less tightly coupled than those of agents interacting over a physically connected network such as a power system

The literature on cooperative problem solving for mechanically interconnected, complex systems such as electricity networks, is particularly limited. Pilot relaying is one early exception to this, and provides a useful example. Pilot relaying is commonly used to identify and interrupt faults along high voltage transmission lines [49, ch. 13]. In this simple scheme, relays on one end of a transmission line inform relays on the other end when a potential fault is detected. The relays employ simple heuristics to reach agreement on whether to open circuit breakers based on local voltages and currents and simple message passing. By cooperating pilot relays can interrupt faults faster and more reliably than by working independently. While this scheme is useful, it does not always result in optimal solutions to the optimal operations problem, and because of the extremely simple nature of the message passing and control actions involved it only marginally fits in the category of real-time multi-agent cooperation. Recently some have presented cooperative relaying schemes that add some additional intelligence to power system protection schemes [50] but do not solve the optimal

operations problem. Camponogara [34] describes some preliminary methods for real-time cooperative control, of which [14] is to some degree an extension. This thesis extends these preliminary methods to clearly demonstrate that real-time cooperative control is feasible for complex networked systems.

1.4.4. Distributed optimization. The agent-based control method described here uses a form of decentralized optimization algorithm. A wide variety of decentralized optimization methods exist in the literature, though the majority focus on the solution of optimization problems on a parallel computer with shared memory (see e.g., [51]). Since agents distributed throughout a large network will not have high-speed access to shared memory, shared memory algorithms are not particularly useful for decentralized control. A few algorithms exist that allow for geographically distant agents to cooperatively solve optimization problems. The ADOPT algorithm [44] is a hierarchical, decentralized algorithm for solving constraint satisfaction problems. While the algorithm has good convergence properties and allows for asynchronous work, it is best suited to agent systems that naturally fit in a tree-like, hierarchical structure and to constraint satisfaction problems. Several algorithms stem from a form of the Augmented Lagrangian optimization method (ALM) for general non-linear optimization problems [52]. The Auxiliary Problem Principle [53, 54] for example, provides a framework for the decentralized solution of general optimization problems. This method has been applied to the solution of the Optimal Power Flow (OPF) problem [54, 55], but experiments performed by the author (see [56]) indicate that the method does not work well when a power system problem is fully decomposed (one sub-problem per node in a power network).

1.4.5. Related methods for controlling cascading failures in power networks. According to [57], Special Protection Schemes (SPS, also known as Remedial Action Schemes, RAS) is a

“protection scheme that is designed to detect a particular system condition that is known to cause unusual stress to the power system and to take some type of predetermined action to counteract the observed condition in a controlled manner. In some cases, SPSs are designed to detect a system condition that is known to cause instability, overload, or voltage collapse. The action prescribed may require the opening of one or more lines, tripping of generators, ramping of HVDC power transfers, intentional shedding of load, or other measures that will alleviate the problem of concern.”

When well designed, a SPS can provide a power network with automated responses to stress that are more in line with the OOP. The primary difference is that most SPS are specifically tuned to react to a small set of high-risk conditions. A scheme that results in nearly optimal actions under one set of conditions may have adverse effects given a different system state. Nevertheless many such schemes have been deployed in power networks world-wide. In some cases an SPS can enable a network to operate with smaller margins, though not without some additional risks [57, 58]. Zima [59] provides a fairly thorough review of the SPS literature.

Since the large blackouts of 2003, substantial progress has been made in the development of advanced SPS-like control methods. The May 2005 edition of the *Proceedings of the IEEE* was devoted to “Energy infrastructure defense systems,” [60] and includes several papers describing the state of the art in SPS technology. Included is a description of new methods being employed by the Bonneville Power Administration (BPA) Wide-area Stability and Voltage Control System [61]. This paper describes the transition at BPA from a feed-forward system that enacts pre-programmed responses to discrete events, to a feedback-based scheme which can react to stress in the system after measurements are obtained. BPA’s scheme differs from the methods described here in that it is largely operated from a central control facility. Similarly, [62] describes several algorithms for the assessment and mitigation of voltage and frequency

stability problems in power networks. As with the BPA system, the algorithms are designed to operate from a centrally located facility using phasor measurement units and other measurement devices located at substations. Refs. [63, 64] describe two other notable, centrally operated, control schemes. The first uses the AC power flow equations to calculate switching actions that can, in some but not all cases, alleviate voltage and current problems. The second describes an algorithm for choosing switching actions that can separate a power network into disjoint sub-networks in order to contain a cascading failure.

Very few SPSs employ decentralized control methods. The Strategic Power Infrastructure Defense (SPID) system described in [65] is one potential exception in that it employs a hierarchical, multi-agent architecture, though the scheme as a whole still relies on centrally located facilities for most reaction scenarios and thus differs substantially from the approach described here.

Looking forward both the US Dept. of Energy [66] and the Electric Power Research Institute [67] are currently involved in major research, development and demonstration programs to improve the control and communications infrastructure for power networks. The EPRI Intelligrid program specifies a communications architecture that could enable a variety of new approaches to controlling cascading failures, though detailed control algorithms are not yet an official part of the program [67]. Similarly, the DOE's Modern Grid Initiative (MGI) [66] specifies a number of goals for improving power network controls but does not yet recommend a particular approach to controlling cascading failures. Both programs may lead to a grid with the ability to respond to stress nearly optimally, according to the OOP, but at the current time these programs include very little specific technology for controlling cascading failures.

1.5. Related Policy Problems

While the goal of this work is to provide a decentralized solution to OOP, it is motivated by and has important implications for important policy problems. The public sector will likely always need to play some role in the mitigation of risk associated with large blackouts in electrical power networks. Because large blackouts rarely confine themselves to the domain of a single private company in a synchronous power network, efforts to control this risk require multi-party coordination, or at least cooperation. System-wide reliability, such as would be affected by a large cascading failure, has many properties of a public good. For example, Joskow and Tirole [68] argue that the when operating reserves are needed to prevent cascading failures, the supply of operating reserves is a public good.

In the United States, largely due to a political recognition of the public-good nature of system reliability after the Aug. 14, 2003 blackout, the federal government has granted NERC authority to develop and enforce rules that facilitate system reliability. NERC (now known as the US-Electricity Reliability Organization, ERO) now has responsibility to manage the public-good aspects of electrical power system reliability. As mentioned above several private (Intelligrid [69]) and public (the Modern Grid Initiative [66]) organizations are developing methods to modernize US electricity infrastructure. Common to all of these efforts is a desire to use advanced control methods to minimize the impact of problems like cascading failures. Because of the public-good properties of cascading failures and system-wide reliability, the public sector, likely through the ERO in the United States and organizations like the UTCE in Europe, will need to play an active role in coordinating the efforts of electricity industry stakeholders as they work to modernize electricity infrastructure.

1.6. Thesis structure

This thesis is organized into seven chapters. Chapter 1 is this introduction. Chapter 2 (Blackouts) contains an empirical analysis of historical blackout records in the

United States. Chapter 3 (Operations) discusses the operations problem in more detail and presents some results that illustrate the value of the approach described by this thesis. Chapter 4 (Cooperation) provides some additional discussion of multi-agent cooperation and reciprocal altruism, and describes the cooperation methods that were employed in the proposed control system design. Chapter 5 (Decomposition) describes the method used to decompose the global optimal operations problem into sub-problems which can be solved by autonomous agents. Chapter 5 also argues that the effectiveness of decentralized control methods depends at least to some extent on the structure of the network to which it is applied. Chapter 6 (Verification) provides a more thorough, simulation-based, analysis of the proposed decentralized control algorithm. Finally, Chapter 7 (Conclusions), discusses the importance of this work to contemporary policy problems and highlights the most important contributions from this thesis. Included in the conclusions is a discussion of several implementation challenges faced by wide-area power systems control technology, and a brief discussion of policy instruments that could facilitate deployment of this type of control technology.

Several technical appendices provide data and details that do not fit within the text body. Included in the appendices is the full blackout data, which is employed in Chapter 2, the complete IEEE 300 bus data system as used in the experiments described herein and a description of the whisker-plot frequency distribution graph employed.

CHAPTER 2

Blackouts

This chapter provides an empirical analysis of the frequency and impact of large blackouts in the United States. From data collected by the North American Electric Reliability Corporation (NERC), one can approximately calculate the expected annual cost of large blackouts, which provides an upper bound for the expected annual cost of large cascading failures. The analysis and methods given here are intended to (1) provide industry members and policy makers with improved means for empirically evaluating the expected cost of large blackouts, and (2) determine what, if any, trends exist in the history of large blackouts in the US. These results are intended to be useful to large consumers, system operators and policy makers by providing them with better information with which to choose among infrastructure and policy changes that could mitigate the frequency and expected cost of large blackouts. While the analysis is based on data available for the United States, the approach may be useful in other contiguous, synchronous electricity networks.

The analysis described here indicates that the annual frequency of large blackouts in the United States is not decreasing in time. In fact, depending on the measure used, a small increase appears. This trend remains even after removing all of the blackouts that resulted from extreme natural events (hurricanes, ice storms, earthquakes, tornadoes) and after adjusting for the natural growth in demand and population. Despite substantial research and investment by government, academia and industry focused on improving power network operations, no decrease in the annual frequency of large blackouts is apparent. This chapter concludes with a brief discussion of plausible explanations for these results.

2.1. The impact and social costs of large blackouts

Large blackouts often come with large social costs. Some of these are relatively direct economic costs. The New York Times reported that the insurance industry would pay out about \$3 billion as a result of the Aug. 14, 2003 blackout [70]. Many impacts, such as leaving subway passengers stranded underground, are more difficult to measure. The social consequences of a blackout are a function of many factors including the size of the blackout, the duration of the blackout, its location and the time of day. Given a large data set of blackout costs, one could probably obtain a good fit between blackout size and blackout cost given the following functional form:

$$(2.1) \quad \text{Cost}_i = \alpha(\text{MW}_i) + \beta(\text{MW}_i)^2 + \gamma(\text{MWh}_i) + \eta(\text{MWh}_i)^2.$$

Unfortunately accurate estimates for the social costs of large blackouts are not widely available. From a study of 24,800 individual customer outages, Larsson et al. [41] found that reported commercial and industry customer costs increased, but not linearly, with outage duration. In this study, per kWh blackout costs increased over the first 9 hours and then decreased thereafter. A follow up study [71] argued from the same data that much of the impact of large blackouts results from the initial interruption (α) rather than the duration adjusted size (γ). On the other hand, after several hours the non-commercial costs of a blackout may increase substantially as services such as cellular telephone service and water distribution systems begin to fail. If one were to perform a regression analysis using eq. 2.1, one would certainly obtain positive multipliers for α and γ , since blackout costs increase with both the initial size (α , geographic dispersion), and the duration adjusted size, γ . The quadratic terms, on the other hand, might have opposite terms. One could argue that costs would grow superlinearly with β , due to compounding social costs that come from the scale of a blackout. For example, a blackout that disabled all of the traffic lights in an entire city for 1 hour would likely be more costly than 2 blackouts that disabled 1/2 of the city's traffic lights each for 1 hour. The larger blackout might remove all

alternate paths for traffic, and cause a much larger traffic problem. The Larrsson et al. [41] study, on the other hand, indicates that costs scale sublinearly with duration (i.e. $\eta < 0$). This may be the result of organizations adapting to the situation as the blackout extends in time. However, this study focused only on commercial and industrial costs. The per MWh non-commercial costs might begin to increase after socially valuable services begin to fail after the first day or so.

Given that extensive data on the costs of large blackouts do not exist, some assumptions about the costs of blackouts are required to provide a quantitative analysis of blackout impact. In the remainder of this thesis the impact of blackouts is measured in MW-interrupted and social cost. When measuring impact in cost terms, I assume that costs scale linearly with MW, though in the simulation results costs vary by location (see Chapter 6 for a description of the simulation model in which costs are measured). While the linear assumption is a simplification of the relationship between event size and cost, there is not enough information either in the NERC data (because duration is not consistently reported) or in the simulation results (because the restoration process is not modeled) to calculate the unserved energy (MWh) resulting from each blackout. Assuming that blackout costs scale linearly with size in MW is equivalent to assuming that $\beta = 0$, that $\eta = 0$ and that all blackouts are of the same duration ($(\text{MWh}) = d(\text{MW})$, where d is a scalar).

2.2. Related research results

Several recent papers note interesting patterns in the North American blackout data available from NERC. Carreras et al. [72, 24] and Talukdar et al. [73] show that blackout sizes in these data have a power-law tail in their probability distributions. Carreras et al. [24] argue that time-correlations in the blackout data (using the Hurst parameter, which measures auto-correlation over multiple time-scales) is evidence of self-organized criticality, which would provide a plausible explanation for the power-law tail. While some have questioned the self-organized criticality conclusion, arguing

that seasonal effects provide a better explanation for the clustering [74], the power-law statistic in the blackout size distribution is not disputed. The analysis described in this chapter uses a more extensive data set (1984-2006) than what is presented in the above analyses and filters the data in several ways to remove effects associated with demand growth, supply shortages, extreme natural events and the spotty reporting of smaller events. The resulting data show a very strong fit to the power-law tail in the blackout size distribution and a statistically significant seasonal increase in risk during the summer months.

Some authors have used various theoretical blackout models to develop high-level risk measures for cascading failures. For example [75] describes a probabilistic model of cascading failure risk, and [76] describes a power system failure model that accounts for hidden failures. The blackout-risk model presented here uses a simple extension of the statistics evident in the blackout data for the United States to produce an empirical, but rough, estimate of the expected costs associated with cascading failures. It differs from the existing models in that one does not need extensive technical network data to estimate the expected cost of large cascading failures.

2.3. Data

Both the US Department of Energy (DOE) and the North American Electric Reliability Council (NERC) require that member organizations submit reports when sufficiently large disturbances occur within their territories. The DOE publishes the resulting data as “Form 417” reports [77], and NERC provides the data through its Disturbance Analysis Working Group (DAWG) database [8]. By law, utilities and other load serving entities must report all disturbances that interrupt more than 300 MW or 50,000 customers [77]. Some smaller disturbances are also included in the reports, but on a less predictable basis. Since the NERC DAWG database is the most complete of the two sources, providing data on blackouts from 1984 to 2006, the statistical analysis presented here is based on the NERC data.

Many of the events in these data sets are smaller than the 50,000 customer / 300 MW limit. Since small event reporting is not required and likely to be spotty, this analysis focuses on the larger events. Initially, all data smaller than 1,000 customers or 100 MW were removed to arrive at a preliminary data set with with 578 events (25.1/year) starting with 3-Jan-1984 and ending with 30-Dec-2006. Subsequent analysis focuses on a subset of these events. Many of the reports list the event size only in MW or customers (not both). To compensate for this, and to avoid dropping data that might otherwise be useful, the events with one or the other entry missing were scaled by the average customers per MW for those events which did include both sizes (450 customers/MW).

Given the number of customers interrupted in each blackout, one can calculate the apparent System Average Interruption Frequency Index¹ (SAIFI). After adjusting for demand growth, such that the data are scaled to year 2000 customers, and dividing by the number of electricity customers in the US in the year 2000, the apparent SAIFI from the NERC data is:

$$SAIFI = \frac{(219,643,512 \text{ interruptions})}{(23 \text{ years})(127,568,517 \text{ customers})} = 0.075.$$

SAIFI in the United States is about 1.2 or 1.3². Thus the transmission system events in the NERC data represent about 6% of the events reported in SAIFI. Since many blackouts do not get recorded in utility's SAIFI numbers³, it is likely that the NERC data represent somewhat less than 5% of all US customer interruptions.

The blackouts described by these data began with a wide variety of initial failures. Since this thesis is primarily concerned with cascading failures, the data were filtered

¹SAIFI measures average number of sustained (>5 minutes) service interruptions within a given region per year. SAIFI is the quotient of the number of interruptions within a region over the year and the number of customers.

²These figures represent the mean SAIFI over many utilities, as reported in [71]. They do not actually represent the SAIFI for the US, as the mean of the indices does not necessarily return the index for the aggregate.

³In most states that require SAIFI reporting, utilities are allowed to excluded from their reported statistics blackouts that were caused by large storms, large cascading failures, and some other events.

to remove events whose size was very likely not affected by a cascading failure. While the event reports are not detailed enough to ensure that all of the non-cascading failures were removed, the below filtering removes most of the events that are certainly not cascading failures. In order to do so, the events were sorted into the following categories:

- (1) Blackouts initiated by extreme natural events including hurricanes, ice storms, tornadoes and earthquakes (17.6%),
- (2) Blackouts (typically due to wind storms) that affected only the distribution system and do not fall in the above category (5.0%),
- (3) Supply shortage events in which operators manually shed load (5.2%), and
- (4) All other events (72.1%).

Figure 2.1 shows the number of blackouts in each category for each year, after removing the very small events.

Within the “other” category, blackout events were initiated by a variety of causes including lightning, smaller storms, fires, device failures and human errors. While many of the failures began with failures in transmission lines, several of the clear cascading failures began with failures at substations (often due to problems with metering transformers that hang off of substation bus conductors). Such substation (node) failures are particularly likely to result in a cascading failure because they result in multiple transmission line outages surrounding the substation.

2.3.1. Scaling to adjust for demand/population growth. Because the total number of customers and the total consumption of electricity increase with time, conclusions drawn about changes over time in the raw data could be misleading. For this reason the customer and MW event sizes are scaled to adjust for population and demand changes in the United States. Population data are drawn from the mid-year (July 1) US Census Bureau population estimates [78]. Demand data are taken from the net annual generation data (energy not power) published by DOE/EIA [79]. The

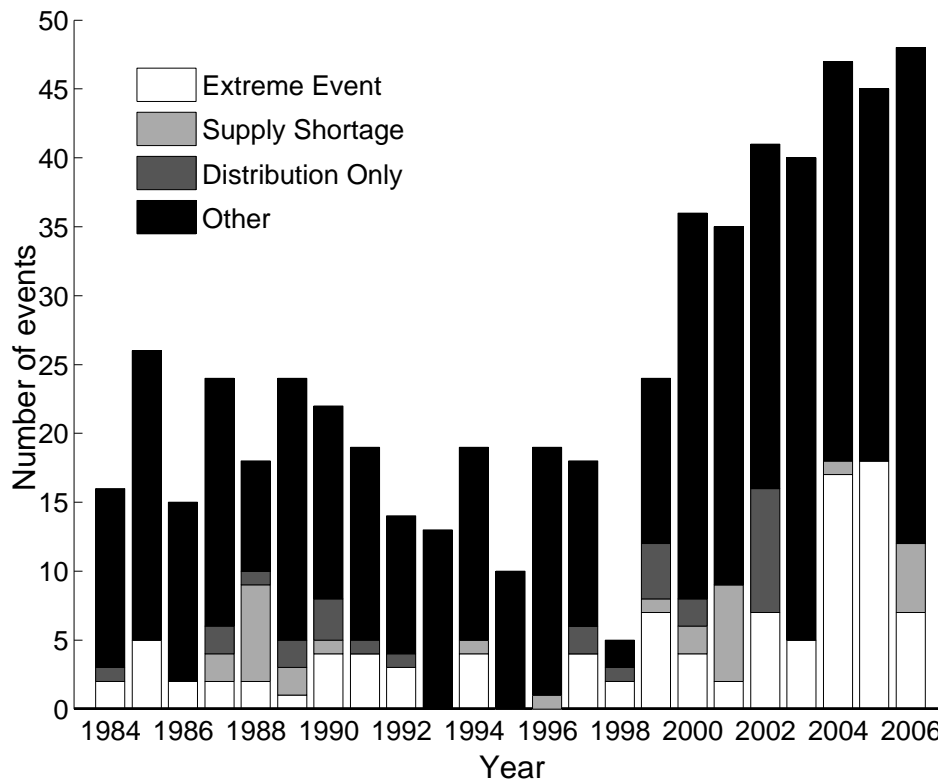


Figure 2.1: The number of blackouts for each year of the NERC DAWG data [8], after removing events smaller than 1,000 customers and 100 MW. The number of reported events has increased in recent years, though this may be the result of increased reporting of small events.

scaled sizes (\hat{S}) are calculated according to the following:

$$\hat{MW}_i = MW_i \times \frac{\text{Demand in year for event-}i}{\text{Demand in year-2000}}$$

$$\hat{Customers}_i = Customers_i \times \frac{\text{Population in year for event-}i}{\text{Population in year-2000}}.$$

Roughly these measures give the relative proportions of all demand/customers interrupted during each event.

2.4. Power-Laws

It is well known that the sizes of large blackouts in the United States follow a power-law probability distribution [73, 72, 24]. There are a number of forms of the power-law probability distribution, but one of the most commonly employed is the

Table 2.1: Power-law fit statistics, showing the parameters for the fit between the tail (largest values) of the event data and a Pareto distribution. The “fit threshold” shown below is the threshold parameter (x_{\max}) in the Pareto distribution given in eq. 2.2. The R^2 values indicate the goodness of fit to the Pareto (power-law) distribution.

<i>Data</i>	<i>Fit threshold</i>	<i>Exponent (k)</i>	R^2
Raw Customers	500,000	1.20	0.977
Scaled Customers	500,000	1.14	0.988
Raw MW	800 MW	1.19	0.997
Scaled MW	800 MW	1.15	0.997

Pareto distribution; named after Vilfredo Pareto who found that the distribution of wealth followed a power-law probability distribution. The cumulative distribution function (cdf) for a random variable x with minimum value x_{\min} , which follows a Pareto distribution, can be written as follows:

$$(2.2) \quad P(x \leq X) = 1 - \left(\frac{X}{x_{\min}} \right)^{-k},$$

where k is the scaling exponent. The probability density function (pdf) is

$$(2.3) \quad P(x = X) = \frac{kx_{\min}^k}{X^{k+1}},$$

and the expected value (mean) is

$$(2.4) \quad E[x] = \begin{cases} \frac{kx_{\min}}{k-1}, & k > 1 \\ \infty, & k < 1 \end{cases}.$$

Figure 2.2 shows the power-law relationship among the sizes of the largest events in the event size data. Table 2.1 gives the power-law fit statistics, which shows exponents (k) in the range of 1.14–1.20. The largest events in this set, particularly with size measured in MW, show an excellent fit to a power-law probability distribution ($R^2 = 0.997$ for the scaled MW data).

The existence of a power-law probability distribution is important because it indicates that large events are substantially more common than one would predict from exponential statistics such as a Gaussian or Weibull, which are commonly used in

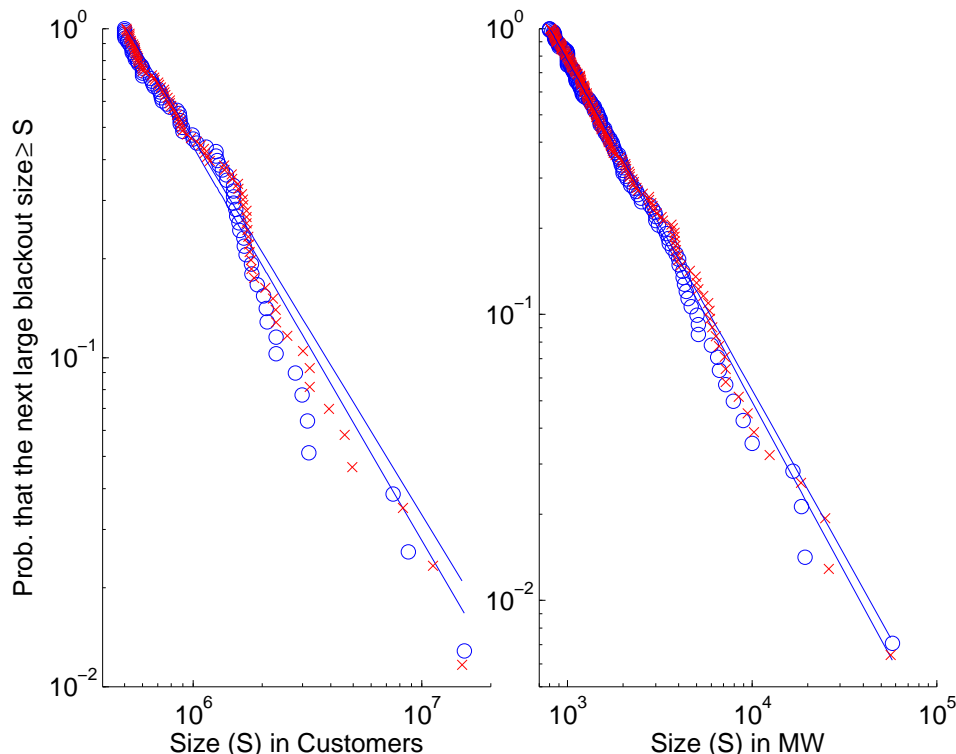


Figure 2.2: The relationship between the size and relative frequency of large blackouts in the United States, in the form of cumulative probability functions. Given that the frequency of large blackouts is not changing in time, this figure indicates the probability that the next large blackout ($\geq 500,000$ customers or ≥ 800 MW) will be greater than an arbitrary size S . “X” marks indicate data scaled to adjust for population and demand growth. “O” marks indicate unscaled data. The lines show power-law fits to each of the four sets, showing that the fit to a power-law distribution is quite good.

engineering reliability analysis. The end result is that a blackout of any size (up to the extent of the entire network) has a non-zero probability. More practically this result indicates that blackout mitigation efforts should focus on the largest events in nearly equal proportion to the smaller events. As evidence of this effect, figure 2.3 shows the relative contributions from blackouts of various sizes to the overall impact of large transmission system blackouts.⁴ Another effect of the power-law distribution is apparent when calculating the size of a 100-year blackout, using methods commonly used for storm impact assessment. Given that the sizes of large blackouts (size

⁴The impact measure shown in figure 2.3 assumes that impact, or blackout consequence, is a constant function of blackout size. Large blackouts may in fact be more costly than small ones on a per unit basis. This is particularly likely to be the case when a large blackout causes massive social disorder. For example the 1977 east coast blackout triggered wide-spread looting and chaos in New York City.

greater than 800 MW) follow a Pareto distribution with $k = 1.15$, and given that an event equal in size to Aug. 14, 2003 occurs once in every 23 years (the extent of the available data) the following gives the size of the 100 year blackout:

$$\begin{aligned} S_{23} &= 56,465 \text{ MW} \\ P_{23} &= P(S \geq 56,465) = 0.006 \\ P_{100} &= P_{23} \left(\frac{23 \text{ years}}{100 \text{ years}} \right) = 0.00138 \\ S_{100} &= 800 (10^{-\log_{10} P_{100}/1.15}) = 246,000 \text{ MW} \end{aligned}$$

By comparison, according to DOE/EIA data, the peak demand (EIA: “Net Internal Demand”) for the continental US in 2000 (the base year for the size measures) was 681,000 MW [80]. Thus, if the observed statistical pattern holds for very large blackouts, and if the US were to see a 100-year blackout next year, it would interrupt about one third of all electricity service in the continental US.

2.5. Time trends in the blackout data

This section provides an analysis of potential time trends in the blackout data for 1984-2006. Specifically, two hypotheses are tested:

- (1) There are no seasonal trends in the data.
- (2) The frequency of large blackouts has decreased with time.

The rationale for hypothesis 1 comes from the observation in [24], that seasonal trends do not exist, and the proposition that self-organized criticality provides a good explanation for the clustering that occurs in the data. The rationale for hypothesis 2 comes from the conjecture that efforts by members of the electricity industry (in terms of changes in technology and policy) have resulted in a decrease in the frequency of large blackouts.

2.5.1. Seasonal trends. Figure 2.4 shows a fairly clear bi-modal distribution in the month-by-month blackout frequency. The trend is apparent in both the “extreme

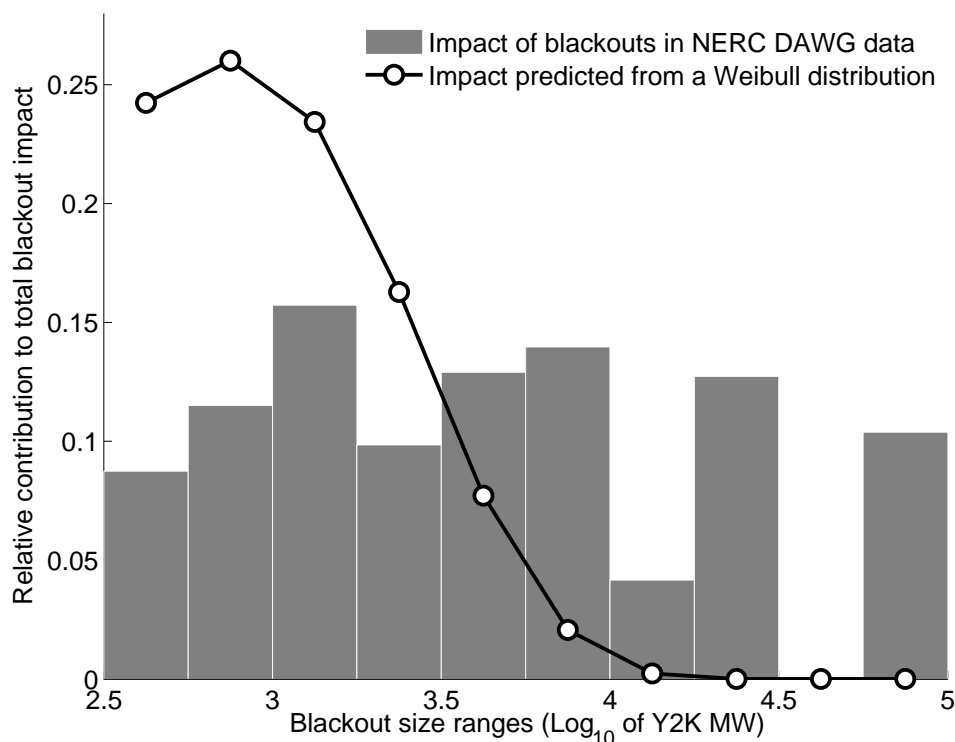


Figure 2.3: A histogram (with a logarithmic y-axis) showing the relative impact of large blackouts. Each bar shows the sum of all blackout sizes within the size range specified, divided by the sum of all event blackout sizes. The line shows the sizes that would be expected if the data were distributed according to a Weibull distribution fit to the data. Clearly, large events contribute to the overall risk much more than would be expected from exponential statistics.

event” (showing a substantial increase during hurricane season) and “other” (with increases during the hot summer months and during the winter storm season) categories. In fact a Kolmogorov-Smirnov t-test, which tests the hypothesis that two data sets come from the same distribution, shows that the difference between the periods June 1-Aug. 31 and Sept. 1-Nov. 30 is statistically significant ($P = 0.0064$). Thus the data show a statistically significant seasonal trend, indicating that the blackout risk increases and decreases seasonally. We should likely reject hypothesis 1.

2.5.2. Longer term trends in the blackout frequency. In this section we test the hypothesis that the frequency of large blackouts has decreased with time over the period 1984 to 2006. Figures 2.5 and 2.6 show the number of large blackouts,

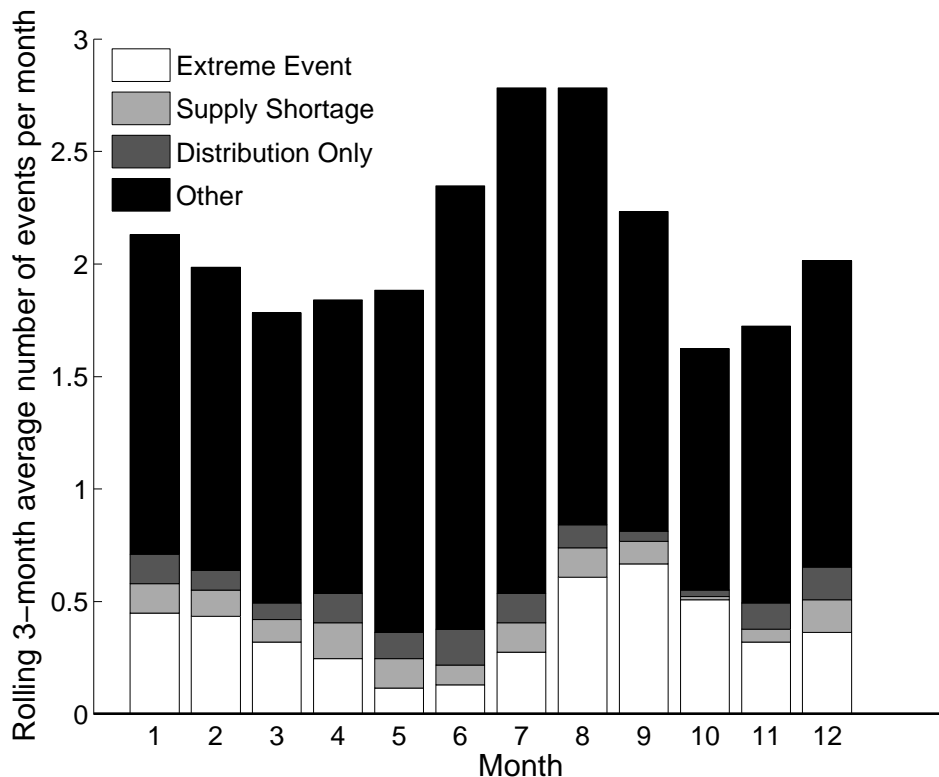


Figure 2.4: The average number of events per month from the full data set, for 3-month periods centered around each month (see [74] for a similar figure). Seasonal variation is apparent in both the “extreme event” and “other” categories.

after removing extreme events, supply shortages and distribution events. Figure 2.7 shows the impact of blackouts in the data set. This figure clearly shows the disproportionately large effect of large events on the total impact.

From these figures it is fairly clear that the overall event frequency is not decreasing. Table 2.2 shows the results of several statistical tests. By some of these measures, the frequency of large blackouts is significantly increasing, and in no case is a decrease apparent. Thus we can conclude with some confidence that the frequency of large blackouts is not decreasing, and reject hypothesis 2.

2.6. Estimating the expected cost of large blackouts

Given the statistics calculated above, one can approximate the overall cost imposed by large blackouts. After filtering out the extreme natural events, supply

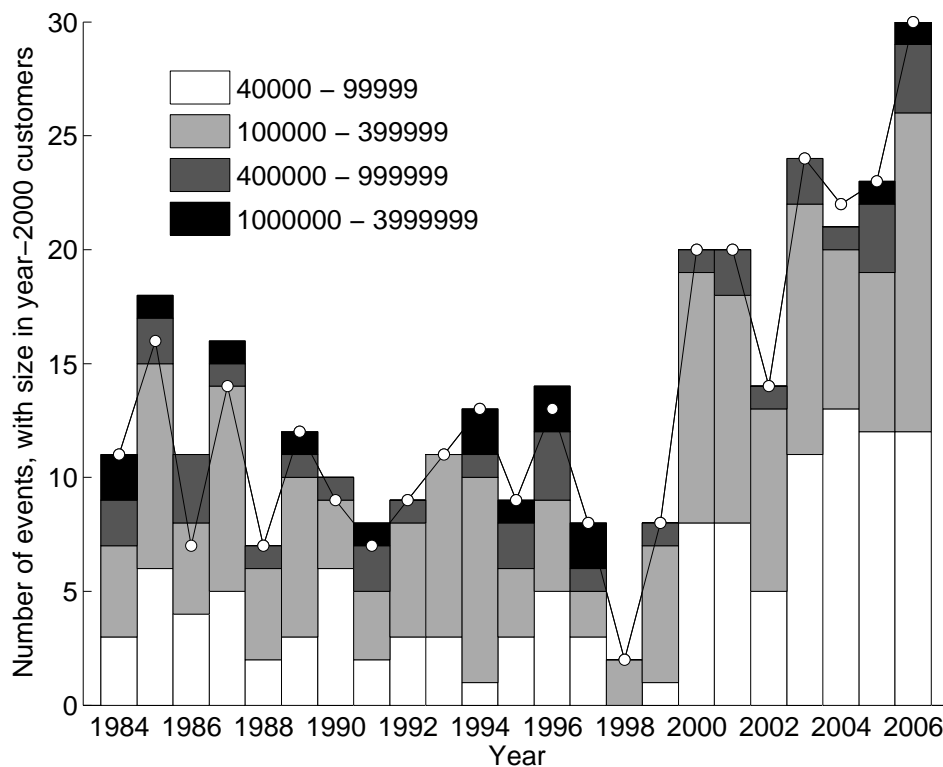


Figure 2.5: The frequency of large blackouts in the United States, with event size measured in customers interrupted. This figure shows the outages that remain after removing extreme natural events, supply shortages and distribution system blackouts. The bars show the data in number of customers interrupted, adjusted for population growth. The line shows the data before this adjustment.

Table 2.2: Results from statistical tests on the blackout data. The “Corr ρ ” column shows the correlation between year and blackout frequency (Corr P gives the significance of ρ). The K-S t-test P values result from a Kolmogorov-Smirnov t-test of the hypothesis that the early and later portions of the data come from the same statistical distribution. In several cases this hypothesis can be rejected, providing some evidence that the frequency of large blackouts is increasing. 1998 is excluded because data for this year are missing in the NERC records.

Data	Threshold	Corr ρ	Corr P	1984-1995		1996-2006, \neq '98		P from K-S t-test
				Median	Mean	Median	Mean	
cust.	50,000	0.59	0.0033	10	10.0	18	16.3	0.0468
y2k cust.	50,000	0.46	0.0285	10	10.7	15	15.3	0.1473
cust.	100,000	0.53	0.0092	7	7.1	10	10.3	0.1473
y2k cust.	100,000	0.34	0.1117	8	8.2	10	10.2	0.9852
MW	300	0.42	0.0457	8	8.5	10	10.7	0.7358
y2k MW	300	0.16	0.4573	10	9.9	10	10.6	1.0000
MW	500	0.40	0.0588	5	4.9	8	6.9	0.1473
y2k MW	500	0.09	0.6900	7	6.3	8	6.8	0.7358

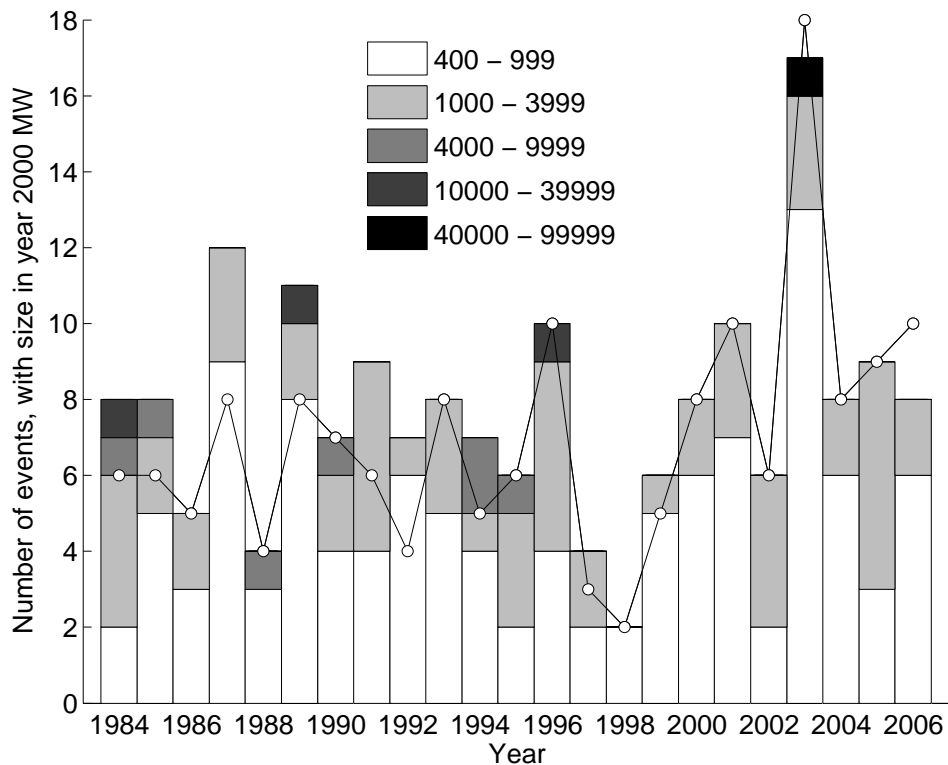


Figure 2.6: The frequency of large blackouts in the United States, with event size measured in MW demand interrupted. This figure shows the outages that remain after removing extreme natural events, supply shortages and distribution system blackouts. The bars show the data in number of customers interrupted, adjusted for demand growth. The line shows the data before this adjustment.

shortages and distribution system events this gives a close upper bound on the costs associated with large cascading failures. If we assume that the expected cost is not changing in time (the data do not indicate any such change) this measure gives an approximation of the expected cost (or risk) associated with large blackouts. While this calculation is necessarily rough, due to the coarse availability of data, it may be useful as a measure against which to compare the costs associated with policy or technical changes that aim to mitigate the frequency or impact of large blackouts. If:

- C is the discounted present value cost of all blackouts for the next 30 years,
- r is a discount rate (assumed below to be the same as the inflation rate),
- n_y is the number of blackouts in year y ,

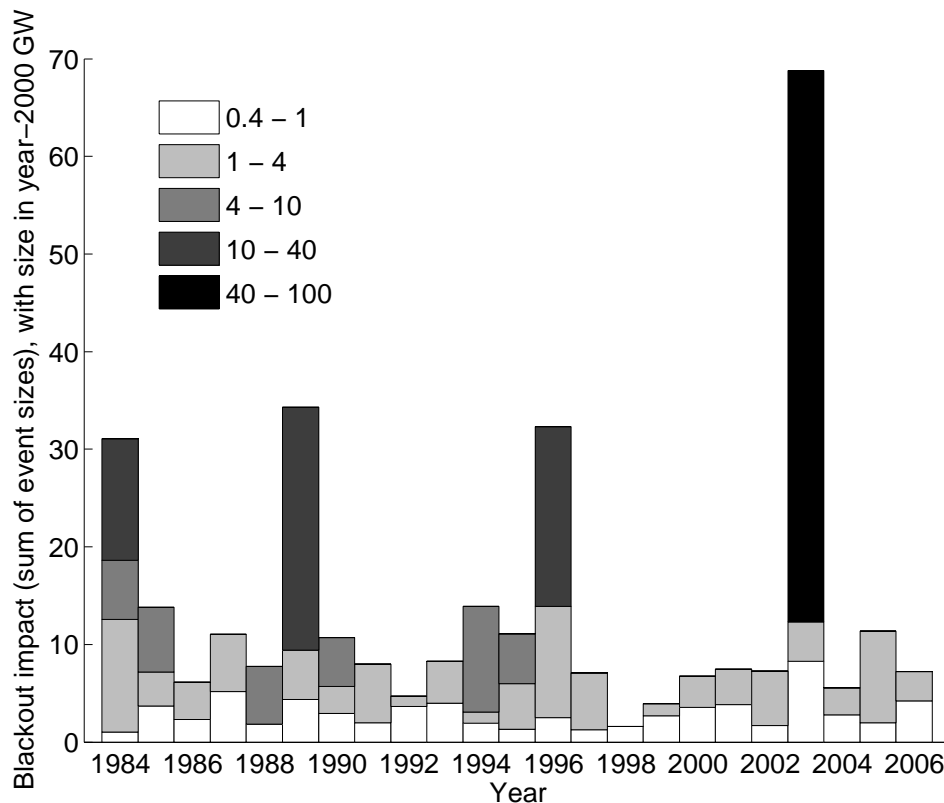


Figure 2.7: The annual impact of large blackouts in the United States, after removing extreme natural events, supply shortages and distribution system blackouts. Impact is defined here as the sum of all blackout sizes, with size measured in demand-adjusted MW, during each year.

- c_y is the average per MW cost of blackouts in year y (assuming that blackout costs scale linearly with blackout size), and
- s_{iy} is the size of blackout i in year y ,

we get the following expression for the total cost of future blackouts:

$$C = \sum_{y=1}^{30} e^{-ry} \sum_{i=1}^{n_y} c_y s_{iy}.$$

Given that we do not know n_y or s_{iy} , it is useful to consider them as random variables with probability mass/density functions $p_n(N)$ and $p_s(S)$ respectively. Assuming that n_y and s_{iy} are independent and that $p_n(N)$ and $p_s(S)$ do not vary with time, the

expected cost is:

$$E[C] = \sum_{y=1}^{30} c_y e^{-ry} E[n_y] E[s_{iy}].$$

Thus given $p_n(N)$ and $p_s(S)$ and c_y , we can calculate the expected net present cost of blackouts. Given the following assumptions:

- the arrival rate of large cascading failures (>300 MW) is distributed according to a Poisson distribution with parameter $\lambda=10$ events/year (the average for events in the “other” category),
- blackout sizes are distributed according to a Pareto distribution with exponent $k=1.15$ (see section 2.3),
- the cost of a large blackout increases linearly with blackout size in MW, at a rate of \$10,000/MW⁵ and increases with inflation, and
- the inflation rate is equal to the discount rate, reflecting a public policy perspective with a fairly low discount rate,

the overall expected cost can be calculated as follows:

$$\begin{aligned} E[C] &= \sum_{y=1}^{30} c_y e^{-ry} (10) \left(\frac{k \min(s_{ij=y})}{k-1} \right) \\ &= \sum_{y=1}^{30} e^{ry} (10,000) e^{-ry} (10) (2300) \\ &= \sum_{y=1}^{30} (10,000) (10) (2300) \\ &= (30 \text{ years}) (\$230,000,000/\text{year}) \\ &= \$6.9 \text{ billion} \end{aligned}$$

⁵Cost estimates for the Aug. 14, 2003 blackout range from \$2 to \$10 billion (see eg. [81]). This works out to about \$35,000/MW to 170,000/MW. The cost of this particular blackout was larger in part due to its location (New York City) and its duration (more than 24 hours in some locations). Smaller blackouts will typically have a smaller per MW cost. \$10,000/MW gives a fairly conservative estimate for the average per MW costs for large blackouts.

While this calculation is necessarily rough and highly sensitive to the assumptions (the total value scales linearly with the most of the uncertain parameters), it provides an estimate of the total costs associated with cascading failures. While a \$230 million annual cost is substantial, it is not as large as some other problems within the electricity industry. For example congestion charges in the PJM territory in 2004 were \$808 million [82]. A control system or policy change that reduces congestion costs in addition to reducing the risk of cascading failures would be substantially more valuable than one that only reduced the risk of cascading failures.

2.7. Explanations for the lack of improvement

Given the lack of a significant decrease in the frequency of cascading failures and given the significant investment in technologies and policies to control the risk of such failures, it is natural to look for an explanation for the existing trend (or lack thereof). Unfortunately the data alone do not provide an explanation, as the granularity is not sufficient to empirically evaluate the effects of any particular policy or technical change. Nevertheless, some discussion of the potential explanations may be useful.

2.7.1. Market restructuring. The restructuring of the electricity industry, beginning with FERC Order 888 which required open access to transmission capacity, has been blamed by numerous problems in the US electricity industry [83]. While it is likely that open access has resulted in additional use of transmission paths for long distance transfers, it is difficult to say from these data that restructuring has had a direct effect on blackout risk. Even if the increased use of transmission infrastructure has increased the risk somewhat, this explanation does not help much in providing a solution as it would be very difficult for the industry to return to a market structure with substantially less open access to transmission services.

2.7.2. Inadequate transmission investment. Industry members often assert that a lack of transmission system investment has led to unsatisfactory performance

of the transmission system. The national transmission grid study [84] notes that the frequency of transmission loading relief (TLR) events (a rough measure of system stress) has increased simultaneously while transmission system investment has decreased. Hirst [85] shows that the quantity of available transmission has over the period (1999 - 2002) has steadily decreased when normalized by summer peak demand. Vajjhala and Fischbeck [86] show that in many US states where new transmission is most needed, it is particularly difficult to build new transmission.

On the other hand, perhaps due to the attention that this issue has received, actual transmission investment has increased fairly steadily since 1999 [85]. And there are many ways to increase the capability of transmission systems without actually building new lines. Composite conductors can increase the thermal ratings, and phase-shifting transformers or FACTS devices can relieve bottleneck constraints by changing the apparent impedance of transmission lines. Finally, Blumsack [87] shows that some transmission construction can have a negative impact on reliability. While transmission investment can have a positive impact on cascading failure risk, and reliability, transmission constriction alone is a costly, and potentially ineffective, solution to reliability problems.

2.7.3. A lack of enforceable reliability rules and system-wide management. After the August 14, 2003 blackout, many in industry and government argued that the voluntary reliability rules, as established and operated by NERC, were an insufficient instrument for managing reliability in a competitive electricity industry. As a result of this discussion, the Energy Policy Act of 2005 gave FERC the authority to appoint an Electricity Reliability Organization (the role that NERC now fills), with the authority to design and enforce mandatory reliability rules nationwide.

Relatedly, Apt et al. [88] argue that insufficient system-wide management of the electricity network (similar to FAA's management of the air-traffic control system in the US) contributes to the overall blackout risk. Apt et al. argue that a systems

approach to risk mitigation has significantly reduced the accident frequency in commercial air travel, and that similar actions within the US electricity system could result in similar risk reductions.

The events of Aug. 2003 do provide some evidence that unenforceable reliability rules contributed to the cascading failure. But, since 2003 FERC and NERC have been fairly diligent in their oversight of transmission assets, and the annual number of large blackouts remains relatively constant. While systems policy changes are necessary to solving the blackout problem, they are not sufficient. The cascading failure problem is the result of both policy and technology failures.

2.7.4. System protection and problem formulation. Another explanation, argued in [89], is that the design of the protection system in electrical power networks is poorly aligned with the objectives of the system as a whole. Protective relays remove components from the network when they experience significant stress. While this approach effectively ensures that problems in the transmission system will not damage equipment, the strategy is frequently sub-optimal with respect to the goal of the system as a whole—delivering energy to customers. A better strategy would protect the equipment, while also seeking to deliver energy to customers. This thesis is an attempt to correct this problem through the design of a decentralized control system that aligns the goals of the components with the goals of the system as a whole.

2.8. Conclusions

The empirical analysis described in this chapter shows that the frequency of large blackouts in general, and cascading failures in particular, is not decreasing in the United States. The data also show a significant seasonal trend, indicating that the risk of cascading failure is a function of time varying factors such as weather and system demand. Finally, given some defensible assumptions about the costs associated with large blackouts, one can calculate that the expected social costs associated

with cascading failures in the United States is on the order of \$230,000,000 / year. While this is a significant risk, it is not as large as some other problems that face the industry. Not every solution to the cascading failure problem is appropriate to the size of the problem. However, a solution that could address other problems at the same time, such as the multi-agent control system proposed in this thesis, might be a cost-effective approach.

CHAPTER 3

Operations

This chapter adapts the general Optimal Operations Problem (OOP) to the more specific problem of reducing the social costs associated with cascading failures in electrical power networks. As defined in Chapter 1, the OOP is to maximize the net benefit from network services (defined within \mathbf{X}) that result from a stream of control actions (\mathbf{U}), given the dynamics of the network (eq. 3.2) and limits on control variables (eq. 3.3).

$$(3.1) \quad \text{OOP} \quad \underset{\mathbf{U}}{\text{Maximize}} \quad V(\mathbf{X}) - C(\mathbf{U})$$

$$(3.2) \quad \text{Subject to} \quad \mathbf{g}(\mathbf{z}_k, \mathbf{z}_{k+1}, \mathbf{e}_k) = \mathbf{0}, \forall k$$

$$(3.3) \quad \mathbf{u}_{\min}(\mathbf{u}_{k-1}) \leq \mathbf{u}_k \leq \mathbf{u}_{\max}(\mathbf{u}_{k-1}), \forall k$$

As discussed in the Introduction, power networks sometimes react to stress sub-optimally. Cascading failures are one consequence of sub-optimal stress reactions. In order to correct this error we need to carefully define a problem that could form the basis for the implementation of an architecture that would have good reflexes—one that would choose good reactions to the stress that is inevitable to occur within a complex system. This chapter presents a formulation, in the form of a Model Predictive Control (MPC) problem derived from the OOP, that aims to meet this need. Results from application of the resulting MPC problem to the IEEE 300 bus network indicate the utility of the approach. Subsequent chapters focus on ways to solve this problem through the use of control agents located throughout the power network (see Chapter 5) and provide more thorough analysis of the approach (see Chapter 6).

In addition to the MPC formulation, section 3.1 provides a high-level description of how the various components of the proposed design could fit together in a multiple layer, multiple time-scale architecture for power system operations. This general concept is not particularly original to this thesis. The conceptual design shares many properties with the structure proposed by EPRI's Intelligrid architecture [69], some of the concepts proposed in the DOE Modern Grid Initiative (MGI) [66], and some designs from the academic literature including the Strategic Power Infrastructure Defense design [65], and the hierarchical structure proposed in [90]. The general architecture is described here to show how the detailed algorithms, which are unique to this thesis, could fit into the overall task of power system operations.

The MPC problem described here is in many ways related to the Optimal Power Flow (OPF) problem, which is used by power system operators to dispatch energy resources given transmission constraints. The literature on the OPF problem is vast, and as such a review of this literature is beyond the scope of this thesis. See [13] for a textbook treatment of the subject and [91, 92] for a thorough review of the (older) OPF literature.

3.1. An Architecture for the Optimal Operation of Power Networks

The purpose of a power network is to facilitate the efficient and reliable delivery of energy for its sources to consumers. To fulfill this goal many thousands of agents, human and non-human, must act in a manner that is at least mostly in line with this goal. When they do not the results can be disastrous. To do so the components of the system need to work in a coordinated fashion along many different time horizons. In general, the agents within a power system can be categorized according to the time horizons of these actions. Table 3.1 gives a rough description of how the optimal operations problem could be implemented within different time horizons. This work is primarily focused on solving problems that act along time horizons with seconds to a few minutes, through the use of decentralized control methods. But, many of the

concepts described in this chapter could be useful in the design of control methods that operate along longer, or potentially even shorter, time horizons.

The proposed design for power system operations has three interaction layers. The lower layer is the physical power system, along with all of its existing components. The top layer is the existing network of human operators, who interact with the power system relatively slowly, making control plans over relatively long time horizons. Between these two layers is a set of control agents, one per node (substation) in the power network, which operate with shorter time horizons and work cooperatively to make short-term corrections to the control plans decided upon by the power system operators. Given the design proposed in this chapter and in Chapter 5, the agents do not make any changes to the operators' control plans unless the system is particularly stressed. When the agents sense extreme stress they operate to mitigate that stress. More specifically, the following lists the actions that operators and decentralized control agents would need to take to enact the proposed design, along each time horizon listed in table 3.1:

- (1) (*months-years*) Policy makers and operators make decisions as to how load reduction costs will be set. If this is not done carefully, some control areas could set costs very high, causing a disproportionate risk to neighboring demand.
- (2) (*hours-days*) Operators choose settings for distributed control agents and transmit these settings to the agents.
- (3) (*minutes*) Operators run a version of the long horizon (minutes) stress mitigation problem (see below) when the system undergoes potentially dangerous stress. The solution of this problem may need to be coordinated with neighboring operators, thus providing a need for a coordinated optimization approach. Future work may look at the potential to apply the proposed approach to decentralized MPC to this problem.

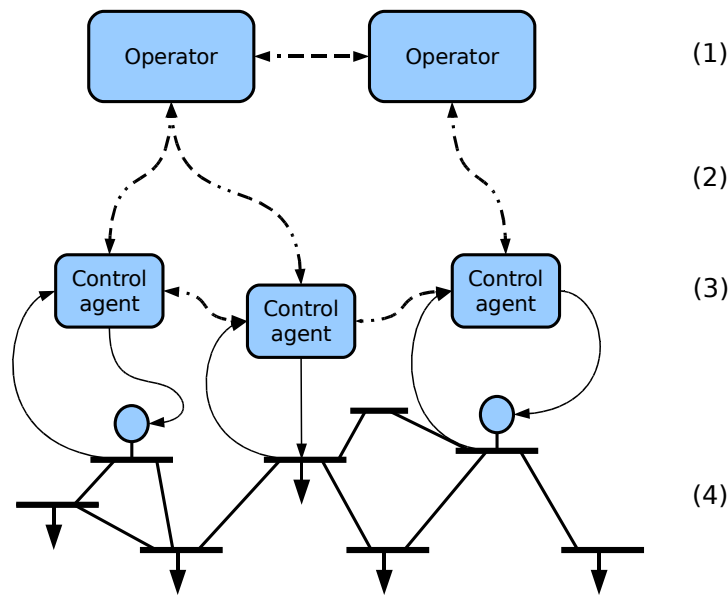


Figure 3.1: A depiction of the proposed power system operations architecture. In this design, centrally located operators (1) set schedules for devices according to some version of the OOP with fairly long time horizons (minutes-hours). These schedules are transmitted to control agents (3), located at many or all buses in the power network, over a communications channel (2). The control agents collect local measurements and make emergency adjustments to local control variables based on a version of the OOP with short time horizons (seconds-minutes). The power network infrastructure (4) remains essentially unchanged; the agents operate with the existing control and measurement hardware.

- (4) (*seconds*) When a power network undergoes extreme stress that operators would not otherwise have time to respond to (response required within seconds to a few minutes), DMPC agents, operating according to reciprocal altruism, calculate and implement emergency control actions. The actions would be approximately equal to those that would be calculated via the full SMP described below.
- (5) (*sub-second*) Future work may look at ways to coordinate agent actions with the settings of high speed devices such as fault protection relays and high speed power electronics. For the time being the agents take these settings as given.

Table 3.1: Time horizons for power network operations and MPC applicability

<i>Time horizon</i>	<i>Description</i>	<i>Relationship to the current problem</i>
(1) Months - Years	Planning and investment. Policy design.	The planning problem is outside the scope of this work, though a rolling horizon/MPC approach may be a useful way to think about some long time-horizon planning problems.
(2) Hours - days	Resource scheduling, market operations	Resource scheduling can be included in the OOP, though this work focuses on the shorter time scale problems. Within this time period operators will need to occasionally communicate settings to the OOP agents which implement the control method described in this thesis. A rolling horizon approach to the scheduling problem can be very useful—the unit commitment problem is one example application.
(3) minutes - 1/2 hour	Resource schedule adjustments	Within this time horizon, energy resources can be rescheduled to relieve local problems from central facilities. The MPC problem presented in this chapter could be applied to this task, though it is intended for the shorter time-horizon below.
(4) 1 second - minutes	Emergency stress management	Within this shorter time horizon voltage collapse problems occur, zone 3 and time over-current relays trip and heavily loaded lines sag into trees. The methods described in this thesis focus on this time horizon, though because centrally located operators cannot observe large networks within this horizon, centrally operated stress management is often impractical.
(5) Sub-second - sub-cycle	Dynamic power system control and protection	Within this time horizon, control decisions must be made in a completely decentralized manner according to simple control laws. An MPC approach, given current technology, is probably not applicable to problems within this time horizon, though future work may look at how DMPC agents could coordinate with such high-speed controllers.

3.2. The Optimal Stress Mitigation Problem for Power Networks

This section adapts the rather general optimal operations problem to the specific problem of controlling cascading failures in electrical power networks. In words the problem is to calculate a set of control actions, to be implemented over a time horizon, that would result in minimal social costs, given the current state of the network and the continuous and discrete dynamics of the network. Cascading failures are

largely a property of the discrete dynamics of power networks. There are a number of ways to account for discrete dynamics in this problem. One approach would be to build a model that can predict the switching actions (discrete events) resulting from persistent stress in the network. A second approach would be to design the formulation to choose control actions that prevent state variables from crossing the thresholds that would initiate a switching event. There are a number of advantages to the first approach, including the potential to arrive at less expensive control actions. For example, given a model with good predictive capabilities, the system may be able to determine that allowing relays to interrupt one line (or perhaps implementing this actions directly) will restore the system to a “normal” state, eliminating the need for expensive mitigating control actions, such as load shedding. On the other hand, in the context of an MPC problem, discrete predictive models require a mixed integer programming approach that may make the problem difficult to solve within an acceptable time period, and may not be particularly accurate, particularly given the modeling errors that will come with a decentralized approach to the problem. For this reason, the optimal stress mitigation problem (SMP) detailed below roughly follows the second approach; the control problem is designed to choose actions that prevent switching actions when possible.

Sections 3.2.1 through 3.2.5 below describe the objective, stress variables, state variables, control variables, and dynamic constraints that make up the adaptation of the Optimal Operations Problem to the task of controlling cascading failures. The resulting formulation is referred to as the optimal stress mitigation problem (SMP) and is described in full in sections 3.2.6 and 3.2.7.

3.2.1. Objective. The objective in the OOP is to maximize the benefit from electricity service net the costs associated with providing this service. In the economics literature this objective is known as “social welfare” maximization [93]. Because the SMP focuses on the shorter time horizon aspects of the OOP, it starts with the assumption that the current schedule is optimal with respect to the more long-term

goals of the system, so long as the stress variables are below their emergency thresholds. When the stress variables cross thresholds above (or below) which relay actions are likely, the current operating point is no longer assumed to be optimal.

From this perspective, the objective can be written as a cost minimization function with three terms (eq. 3.5). The result is essentially equivalent to the original OOP objective (eq. 3.4), but with the opposite sign.

$$(3.4) \quad \underset{\mathbf{U}}{\text{Maximize}} \quad V(\mathbf{X}) - C(\mathbf{U})$$

$$(3.5) \quad \underset{\mathbf{U}}{\text{Minimize}} \quad C_u(\mathbf{U}) + C_d(\mathbf{X}) + C_s(\mathbf{X})$$

The first term estimates the cost of control actions ($C(\mathbf{U})$ in eq. 3.4) and the second and third terms estimate losses to the benefits of services provided by of the network (losses to $V(\mathbf{X})$ in eq. 3.4). The first term, $C_u(\mathbf{u}_k, \mathbf{u}_{k+1})$, gives the control costs associated with making changes to the various controllers in the system (generator outputs, circuit breakers, etc.). The second, $C_d(\mathbf{x}_{D,k}, \mathbf{x}_{D,k+1})$, gives the social costs (or lost benefit) associated with demand curtailment resulting from control actions. (Real power demand at time k is given by $\mathbf{x}_{D,k}$, where D in this case is the set of all x associated with real power consumption at time t_k , i.e. $\mathbf{x}_{D,k} = \mathbf{P}_{D,k}$.) The third term, $C_s(\mathbf{y}_k, \mathbf{y}_{k+1})$, where \mathbf{y}_k is a set of stress variables and a function of \mathbf{x}_k , approximates the costs associated with allowing stress variables to persist above their thresholds. In order to give the system some preference for delayed control actions the objective function uses a discounted sum of the predicted costs over the time horizon, with discount factors: $\rho^0, \rho^1, \dots, \rho^{K-1}$. Eq. 3.6 shows the combined objective function

and eqs. 3.7-3.9 describe some of its properties in more detail.

$$(3.6) \quad \underset{\mathbf{U}=[\mathbf{u}_0, \mathbf{u}_1, \dots, \mathbf{u}_K]}{\text{Minimize}} \quad \sum_{k=0}^{K-1} \rho^k (C_u(\mathbf{u}_k, \mathbf{u}_{k+1}) + C_d(\mathbf{x}_{D,k}, \mathbf{x}_{D,k+1}) + C_s(\mathbf{y}_k, \mathbf{y}_{k+1}))$$

$$(3.7) \quad C_u(\mathbf{u}_k, \mathbf{u}_{k+1}) \begin{cases} = 0 & \text{if } \mathbf{u}_k = \mathbf{u}_{k+1} \\ > 0 & \text{otherwise} \end{cases}$$

$$(3.8) \quad C_d(\mathbf{x}_{D,k}, \mathbf{x}_{D,k+1}) \begin{cases} = 0 & \text{if } \mathbf{x}_k = \mathbf{x}_{k+1} \\ \neq 0 & \text{otherwise} \end{cases}$$

$$(3.9) \quad C_s(\mathbf{y}_k) \begin{cases} = 0 & \text{if } \mathbf{y} \in [\mathbf{y}_{\min}, \mathbf{y}_{\max}] \\ > 0 & \text{otherwise} \end{cases}$$

Under normal conditions, where none of the stress variables exceed their thresholds, 3.9 evaluates to zero. All of the cost functions are designed to evaluate to no less than zero, thus making it sub-optimal to change the control variables in the unstressed condition. When the control variables do not change eq. 3.7 evaluates to zero and, given a fairly simple dynamic model $x_{D,k} = x_{D,k+1}$ will be true and eq. 3.8 will also evaluate to zero. The result is that the optimal solution to SMP when $y \in [y_{\min}, y_{\max}]$ is to make no changes to the control variables, i.e.:

$$y_0 \in [y_{\min}, y_{\max}] \Rightarrow \mathbf{u}_{k+1} = \mathbf{u}_k, \forall k \in \{0, \dots, K-1\}.$$

3.2.2. Stress variables. Stress variables are those that could trigger a relay action if allowed to persist outside of the threshold values. When the stress variables are a linear function of the state variables (as is the case in the models used here) we get:

$$\mathbf{y}_k = \mathbf{C}\mathbf{x}_k,$$

which is the output equation in a linear state-space model.

There are many power system variables that could be included in the stress variable category. Among these include:

- Apparent (complex) impedance ($Z = V/I$): a measure used by distance relays to detect and interrupt faults. A distance relay will open when Z approaches the origin (the actual threshold depends on the relay, and its settings).
- Measured, or calculated proximity of transmission lines to vegetation. This metric can be estimated through the use of temperature and current measurements or through the use of sensors along the transmission path.
- Measured transformer temperature. Many transformers have relays with temperature thresholds.
- Frequency or machine rotational speed (ω). Generators typically include relays that will disconnect the machine when the rotational speed or the measured bus voltage frequency deviates from the nominal value. Generators may also have out-of-step relays that trip the machine when its machine rotational angle diverges substantially from the measured bus voltage angle.
- Branch current magnitude ($|\mathbf{I}|$). While not all transmission lines include over-current protection, very high currents quickly cause lines to sag (or transformers to overheat), which can trigger a relay action. High currents also move the apparent impedance toward the origin, increasing the chance of a distance relay trip, particularly when transmission lines include time-delayed zone 3 (backup) distance relays.
- Bus voltage magnitude ($|\mathbf{V}|$). Low voltages increase the risk of voltage collapse¹, increase the likelihood of a distance relay trip, and result in degraded service.

¹Voltage collapse occurs (essentially) when the power being transferred from one end of a line to the other approaches a theoretical maximum. As the power transfer increases the voltage magnitude typically decreases until it approaches the edge of what is known as the nose curve (see [94, p. 45]).

As currently implemented, the SMP formulation uses the following sets of variables: (1) voltage magnitudes at all non-generator buses $|\mathbf{V}_{\bar{G}}|$, (2) branch current magnitudes $|\mathbf{I}|$ (see section 3.2.2.1 for a discussion of why and how current magnitudes should be used as a measure of branch flow in OPF-like problems, rather than real or apparent power flow), and (3) a measure of frequency deviation ($\Delta\theta_r$, or the change in the voltage phase angle at the reference/slack bus) that comes out of the AC power-flow equations. With these stress variables, we can write the complete stress vector as follows:

$$y = \begin{bmatrix} |\mathbf{V}_{\bar{G}}| \\ |\mathbf{I}| \\ \Delta\theta_r \end{bmatrix}.$$

The stress thresholds ($|\mathbf{V}|_{\min}$ and $|\mathbf{I}|_{\max}$) are calculated and set by the operator, and therefore are treated as an exogenous variable to our problem. $\Delta\theta_r$ is limited on both sides at zero at every time step.

During most of the recent large cascading failures high currents combined with low voltages caused numerous distance relays to trip. Zone 3 (backup) distance relays typically operate with time delays greater than 1 second, and can trip when the transmission line is very heavily loaded, but is not feeding an actual fault. Maintaining currents and voltages below the zone 3 thresholds can greatly reduce the likelihood of a large cascading failure. Similarly, low voltages can cause significant stress on the system, in addition to increasing the likelihood of a distance relay trip. One of the key recommendations of the US-Canada Power System Outage Task Force, which investigated the Aug. 14, 2003 blackout [2], was to improve the practices of under-voltage load shedding and reactive power management. The inclusion of voltage magnitude as a stress variable effectively results in an implementation of this recommendation.

3.2.2.1. *On the use of current magnitude as a measure of branch flow.* This section provides some explanation of why (and how) one should use branch current magnitude

as a measure of branch flows in OPF-like power-systems problems, as opposed to measures based upon the measured power-flow on the branch. It is thus a minor diversion from the text, but the results are used in later sections within this chapter.

For mostly historical reasons most optimal power flow (OPF) formulations use branch apparent power ($|S_{ij}| = |V_i I_{ij}^*|$) or real power ($P_{ij} = \Re(V_i I_{ij}^*)$) as measures of branch flow, for which limits are set. Both are rather arbitrary, and potentially misleading, measures to use. The branch current magnitude provides a better measure because (in most cases) it corresponds more closely to the risk associated with a branch being taken out of service due to an overload. When a transmission line sags into a tree, it does so because the line has heated (due to $I^2 R$ losses) and stretched to the point at which it made contact with a grounded structure or vegetation. In an extremely stressed system, if a branch exceeds its zone 3 distance limit, it does so essentially because the ratio of current to voltage ($|I|/|V|$) had crossed a threshold. When distance relays are used, the branch moves closer its limits as $|V|$ decreases, and as $|I|$ increases. If we use either power-based measure of branch flow ($|S_{ij}|$ or P_{ij}) to assess proximity to the physical limit, the measure will decrease as the voltage decreases—indicating that the branch is moving away from the limit when it is actually moving in the opposite direction. Since the branch current magnitude is mostly independent of voltage, it lacks this misleading aspect.

In order to use the branch current magnitude in an OPF-like optimization problem (such as the SMP described here) one needs the derivatives with respect to other measurable variables in the problem; in this case the voltage magnitudes on both ends of the branch and the phase angle difference between the two ends of the branch. We can compute these derivatives by writing the branch current in phasor form and using some properties of triangles.

Given two buses (a and b) with voltages $V_a = |V_a|e^{j\theta_a}$ and $V_b = |V_b|e^{j\theta_b}$, and defining admittance values $y_{aa} = |y_{aa}|e^{j\phi_{aa}}$ and $y_{ab} = |y_{ab}|e^{j\phi_{ab}}$ such that the complex

current at bus a headed toward bus b is

$$I_{ab} = y_{ab}V_a + y_{ab}V_b = |y_{aa}||V_a|e^{(\phi_{aa}-\phi_{ab}+\theta_a-\theta_b)} + |y_{ab}||V_b|,$$

we can draw a triangle with one known angle, and the length of all three sides known. If side a has length $a = |y_{aa}||V_a|$, side b : $b = |y_{ab}||V_b|$, side c is the current magnitude: $c = |I_{ab}|$, and the angle opposite the current magnitude is C : $C = \pi - (\phi_{aa} - \phi_{ab} + \theta_a - \theta_b)$, where $\delta_{ab} = \theta_a - \theta_b$, by the law of cosines ($c^2 = a^2 + b^2 + 2ab \cos C$) we can calculate the derivatives that we need for the OPF problem

$$(3.10) \quad \frac{\partial c}{\partial a} = \frac{a - b \cos C}{c} \Rightarrow$$

$$(3.11) \quad \frac{\partial |I_{ab}|}{\partial |V_a|} = \frac{|y_{aa}|^2 |V_a| - |y_{aa}||y_{ab}||V_b| \cos(\pi - (\phi_{aa} - \phi_{ab} + \theta_a - \theta_b))}{|I_{ab}|}$$

$$(3.12) \quad \frac{\partial c}{\partial b} = \frac{b - a \cos C}{c} \Rightarrow$$

$$(3.13) \quad \frac{\partial |I_{ab}|}{\partial |V_b|} = \frac{|y_{ab}|^2 |V_b| - |y_{aa}||y_{ab}||V_a| \cos(\pi - (\phi_{aa} - \phi_{ab} + \theta_a - \theta_b))}{|I_{ab}|}$$

$$(3.14) \quad \frac{\partial c}{\partial C} = \frac{ab \sin C}{c} \Rightarrow$$

$$(3.15) \quad \frac{\partial |I_{ab}|}{\partial \delta_{ab}} = -\frac{|y_{aa}||y_{ab}||V_a||V_b| \sin(\pi - (\phi_{aa} - \phi_{ab} + \theta_a - \theta_b))}{|I_{ab}|}$$

Figure 3.2 describes the locations of these variables graphically.

With these derivatives (eqs. 3.10-3.15) we can calculate the sensitivity of a given branch current magnitude to changes in the parameters on either end of the line, and thus calculate how small changes in the network will effect the branch current magnitudes. These derivatives are used in the linear MPC formulation described in section 3.2.7.

3.2.3. State variables. While there are many variables that could be included in the SMP, the SMP as implemented here includes voltage magnitudes ($|\mathbf{V}|$), voltage phase angles (θ), current magnitudes ($|\mathbf{I}|$), and real and reactive power consumption ($\widehat{\mathbf{P}}_D$, $\widehat{\mathbf{Q}}_D$ as opposed to actual demand, which is \mathbf{P}_D and \mathbf{Q}_D) at each load in the

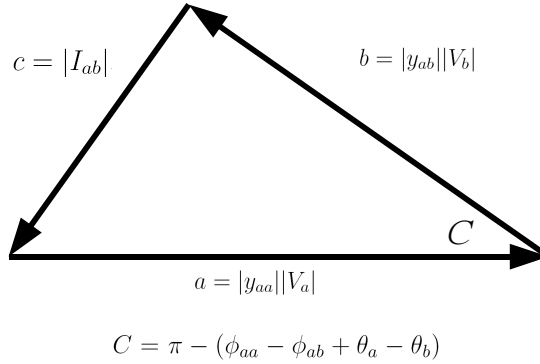


Figure 3.2: The derivatives of branch current magnitude with respect to bus voltage magnitudes and angles can be found by writing the equation $I_{ab} = y_{aa}V_a + y_{ab}V_b$ in phasor form. The diagram above illustrates the two phasors and their sum (I_{ab}). a , b , and c represent the phasor magnitudes and C the angle between the two initial phasors. In phasor form one can see how a change in $|V_a|$, $|V_b|$, or $\theta_a - \theta_b$ would affect the current magnitude $c = |I_{ab}|$.

system. When combined the state vector has the following values:

$$\mathbf{x} = \begin{bmatrix} \theta \\ |\mathbf{V}| \\ |\mathbf{I}| \\ \widehat{\mathbf{P}}_D \\ \widehat{\mathbf{Q}}_D \end{bmatrix}.$$

In actual implementation, the voltage state variables are limited to those that are not located at generator buses ($|\mathbf{V}_{\overline{G}}|$), but the notation is somewhat simpler in the above form. The SMP formulation does not explicitly limit the state variables, but limits do result from constraints on control and stress variables.

3.2.4. Control variables. The number of control variables that could be included in this problem is enormous. Table 3.2 lists some of these. This work focuses on the use of real power output from generators (\mathbf{P}_G), voltage magnitude set points at generator buses ($|\mathbf{V}_G|$, adjusted using machine excitation controls), and demand reduction (changes to \mathbf{S}_D). Demand reduction is controlled through a continuous variable in the range zero to one ($\mathbf{\Lambda}$), referred to as the “demand reduction factor.” The

demand reduction factors reduce the demand according to the following relationships:

$$\begin{aligned}\widehat{\mathbf{P}}_D &= \mathbf{\Lambda} \odot \mathbf{P}_D, \Lambda_i \in [0, 1], \forall i \\ \widehat{\mathbf{Q}}_D &= \mathbf{\Lambda} \odot \mathbf{Q}_D, \Lambda_i \in [0, 1], \forall i\end{aligned}$$

(where \odot represents an element-wise product of two vectors). Λ_i could be an integer variable in a mixed integer formulation and represent the status of a feeder circuit-breaker for a given distribution circuit. In this implementation, Λ_i is assumed to be continuously adjustable in the $[0, 1]$ range. While this assumption is not always precisely correct, from the perspective of a large transmission substation this is a reasonable approximation of actual behavior. A large transmission substation with demand connected, will typically feed many distribution feeders with at least one circuit breaker on each feeder. By choosing to switch a subset of these circuit-breakers demand can be set to a fairly large range of values between zero and the full amount. Additionally, there is growing interest in appliances (air conditioners or electric water heaters for example) with intelligent controllers that can be switched on and off through signals on a communication channel, such as the Internet (see for example Borenstein et al. [95]). With a sufficient number of these devices on a circuit, the continuous load reduction assumption is certainly reasonable.

Control variables in this problem can have two types of limits. All of the control variables have absolute limits (for example a generator can produce no more than P_{\min} MW and no more than P_{\max} MW). Most of the variables will also have limits on the amount that the variable can change within a time range. For example a generator can only increase or decrease within the time step $[t_k, t_{k+1}]$ according to its ramp rate. The control limits are written in generic form as follows:

$$\begin{aligned}\mathbf{u}_{\min} &\leq \mathbf{u}_k \leq \mathbf{u}_{\max} \\ \Delta \mathbf{u}_{\min} &\leq \mathbf{u}_{k+1} - \mathbf{u}_k \leq \Delta \mathbf{u}_{\max}.\end{aligned}$$

Table 3.2: Control variables that could be included in the stress mitigation problem. Those that are employed in this study are indicated with an asterisk*.

<i>Control Variable</i>	<i>Notes</i>
Real power output from generators*	Output can be reduced quickly using fast valving or a breaking resistor. Output power can also be increased, but more slowly.
Reactive power output from generators	Adjusted through the use of exciter control systems. Reactive output can be changed quickly relative to real power.
Generator voltage set points*	Requires adjustment of exciter set points as above.
Circuit breaker statuses	Located on transmission lines, transformers, distribution feeder circuits, etc. Circuit breakers can be switched quickly.
Transformer tap changers	If a phase-shifting transformer is used, tap changers can change power transfer along a line. Otherwise changes the voltage ratio. Changes can be implemented in a few seconds.
Load served by a substation*	Controlled through circuit breakers or other intelligent, demand-side devices. Changes can be affected quickly given the appropriate control and communications infrastructure.
Reactive power output from reactive power sources	Could include switched capacitors, synchronous var compensator's, or power-electronic devices with reactive power production capabilities. All can be switched quickly.
Power electronic flow-control device settings (FACTS devices)	Flow-control FACTS devices have a wide variety of settings, including real and reactive power flows, that could be included in this problem. Ref. [63] describes a SMP-like method for FACTS control. FACTS device changes can be implemented within cycles.

3.2.5. Dynamic constraints. The dynamic constraints in the OOP have the following form:

$$\mathbf{G}(\mathbf{u}_k, \mathbf{x}_k, \mathbf{e}_k, \mathbf{x}_{k+1}) = \mathbf{0}, k = 0, 1, \dots, \infty.$$

While one may not know the exogenous variables (\mathbf{e}_k) exactly for time t_0 , their behavior in future time steps is uncertain by definition, thus making \mathbf{e}_k a random variable for $k \in \{0, \dots, K\}$. There are a number of ways to model the random variables in \mathbf{e}_k . A common approach in feedback-based control system design is to assume that \mathbf{e}_k does not change over the time horizon ($\mathbf{e}_k = \mathbf{e}_{k+1}$) and to design the controller to compensate for unpredicted changes through feedback. Alternatively, stochastic programming can be used to explicitly model the effects of the random variables. For the sake of simplicity the former approach is used in this paper. The stochastic programming approach is a potential direction for future research. Thus ignoring

future changes in the exogenous variables, the dynamic constraint has the following simplified form:

$$\mathbf{G}(\mathbf{u}_k, \mathbf{x}_k, \mathbf{e}_0, \mathbf{x}_{k+1}) = \mathbf{0}, \quad k = 0, 1, \dots, \infty.$$

While a full machine-rotor dynamic model could be of some benefit to the SMP formulation, cascading failures generally begin well before machine rotor-angles begin to change rapidly. During early portions of a cascading failure, the AC power-flow equations provide a reasonable basis for approximating the network's reactions to various changes. Because the AC power flow constraints are memory-less, only the variables for time t_k show up in the set of constraints for time t_k . The time-dependence shows up in the constraints associated with the control variables. In complex form, the AC power-flow constraints have the following form:

$$(3.16) \quad \mathbf{S}(\mathbf{u}_k, \mathbf{x}_k) = \mathbf{V}(\mathbf{u}_k, \mathbf{x}_k) \odot (\mathbf{Y}_{BUS}(\mathbf{e}_k) \mathbf{V}(\mathbf{u}_k, \mathbf{x}_k)^*),$$

where \mathbf{S} is the vector of complex power injections resulting from generation and demand. The system impedance matrix (\mathbf{Y}_{BUS}) is shown as a function of the exogenous variables, because random transmission line faults will result in changes to the configuration of the network, and thus the \mathbf{Y}_{BUS} matrix. In order to more precisely show the equations, it is useful to write eq. 3.16 in their sine-cosine form:

$$(3.17) \quad P_i = |V_i| \sum_{j=1}^{n_V} (g_{ij}|V_j| \cos(\theta_i - \theta_j) + b_{ij}|V_j| \sin(\theta_i - \theta_j))$$

$$(3.18) \quad Q_i = |V_i| \sum_{j=1}^{n_V} (g_{ij}|V_j| \sin(\theta_i - \theta_j) - b_{ij}|V_j| \cos(\theta_i - \theta_j))$$

If bus i is a voltage controlled generator bus (if $i \in G$), $|V_i|$ and P_i are decision variables in \mathbf{u}_k and θ_i and Q_i are state variables in \mathbf{x}_k . Otherwise (if $i \notin G$), $|V_i|$ and θ_i are state variables. When there is load at a bus i , P_i and Q_i can be controlled by adjustments to Λ_i . At the reference bus, which is a member of G , the phase angle is loosely fixed at zero ($\theta_r = 0$) through the use of the θ_r as a stress variable.

3.2.6. Non-linear Stress Mitigation Problem (SMP). By combining the above components we can write the stress mitigation problem for power networks in non-linear form:

$$\begin{aligned}
 \text{Minimize}_{\mathbf{U}} \quad & \sum_{k=0}^{K-1} \rho^k (C_u(\mathbf{u}_k, \mathbf{u}_{k+1}) + C_d(\mathbf{x}_{D,k}, \mathbf{x}_{D,k+1}) + C_s(\mathbf{y}_k, \mathbf{y}_{k+1})) \\
 \text{Subject to} \quad & P_{ik}(P_{Gk}, \widehat{P_{Dk}}) = \\
 & |V_{ik}| \sum_{j=1}^{n_b} (g_{ij}|V_{jk}| \cos(\theta_{ik} - \theta_{jk}) + b_{ij}|V_{jk}| \sin(\theta_{ik} - \theta_{jk})), \forall i \in \{1, \dots, n_V\} \\
 & Q_{ik}(Q_{Gk}, \widehat{Q_{Dk}}) = \\
 & |V_{ik}| \sum_{j=1}^{n_b} (g_{ij}|V_{jk}| \sin(\theta_{ik} - \theta_{jk}) - b_{ij}|V_{jk}| \cos(\theta_{ik} - \theta_{jk})), \forall i \in \{1, \dots, n_V\} \\
 & \widehat{\mathbf{P}}_D = \mathbf{\Lambda} \odot \mathbf{P}_D, \Lambda_i \in [0, 1], \forall i \in D \\
 & \widehat{\mathbf{Q}}_D = \mathbf{\Lambda} \odot \mathbf{Q}_D, \Lambda_i \in [0, 1], \forall i \in D \\
 & |I_i| = |y_{a_i b_i} V_{a_i} + y_{a_i b_i} V_{b_i}| \quad \forall i \in \{0, \dots, n_I\} \\
 & \mathbf{u}_{\min} \leq \mathbf{u}_k \leq \mathbf{u}_{\max} \\
 & \Delta \mathbf{u}_{\min} \leq \mathbf{u}_{k+1} - \mathbf{u}_k \leq \Delta \mathbf{u}_{\max}.
 \end{aligned}$$

The objective is the same as the one given in section 3.2.1. The first two constraints show the AC power-flow equations. The second pair of constraints limit the extent to which demand can be controlled at each bus. The branch current constraint defines the branch current magnitude. In this constraint a_i and b_i are the bus indices on either end of branch i . The final two constraints represent the generic control limits for each time step. In actual implementation these will include upper and lower bounds on the real power output of generators, bounds on the $\mathbf{\Lambda}$ vector, and bounds on the generator bus voltage magnitudes. Also included are bounds on the extent to which generator real power output can ramp up or down (actually generators are limited to only ramp down), and on the extent to which generator bus voltages can

increase or decrease within a time step. The effect of this latter limit is explored in the results given below.

While the non-linear form is relatively general, the solution of the problem becomes difficult to solve in reasonable time for larger networks. On the other hand, because the SMP is defined along discrete time steps, it is fairly straight-forward to linearize the AC power flow equations given around the measured operating point $(\mathbf{x}_0, \mathbf{u}_0)$ and formulate a linear MPC problem. The linear formulation is substantially easier to solve, and allows one to use linear algebra to remove unimportant portions of the problem before attempting to solve it. The linearized approach is described below, and the details of the decomposition method, which includes a discussion of problem reduction methods, are discussed in some detail in Chapter 5.

3.2.7. Linear formulation of SMP. This section describes the means by which the non-linear SMP can be formulated as a linear time-varying (LTV) MPC problem. If we define $\Delta \mathbf{z}_k = \mathbf{z}_{k+1} - \mathbf{z}_k$ (and similarly for each sub-vector in the problem), the linear MPC problem takes the following generic form (LSMP):

$$(3.19) \quad \underset{\mathbf{U}}{\text{Minimize}} \quad \sum_{k=0}^{K-1} \rho^k (\mathbf{c}_U^T |\Delta \mathbf{u}_k| + \mathbf{c}_X^T |\Delta \mathbf{x}_k| \dots$$

$$(3.20) \quad + \mathbf{c}_Y^T \max(\mathbf{y}_{\min}(k) - \mathbf{y}_k, \mathbf{y}_k - \mathbf{y}_{\max}(k), \mathbf{0}))$$

$$(3.21) \quad \text{Subject to} \quad \mathbf{A}(\mathbf{x}_0, \mathbf{u}_0) \Delta \mathbf{x}_k = \mathbf{B}(\mathbf{x}_0, \mathbf{u}_0) \Delta \mathbf{u}_k$$

$$(3.22) \quad \mathbf{y}_k = \mathbf{C} \mathbf{x}_k$$

$$(3.23) \quad \mathbf{u}_{\min} \leq \mathbf{u}_k \leq \mathbf{u}_{\max}$$

$$(3.24) \quad \Delta \mathbf{u}_{\min} \leq \Delta \mathbf{u}_k \leq \Delta \mathbf{u}_{\max}$$

This formulation is a slight modification of the standard MPC formulation with a linear state-space plant model, and a linear objective function.

The absolute value and $\max(\dots)$ terms in the objective function can be implemented in a linear program (LP) through the use of slack variables. As this is a fairly

common method in LP design, the implementation details are not described in detail here. The cost vectors in eq. 3.19 come from the costs associated with changes to generator power output and voltage set points (\mathbf{c}_U), decreases in the actual demand served (\mathbf{c}_X), and stress costs (\mathbf{c}_Y) which would need to be set by operators. The dynamic constraints (\mathbf{A} and \mathbf{B}) give a linearization of the equality constraints in the non-linear formulation, and are discussed in more detail below. Because \mathbf{A} and \mathbf{B} are updated each time the time horizon is advanced, the problem is an LTV problem, rather than a linear time invariant one. The \mathbf{C} matrix is a binary matrix that merely selects the elements from \mathbf{x}_k that are stress variables. The absolute control limits (eq. 3.23) bound the absolute set points for the generator power outputs and voltages, and load reduction, as described in section 3.2.6. Similarly, the incremental control limits (eq. 3.24) limit the voltage, generator output, and load reduction that can occur in a single time step. Section 3.3 describes results that illustrate the effects of changes to the above exogenous set limits.

3.2.7.1. *Linearized AC power-flow constraints.* The constraint $\mathbf{A}(\mathbf{x}_0, \mathbf{u}_0)\Delta\mathbf{x}_k = \mathbf{B}(\mathbf{x}_0, \mathbf{u}_0)\Delta\mathbf{u}_k$ is the generic form of linear dynamic constraints for the SMP. These constraints essentially comprise a linearization of the AC power flow constraints and a mapping from voltage changes to current magnitude changes. The linearization is not particularly unique to this work, with the possible exception of the use of current magnitudes. The following eqs. describe the constraints that compose \mathbf{A} and \mathbf{B} .

$$\begin{aligned} \Delta|\mathbf{I}_k|(\Delta\mathbf{x}_k) &= \left[\frac{d|\mathbf{I}|}{d|\mathbf{V}|} \right] \Delta\mathbf{V}_k(\Delta\mathbf{x}_k) + \left[\frac{d|\mathbf{I}|}{d\boldsymbol{\theta}} \right] \Delta\boldsymbol{\theta}(\Delta\mathbf{x}_k) \\ \Delta\mathbf{V}_{Gk}(\Delta\mathbf{x}_k) &= \Delta\mathbf{V}_{Gk}(\Delta\mathbf{u}_k) \\ \left[\frac{d\mathbf{P}_{\bar{r}}}{d|\mathbf{V}|} \right] \Delta|\mathbf{V}|(\Delta\mathbf{x}_k) + \left[\frac{d\mathbf{P}_{\bar{r}}}{d\boldsymbol{\theta}_{\bar{r}}} \right] \Delta\boldsymbol{\theta}_{\bar{r}}(\Delta\mathbf{x}_k) &= \Delta\mathbf{P}_{\bar{r}}(\Delta\boldsymbol{\Lambda}(\Delta\mathbf{u}_k), \Delta\mathbf{P}_G(\Delta\mathbf{u}_k)) \\ \left[\frac{d\mathbf{P}_r}{d|\mathbf{V}|} \right] \Delta|\mathbf{V}|(\Delta\mathbf{x}_k) + \left[\frac{d\mathbf{P}_r}{d\boldsymbol{\theta}} \right] \Delta\boldsymbol{\theta}(\Delta\mathbf{x}_k) &= \Delta\mathbf{P}_r(\Delta\boldsymbol{\Lambda}(\Delta\mathbf{u}_k), \Delta\mathbf{P}_G(\Delta\mathbf{u}_k)) \\ \left[\frac{d\mathbf{Q}}{d|\mathbf{V}|} \right] \Delta|\mathbf{V}|(\Delta\mathbf{x}_k) + \left[\frac{d\mathbf{Q}}{d\boldsymbol{\theta}_{\bar{r}}} \right] \Delta\boldsymbol{\theta}_{\bar{r}}(\Delta\mathbf{x}_k) &= \Delta\mathbf{Q}(\Delta\boldsymbol{\Lambda}(\Delta\mathbf{u}_k), \Delta\mathbf{Q}_G(\Delta\mathbf{x}_k)) \end{aligned}$$

where \bar{r} denotes the set of all buses except for the slack/reference bus r . It is important to note the minor difference in the real valued power injection constraints on the non-reference buses (\bar{r}) and the reference bus (r). In order to obtain reliably good results, it is necessary to ensure that the reference bus angle appears in only one constraint as shown above. This follows the procedure that is common to most linearized OPF formulations. The derivative terms:

$$\left[\frac{d\mathbf{P}}{d|\mathbf{V}|} \right], \left[\frac{d\mathbf{P}}{d\boldsymbol{\theta}} \right], \left[\frac{d\mathbf{Q}}{d|\mathbf{V}|} \right], \left[\frac{d\mathbf{Q}}{d\boldsymbol{\theta}} \right]$$

are calculated by differentiating eqs. 3.17 and 3.18 with respect to voltage magnitudes and angles. These combine to form the standard AC power-flow Jacobian (see for example [?] for a detailed description of these matrices).

In the actual MATLAB implementation of the LP, some of the above equations are reduced slightly for the sake of computational efficiency, but they remain functionally equivalent to the linear equations above.

3.2.7.2. Linear stress cost function details. The linear stress cost term ($\mathbf{c}_Y^T \max(\mathbf{y}_{\min}(k) - \mathbf{y}_k, \mathbf{y}_k - \mathbf{y}_{\max}(k), \mathbf{0})$) may require some additional explanation. The two terms $\mathbf{y}_{\min}(k)$ and $\mathbf{y}_{\max}(k)$ are designed to allow the limits as enforced by the MPC problem to gradually approach the actual limit on the stress variable. In this implementation $\mathbf{y}_{\min}(k)$ and $\mathbf{y}_{\max}(k)$ are set such that the threshold is always set at the measured or predicted value minus a percentage (the reduction/increase rate) times the limit. The limit thus approaches the actual threshold in equal steps until the actual threshold (plus a margin) is reached. For a branch current limit, if $|I_0|$ is the presently measured value, and $|I|_{\max}$ is the actual limit ($|I_0| > |I|_{\max}$), $|I|_{\max}(1)$ is set as follows:

$$|I|_{\max}(1) = \max(|I_0| - \alpha_I |I|_{\max}, |I|_{\max} - \beta_I)$$

where α_I is the current reduction rate and β_I is the limit margin for branch currents. Figure 3.3 illustrates this effect. The limits for voltages are set similarly.

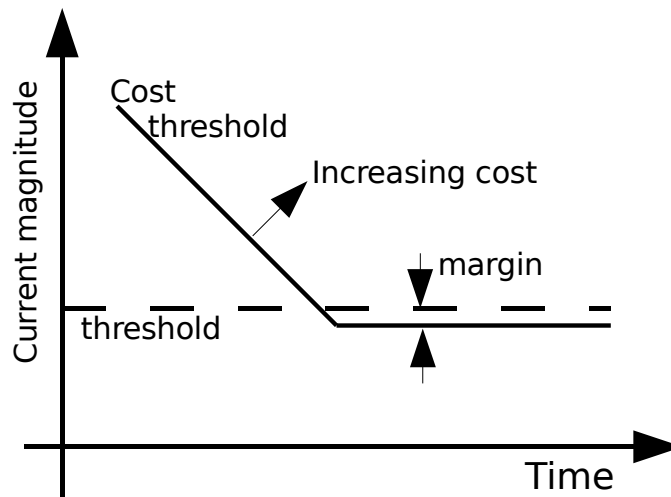


Figure 3.3: Illustration of the stress cost (penalty) function ($C_s(\mathbf{y}_k)$) for current magnitudes. Below the cost threshold the function evaluates to zero. Above the threshold the costs increase with the magnitude of the violation. The resulting measure roughly correlates with the blackout risk associated with allowing violations to persist.

The result is an MPC problem that acts incrementally to mitigate stress, instead of waiting to act entirely at the beginning or end of the time horizon. The discount factors ρ^k have the effect of making delayed actions less costly, whereas the incrementally constricting stress limits have the opposite effect.

3.2.8. The time horizon. In order to set up the discrete time MPC problem, the algorithm needs to choose a time horizon length and a step size. The choice of a step size (Δt) will affect the control variable limits $\Delta \mathbf{u}_{\min}$ and $\Delta \mathbf{u}_{\max}$ in several ways. For example, the Δ limits on the generator real power outputs come from the ramp rate of the machines, so as Δt increases, the feasible control range for $\Delta \mathbf{P}_G$ increases. One may also want to restrict the quantity of load that can be shed during a single time step. This could restrict the control space to a range that would not likely cause or exacerbate machine dynamic stability problems.

The length of the time horizon (K) is an exogenous parameter that will need to be set by an operator. Experimental results indicate that the choice of K does tremendously affect the results so long as it is greater than 4 to 6 time steps. Because

Table 3.3: Typical input parameters for the SMP experiments. Note that the stress costs $c_{|I|}$ and $c_{|V|}$ do not necessarily reflect the costs associated with the respective variables, but were determined experimentally to ensure that the resulting trajectories generally fall within the stress boundaries.

Setting	Symbol	Value	Units
Gen. voltage change limit	$\Delta V_G _{\max}$	0.01	p.u. V
Current stress cost	$c_{ I }$	10^6	$\frac{\$}{(p.u.A)(sec.)}$
Voltage stress cost	$c_{ V }$	10^8	$\frac{\$}{(p.u.V)(sec.)}$
Slack bus phasor error cost	c_θ	10^{12}	$\$ / \text{radian}$
Current threshold margin	β_I	0.5	p.u. A
Current reduction rate	α_I	10%	relative to $ I _{\max}$
Voltage increase rate	α_V	0.01	p.u. V

prediction accuracy decreases in time, the prediction of distant control actions does not dramatically affect the choice for current control actions.

The results that follow reflect the assumption that the time step is set to 1 second, and the time horizon is set to a maximum of 6 time steps.

3.3. Results

This section provides some example results that illustrate the utility of this approach. Table 3.4 shows the outcome of 15 tests of the control method, applied to test case 300-1-1 (see Figure 3.4). In this case, seven branch outages were applied to the IEEE 300 bus test network. Because the loads at each bus were randomly assigned blackout costs ($\$/\text{MW}$), one can approximately measure the outcome of the load shedding that results from the method in cost terms. Without mitigating control actions, a large cascading failure would result from this initial disturbance. These experiments show that approximately 100 MW (about 0.4% of the total) of carefully chosen demand and generator reduction can restore all voltages and currents to within limits. Figure 3.5 shows how the method reduces demand and generation incrementally to gradually restore the branch currents to below their limits.

The experiments described in Table 3.4 show the effect of varying various parameters in the model. Experiments 1-9 show that increasing the amount by which generator voltages can change at each time step ($\Delta|V_G|_{\max}$), dramatically increases

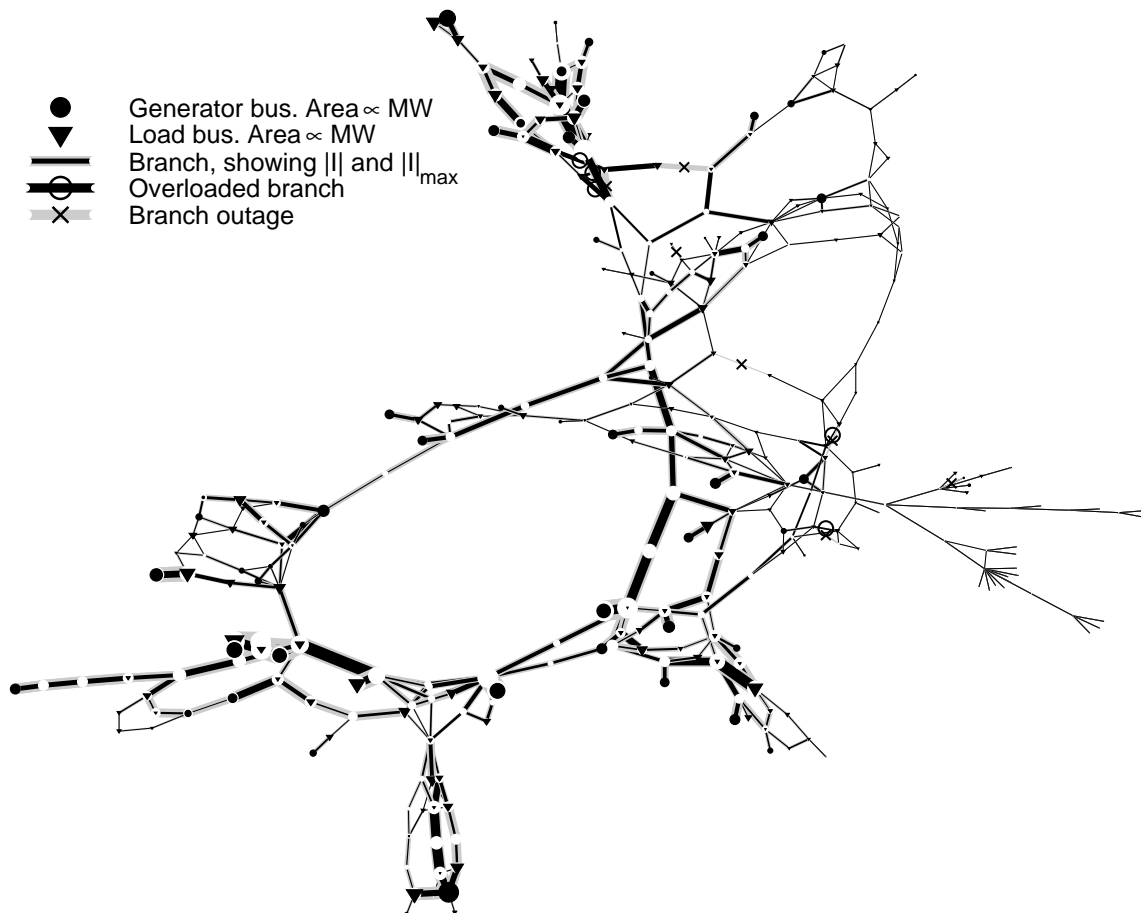


Figure 3.4: An illustration of the test case for examples in Chapter 3 (case300-1-1). In this figure, triangles indicate loads and circles generators, scaled according to the size of the figure. Current flows are shown as black lines between buses, with limits in gray. The 7 locations of the initial branch outages are marked with X's. The 5 locations of the subsequent over-currents are marked with an O. The initial branch outages cause current violations in the upper and right sections of the network.

the quality of the control outcomes. When the algorithm can use generator voltage changes to correct problems, it does not need to shed as much of the high-value load. This illustrates the more general result that larger decision spaces (more possible solutions) result in superior outcomes. It is likely that the addition of other variables, such as circuit breaker and flow-control device controls as described in Shao and Vittal [63, 96], would result in additional improvements.

Experiments 10-14 show the effect of changes to the voltage control cost parameter, $c_{\Delta|V_G|}$. Changes to $c_{\Delta|V_G|}$ do not have a large effect on the quality of the outcomes.

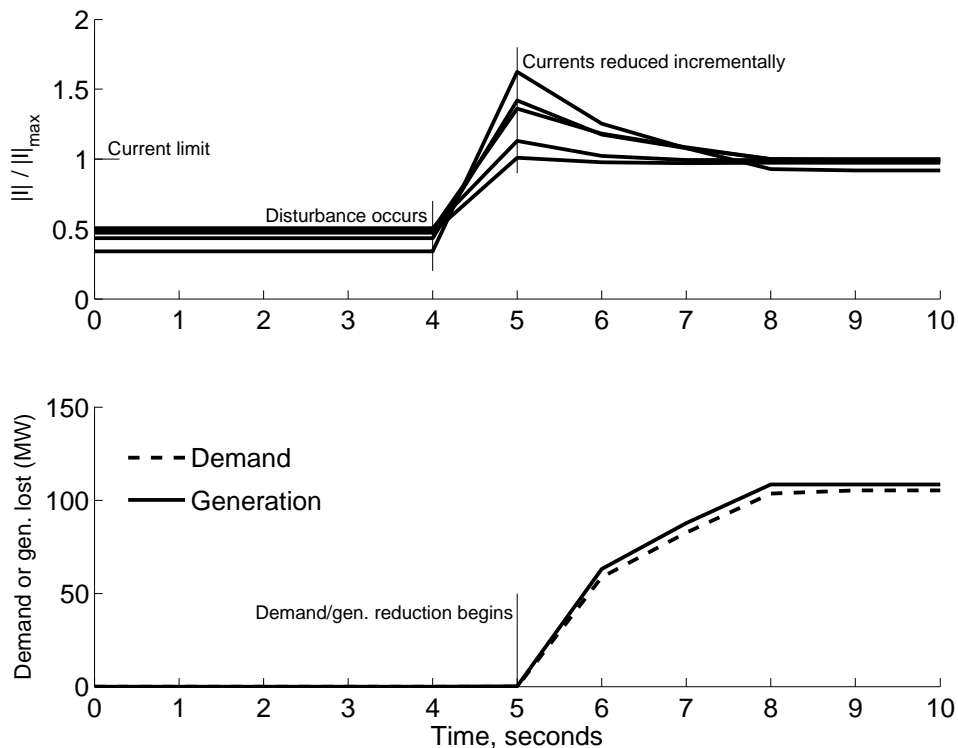


Figure 3.5: The trajectory of branch currents and load/generation shedding for test 6, as shown in table 3.4. The top figure shows the trajectory of the 5 branch currents that exceeded their limits as a result of the initial disturbance, normalized so that their limits are at 1.0. The bottom figure shows the demand and generation reductions which acted to reduce the currents to below their limits. The control actions are taken incrementally until the stress (excess current) is removed from the system.

However, a small $c_{\Delta|V_G|}$ results in the algorithm choosing to change the voltage at many generator buses at each time step. A larger $c_{\Delta|V_G|}$ results in simpler solutions, which may be a desirable outcome. The final experiment (test 15) shows that reducing the rate at which the algorithm tries to reduce currents (essentially the slope of the line in Figure 3.3) substantially increases the amount of time required to eliminate the excess stress (high currents).

A more thorough evaluation of this approach is available in Chapter 6 (Verification). The data are modified from the IEEE 300 bus network which are available from [1] or [97]. The data are described in some detail in Appendix B. The test case used here is listed as case300-1-1 in Appendix B. The disturbance for this case is a set of 7 branch outages that initially cause 5 current overloads and 4 voltage violations

Table 3.4: Results that show the effects of changes to some of the parameters in this model

Test #	$\Delta I $ rate	$c_{\Delta V_G }$	$\max \Delta V_G $	Steps	P_G lost	P_D lost	Cost
1	0.100	20000	0.000	6	173.41	164.49	\$370,500
2	0.100	20000	0.002	6	150.46	143.05	\$259,045
3	0.100	20000	0.004	6	134.61	124.49	\$155,740
4	0.100	20000	0.006	6	117.41	109.18	\$76,049
5	0.100	20000	0.008	5	108.23	102.06	\$47,064
6	0.100	20000	0.010	5	105.51	100.69	\$46,486
7	0.100	20000	0.012	4	105.71	100.65	\$46,471
8	0.100	20000	0.014	5	107.18	100.57	\$46,635
9	0.100	20000	0.016	5	107.63	100.48	\$46,660
10	0.100	500	0.010	5	110.22	97.2	\$45,265
11	0.100	1000	0.010	5	110.47	97.41	\$45,303
12	0.100	10000	0.010	4	106.57	100.49	\$46,347
13	0.100	20000	0.010	5	105.51	100.69	\$46,486
14	0.100	100000	0.010	5	107.37	101.83	\$46,883
15	0.020	100000	0.010	12	119.25	113.73	\$48,585

Table 3.5: Detailed control actions from case300-1-1, test 3. The control actions column shows the location and amount of change in generator bus voltage (dVg), generator power output (dPg), or load (dPd) at each time step.

Time	Control actions	$\max(I / I _{\max})$	Worst $ V $	$ V _{\min}$
5	[Pre-disturbance condition]	0.7786	0.9290	0.92
6	[Post-disturbance condition]	1.6252	0.8548	0.92
7	dPd_141=-42.9 dPg_7=-36.5 dPg_8=-10.2 dVg_7=0.0080 dVg_8=0.0080 dVg_10=0.0061 dVg_32=0.0160 dVg_34=0.0075	1.3363	0.8749	0.92
8	dPd_141=-24.7 dPg_7=-13.4 dPg_8=-9.9 dVg_10=0.0018 dVg_34=0.0160	1.2073	0.8976	0.92
9	dPd_141=-24.7 dPg_8=-3.0 dPg_33=-28.9 dVg_30=0.0049 dVg_34=0.0077 dVg_41=0.0160	1.0312	0.9124	0.92
10	dPd_141=-8.1 dPg_30=-5.8 dPg_41=-1.8 dVg_34=0.0053 dVg_41=0.0036 dVg_43=0.0100	1.0003	0.9201	0.92
11	dPg_42=-0.0 dVg_41=0.0000	0.9992	0.9201	0.92
12	[Final condition]	0.9992	0.9201	0.92

(see figure 3.4). Without emergency control, these violations would result in a severe cascading failure, given the simulation method discussed in Chapter 6.

3.4. Discussion

The optimal stress mitigation problem (SMP) described in this chapter has a number of properties that make it a good starting point for this work. The method can mitigate stress variables along relatively short time horizons as designed, even with imperfect linear models. Because we can use linear models, the problem is computationally tractable even for relatively large networks (solution time is discussed further in Chapter 5). The results shown here add empirical evidence to the assertion that larger decision spaces result in superior solutions. Specifically, allowing the controller to manipulate bus voltages results in substantially less costly control actions. On the other hand, because the MPC controller uses linear dynamic models for a non-linear system, experimental results show that if the voltage magnitude change limits are too large, the control outcomes can be worse relative to a case with somewhat tighter limits on these variables.

This method is not without its limits. For one, the random variables in the problem are not modeled directly. The approach could be improved by modeling measured data as random variables and incorporating some method of estimation, such as a Kalman filter. Similarly, the exogenous variables, such as hidden relay failures and load changes over time, could be more explicitly modeled in the MPC problem through the use of stochastic programming methods. Nevertheless, relying on feedback to compensate for these approximations appears to work fairly well in practice. Also, the computational complexity of the problem is non-trivial. The problem could be difficult to solve within a sub-second time step for very large networks (thousands of buses). For this reason, Chapter 5 discusses two ways that the size of the LP can be reduced without substantially changing the control outcomes.

CHAPTER 4

Cooperation

Chapters 1-3 describe the consequences of operating power networks poorly (black-outs) and provide a Model Predictive Control problem formulation that can be used to improve the operation of power networks (the Stress Mitigation Problem). As described earlier one goal of this thesis is to provide methods for adapting complex network problems to be solved by agents that are scattered throughout a network. In order for such agents to make good decisions with respect to the overall problem, they will need to coordinate their actions in some way. In other words the agents will need to cooperate. This chapter describes the process of inter-agent cooperation rather generally, and introduces the Reciprocal Altruism cooperation method that underlies the agent-based control system described in Chapter 5.

Agents generally make decisions according to goals. Goals can come in the form of objective functions to be minimized/maximized or constraints that need to be satisfied. When an agent helps another to meet the other's goals, it is said to cooperate. More specifically, agent A cooperates with agent B when A helps B to meet its local goals [16]. In many, if not all, cases agents must exchange information to help one another in this way. Information exchange can occur either through direct message passing or by posting messages to some form of shared memory (a bulletin board for example).

Given the above definitions, a cooperative agent that exchanges information with its neighbors¹ makes three types of decisions.

- (1) It must decide the manner in which it will help with its neighbor's goals.

¹“Neighbor” is generally used in this thesis to refer to agents that are in some way connected, either by a physical link such as a transmission line, or by at least one shared goal.

- (2) It must decide what sort of information it will share (if any) with its neighbors.
- (3) It must decide what actions to take upon its local environment while considering both local and neighbors' goals.

For biological agents, the first and second decisions are typically made while considering the long-term consequences of cooperative and non-cooperative behavior. For software agents, these decisions largely result from design choices. In both cases the third decision process can be represented by optimization problem that results from decisions 1 and 2.

This chapter presents an optimization model of cooperation, particularly focusing on Reciprocal Altruism. Two agents practice Reciprocal Altruism (RA) when they share goals; one adopts some goals of the other in the expectation that the other will reciprocate. In the case of software agents, a key design parameter is the size of an agents' reciprocal set, or the set of non-local goals that an agent adopts. As the reciprocal set gets larger an agent will need more information exchange to accurately model remote goals. This expansion can overburden communication channels and lead to complex agent problem formulations. The choice of a reciprocal set, or neighborhood size, is further discussed in Chapter 5.

4.1. The cooperative agent problem

Consider a set of n_a agents that act within a network. Each agent has a set of local control and state variables. For agent n these variables are represented by \mathbf{u}_{N_n} and \mathbf{x}_{N_n} (for simplicity the subscript n will be dropped leaving \mathbf{u}_N and \mathbf{x}_N). From agent n 's perspective, non-local variables in the network are represented by the vectors $\mathbf{u}_{\bar{N}}$ and $\mathbf{x}_{\bar{N}}$. Each agent also has local goals in the form of an objective function, $f_n(\mathbf{u}_N, \mathbf{x}_N)$ and a set of constraints $\mathbf{g}_N(\mathbf{u}_N, \mathbf{x}_N, \mathbf{u}_{\bar{N}}, \mathbf{x}_{\bar{N}}) \leq 0$. If it is not cooperative, agent n will combine these goals and make decisions according to problem formulation

given in eqs. 4.1.

$$(4.1) \quad \begin{aligned} \text{Maximize}_{\mathbf{u}_N} \quad & f_n(\mathbf{u}_N, \mathbf{x}_N) \\ & \mathbf{g}_N(\mathbf{u}_N, \mathbf{x}_N, \mathbf{u}_{\bar{N}}, \mathbf{x}_{\bar{N}}) \leq 0 \end{aligned}$$

If some of the external variables ($\mathbf{u}_{\bar{N}}$ and $\mathbf{x}_{\bar{N}}$) significantly affect the agent's constraints it will need some mechanism for estimating the important external variables. Without this information the agent will not perform well with respect to its goals. The method of prediction/estimation varies among agents. In order to make predictions agents need to gather information about their surroundings. If \mathbf{w}_n is the information that agent n has gathered, and it uses prediction methods \mathcal{U}_n and \mathcal{X}_n to predict external state and control variables, agent n 's problem becomes:

$$\begin{aligned} \text{Maximize}_{\mathbf{u}_N} \quad & f_n(\mathbf{u}_N, \mathbf{x}_N) \\ & \mathbf{g}_N(\mathbf{u}_N, \mathbf{x}_N, \mathbf{u}_{\bar{N}}, \mathbf{x}_{\bar{N}}) \leq 0 \\ & \mathbf{u}_{\bar{N}} = \mathcal{U}_n(\mathbf{w}_N) \\ & \mathbf{x}_{\bar{N}} = \mathcal{X}_n(\mathbf{w}_N) \end{aligned}$$

Assuming that all of the goals in the network are assigned to only one agent, and that the global objective function is a simple sum of the agent objectives (utility functions), the global network problem is the following:

$$(4.2) \quad \begin{aligned} \text{Maximize}_{\mathbf{u}} \quad & f(\mathbf{u}, \mathbf{x}) = \sum_{n=1}^{n_a} f(\mathbf{u}_{N_n}, \mathbf{x}_{N_n}) \\ & \mathbf{g}(\mathbf{u}, \mathbf{x}) \leq 0 \end{aligned}$$

where \mathbf{g} is the combined vector function of all constraints in the network. Under some very restrictive conditions, such as perfect economic competition without externalities, agents acting according to formulation 4.1 will arrive at a solution to the global goals given in 4.2. In most real systems the conditions do not hold and agents

must work cooperatively to arrive a solutions that are acceptable with respect to the global problem (problem 4.2).

4.1.1. Cooperation through voting. Cooperation can take many forms. Among these is voting in which agents choose actions by submitting votes and agreeing to abide by the preferences of the majority. The following is a brief discussion of the decision problem for agents that cooperate through voting. As with all cooperation methods, voting requires that agents exchange information and then adjust their local problems to consider the goals of other agents. The initial posting of votes (message posting) can be used to determine constraints that are preferred by the majority of agents within the network. If all of the agents cooperate, the agents incorporate the constraints (goals) that result from each election into their local decision process. The agreed-upon constraints may also come with penalties for diverging from these constraints. For example, residents of a city may vote for a law to respect property rights and appoint a police force to enforce these property rights. If $\mathbf{v}(\dots) \leq 0$ represents the constraints that result from the voting scheme, the decision process for an agent within a democratic system might be the following:

$$\begin{aligned} \text{Maximize}_{\mathbf{u}_N} \quad & f_n(\mathbf{u}_N, \mathbf{x}_N) \\ & \mathbf{g}_N(\mathbf{u}_N, \mathbf{x}_N, \mathbf{u}_{\bar{N}}, \mathbf{x}_{\bar{N}}) \leq 0 \\ & \mathbf{u}_{\bar{N}} = \mathcal{U}_n(\mathbf{w}_N) \\ & \mathbf{x}_{\bar{N}} = \mathcal{X}_n(\mathbf{w}_N) \\ & \mathbf{v}(\mathbf{u}_N, \mathbf{x}_N, \mathbf{u}_{\bar{N}}, \mathbf{x}_{\bar{N}}) \leq 0 \end{aligned}$$

If designed well, the voted-upon constraints will result in agent actions that are close to what one would get from the global problem (eqs. 4.2). Unfortunately, voting schemes do not generally result in globally optimal outcomes (see e.g. Arrow [98]).

4.1.2. Complete Cooperation. One way to guarantee that all agents act optimally with respect to the global problem is to force (design) all of the agents to always use all of the goals in the global problem, with equal weight, at all times. Ideally this would result in agent problems that are identical to the global formulation. In order to arrive at the ideal every agent would need to pass all of its information to every other agent on a regular basis. At every cycle every agent would need to send and receive n_a message packages. In an engineered multi-agent system, total message traffic would scale with the square of the number of agents, resulting in a scheme that is impractical or impossible for large networks. This approach is here referred to as complete cooperation.

4.1.3. Reciprocal Altruism. Between complete cooperation and competition lies the method that is employed in this thesis, which is roughly equivalent to reciprocal altruism, as found in many biological systems. According to [21], altruism can be defined as “behavior that benefits another organism, not closely related, while being apparently detrimental to the organism performing the behavior, benefit and detriment being defined in terms of contribution to inclusive fitness.”

Reciprocal Altruism (RA) is a form of altruism in which an organism expects other organisms to respond to altruistic behavior with similarly altruistic behavior. Such behavior has been observed in many organisms including vampire bats, which will share food (blood) with others who were not successful in gathering food [99]. In the case of vampire bats, Wilkinson [99] found that the two most important factors in a bats decision to share food, were kinship (relational proximity) and potential for reciprocation. To ensure reciprocation in biological systems, mechanisms exist, such as social norms and guilt, that encourage conformance to the reciprocal altruism rule. In an engineered multi-agent system, however, such enforcement mechanisms are not generally necessary as agents can reciprocate by design. The kinship aspect of RA, however, is equally important to engineered and biological systems. In both

cases it is impractical for an agent to cooperate equally with all other agents. Therefore agents tend to cooperate more with others to whom the agent is related. The proposed decentralized control scheme incorporates this structure through the use of neighborhoods or “reciprocal sets.”

A community of RA agents will consider both local goals and neighbors’ goals while making decisions. Eqs. 4.3 represent the decision process of an RA agent.

$$\begin{aligned}
 (4.3) \quad \text{Maximize}_{\mathbf{u}_N} \quad & f_n(\mathbf{u}_{N_n}, \mathbf{x}_{N_n}) + \sum_{i \in M} \alpha_i f_i(\mathbf{u}_{N_i}, \mathbf{x}_{N_i}) \\
 & \mathbf{g}_N(\mathbf{u}_N, \mathbf{x}_N, \mathbf{u}_{\bar{N}}, \mathbf{x}_{\bar{N}}) \leq 0 \\
 & \mathbf{g}_M(\mathbf{u}_N, \mathbf{x}_N, \mathbf{u}_{\bar{N}}, \mathbf{x}_{\bar{N}}) \leq 0 \\
 & \mathbf{u}_{\bar{N}} = \mathcal{U}_n(\mathbf{w}_N) \\
 & \mathbf{x}_{\bar{N}} = \mathcal{X}_n(\mathbf{w}_N)
 \end{aligned}$$

Here M represents the set of external goals that agent n incorporates into its local problem. Thus $\mathbf{g}_M(\dots)$ is the set of external constraints, and $f_i(\dots)$, $i \in M$ is the set of objective functions (weighted by α_i), that are shared with other agents. M can be thought of as agent n ’s “reciprocal set.” When two RA agents (agent A and agent B) act precisely reciprocally, A considers all of B ’s goals and B reciprocates by considering all of A ’s goals. As describe here, reciprocal altruism is a pair-wise symmetric form of cooperation. Each pair of agents share goals in a symmetric fashion.

When agent n thus formulates its decision problem, it will consider the effects of its local actions on its neighbors, while its neighbors do likewise. Agent n may choose to take actions that are locally costly in order to help meet some of the other goals in its reciprocal set. In doing so it expects that other agents will act optimally with respect to their own local problems. This is the assumption that forms the basis of the prediction functions, \mathcal{U}_n and \mathcal{X}_n . The details of this implementation are discussed in Chapter 5.

The challenge in engineering a multi-agent system that uses reciprocal altruism lies in designing agents to use appropriate reciprocal sets and to exchange appropriate information during operation. The goal is to design the cooperation protocols (both the reciprocal sets and the information exchange) such that the global performance approaches that which would be achieved from the global problem formulation with perfect information. If the reciprocal sets are too small, the agents will act rather myopically. Large reciprocal sets on the other hand require a lot of data exchange to model the larger set of constraints. Similarly if agents exchange too little or the wrong types of information, their solutions will be far from optimal. If the agents exchange too much or misleading information communication channels can become an obstacle to reliable operation.

4.2. Cooperation in the decentralized solution of the SMP

This section provides details for the data exchange protocols associated with the two cooperation methods employed in this work. Additional details are provided in Chapter 5. In method 1 agents apply the general principle of reciprocal altruism and exchange carefully selected packets of measurements that they expect will be useful to neighboring agents. This method is referred to as “simple reciprocal altruism.” Method 2 extends “simple reciprocal altruism such that agents iteratively negotiate their actions (using an admittedly crude negotiation protocol) after their initial decision process. These two methods are described in detail below.

4.2.1. Cooperation method 1: simple reciprocal altruism. In the simple reciprocal altruism scheme, as described in Chapter 5, each agent divides the network into 3 regions, not including the agent’s home node. Region 1 is the local neighborhood (M), and includes all nodes and agents that can be reached by traversing no more than r_l links/branches. Region 2 is the agent’s extended neighborhood (R) is the set of nodes/agents that can be reached by traversing no more than r_e links (see figure 5.1).

Once per time step, agent n creates a message that includes all of its local state variables and control variable set points, and send these to each of its local neighbors (M). Essentially, the message has the following form:

$$w_0(n, m) = \begin{bmatrix} \mathbf{u}_{0N} \\ \mathbf{x}_{0N} \end{bmatrix},$$

where the 0 represents the current time period, t_0 . In a power network this message will include the voltage at bus n , all of the currents that can be measured at bus n , the status (open or closed) of each branch connected to bus n , and the state of each load and generator connected to bus n .

In addition agent n will build a smaller message that includes only the variables that indicate stress at agent n 's location. For a power network these include voltages and currents that are outside of their limits, or the status of branches that have tripped. This message is sent to some or all of the agents in R .²

4.2.2. Cooperation method 2: simple reciprocal altruism with negotiation. Cooperation method 2 extends the simple reciprocal altruism scheme with a simple negotiation protocol to improve upon agents' initial control decisions. In this scheme the agents perform the message passing described above and then follow the procedure below to calculate control actions at each time step. The following is the negotiation protocol for agent n .

- (1) Calculate an initial control vector according to the local control problem.

Prepare a message that indicates the control variables adjustments that agent n believes are optimal given its model of the network. Let $\Delta \mathbf{u}_{\Upsilon_n, 0}^{[n]}$, where $\Upsilon_n = n \cup M_n \cup R_n$, represent this vector for the current time period (t_0). Because of the structure of the agent problems, all $\Delta u_{i, 0}^{[n]}$ will be zero for $i \notin \Upsilon_n$.

²In the current implementation this stress message is sent to all agents in R . This is actually inefficient, because these data are irrelevant to most of the agents in R . The communication requirements could be reduced somewhat by only sending stress messages to a subset of agents in R .

- (2) Given $\Delta \mathbf{u}_{\Upsilon_n,0}^{[n]}$, choose a set of agents to negotiate with (Φ). For a power network, agent n chooses Φ according to $\Phi = \{i : |\Delta \mathbf{u}_{N_i,0}^{[n]}| > \epsilon\}$, where ϵ is a small value to indicate that Δu_i is significantly different from zero. In words agent n chooses to negotiate with a set of agents that it thinks need to make some significant change to their control variables.
- (3) Agent n sends its current control vector $\Delta \mathbf{u}_{\Upsilon_n,0}^{[n]}$ to each member of Φ along with a message that indicates the data in agent n 's model that is relatively current (measured within the last 2 seconds).
- (4) In response to the message from agent n , each member of Φ will compare its local control vector with agent n 's. For example if agent m is a member of Φ_n , it will calculate $\delta = \left\| \Delta \mathbf{u}_{\Upsilon_n,0}^{[n]} - \Delta \mathbf{u}_{\Upsilon_n,0}^{[m]} \right\|$. If δ is significantly different from zero, agent m will respond with a set of measurements that are current in agent m 's model, but are not current in agent n 's model.
- (5) Each agent waits for a moment to allow for message passing, and then recalculates their control vectors $\Delta \mathbf{u}_{\Upsilon_n,0}^{[n]}$.
- (6) If more time remains before the time at which agents agree to implement the control actions for the current time period, repeat from step 2.

While it is perhaps not intuitively obvious, this protocol is similar to the manner in which groups of people negotiate difficult decisions that require consensus. Each person will take the information that they currently have and then tell their neighbors what they think should be done about the current circumstance. When two neighbors disagree they exchange information about why they think their decision makes sense. If the neighbors share similar values, the neighbors will iteratively consider the information being discussed, and update their decision process. In the case of agents at nodes of a power network, consensus typically occurs within a few iterations of this process. For difficult decisions within human organizations, this process often requires much more time.

Table 4.1: Results that show the difference between cooperation methods 1 and 2 in terms of control quality and communication requirements. In all cases $r_e = 10$, $r_c = 6$ (except for the last two tests where $r_c = 5$), and $c_{\Delta|V_G|} = \$20,000$. Other parameters are the same as those used in other tests.

<i>Case</i>	r_l	P_D lost	<i>Social Cost</i>	<i>Comm. Burden</i>
Global MPC	-	100.7	\$46,486	-
Simple coop	2	109.7	\$64,873	7.43
Simple coop	3	110.7	\$66,785	10.95
Negotiate	2	103.4	\$49,572	237.3
Negotiate	3	103.1	\$49,359	247.4

4.3. Cooperation results

To illustrate the difference between cooperation methods 1 and 2 table 4.1 compares the results from the application of the SMP control method to case300-1-1 using a single global MPC controller, a network of agents operating with simple RA only (method 1), and a network of agents operating according to cooperation method 2. While the simple RA method does not require much communication bandwidth (<10 kB output per agent per second), the quality is substantially less that what comes from the negotiation protocol. On the other hand the negotiation increases the burden on the communication system substantially. Method 1 is certainly well within the capability of current communications technology. Method 2 may be near the upper end of what can be expected from current technology in terms of communications bandwidth.

4.3.1. Scaling properties of methods 1 and 2. In both of the above cooperation methods, the quantity of inter-agent communication is proportional to the size of each agent’s local (M) and extended (R) neighborhood (reciprocal sets). In other words the per-agent communication bandwidth requirements of this method will not increase with the number of agents (n_a) so long as the average size of M and R do not increase with n_a .

As implemented here, M and R are defined by the graph distance between agents. Agent n ’s local neighborhood (M_n) is the set of nodes/agents that can be reached

Table 4.2: The average number of buses that can be reached by crossing no more than r branches for several power networks and several radii (r). The IEEE networks come from [1]. The data for NERC regions come from FERC Form 417 filings, which were obtained from FERC in 2004.

Network	n_{BUS}	$r = 2$	$r = 4$	$r = 6$	$r = 8$	$r = 10$
IEEE 39	39	6.9	18.3	30.4	37.9	39.0
IEEE 57	57	8.9	26.5	44.3	53.9	56.7
IEEE 118	118	11.2	36.6	68.4	95.5	110.6
IEEE 300	300	11.4	38.8	84.8	146.2	208.2
ECAR	27096	6.5	39.9	172.1	493.5	1016.3
ERCOT	5251	3.6	12.8	40.9	110.3	258.5
FRCC	4488	8.8	30.9	77.9	159.3	290.0
MAAC	23801	6.5	39.8	171.3	491.7	1012.6
MAIN	42603	6.6	40.5	174.3	502.8	1038.1
MAPP	21629	6.1	35.7	127.6	280.5	466.1
NEPOOL	40499	6.8	42.0	177.6	506.9	1043.8
NYISO	45342	6.5	39.9	172.1	493.9	1022.2
SERC	42871	6.8	41.1	176.2	508.9	1051.4
SPP	34954	6.6	43.1	191.5	549.2	1094.7

by crossing no more than r_l links. Its extended neighborhood (R_n) is the set of nodes/agents that can be reached by crossing no more than r_e links, excluding those nodes in M_n . In actual power networks, the size of a neighborhood defined in this way remains independent of size for small radii, but increases with size when the radius (r_e typically) is larger than 4. Table 4.2 shows how the size of various neighborhoods defined in this way would increase for several actual power networks. The reason for this likely has to do with the presence of long transmission lines that connect remote portions of the grid, thus linking otherwise separate network regions. Because of this effect it is reasonable to define the local neighborhood using the graph radius method, but it may be necessary to define the extended neighborhood in some other way in order to preserve reasonable scaling properties for the method. Such a redefinition will be explored in future work.

4.4. Discussion

This chapter describes a model of cooperation among software-based control agents. Optimization formulations for several forms of multi-agent cooperation are described:

competition, voting, complete cooperation and reciprocal altruism. The proposed agent-based control scheme is based on the latter model, which is extended through the use of two simple cooperation schemes. Simulation of these two schemes show that system-wide performance can be substantially improved through the use of a negotiation protocol, but at the cost of substantial increase in bandwidth requirements for the communications system.

Many other modes of cooperation exist. This work focuses on a scheme that is closely akin to reciprocal altruism, as found in some animal species. Other modes of cooperation include hierarchies, submission and peer-pressure (which is arguably a form of reciprocal altruism). Future work will include a more thorough comparison of different approaches to cooperation among software agents.

CHAPTER 5

Decomposition

The primary goal of this thesis is to provide network operators with improved tools for the real-time operations of complex networked systems. The optimal operations problem formulation given in Chapter 1 provides one way to structure this problem. Chapter 3 describes a way to adapt the general OOP to the more specific problem of controlling electrical power networks and reducing the costs associated with cascading failures. The result was a linear time-varying (LTV) MPC problem that can be used to mitigate stress in a power network (the stress mitigation problem—SMP). Chapter 4 presents the concept of reciprocal altruism, which describes the process by which agents agree to consider the goals of neighboring agents while making local decisions, assuming that other agents will respond in kind. This sharing of goals provides the foundation for the problem decomposition method that is described in more detail in this chapter. In particular this chapter describes a method for solving the SMP through the use of agents dispersed throughout a power network. Essentially the agents operate by incrementally solving a the global SMP by using a locally maintained, simplified, network models and the LSMP MPC problem. If we think of the objective terms and constraints that comprise the SMP as goals assigned to individual agents, our decomposition method is based upon agents who choose their actions based upon both local goals and a set of goals that actually belong to neighboring agents. These neighboring agents' goals make up an agent's reciprocal set, as described in Chapter 4.

There are three primary reasons to take a decentralized approach to the real-time operation of complex networks: robustness, reaction time, and organizational simplicity. Centralized systems are highly susceptible to failures in a small set of

components. When a centrally located decision process fails the system as a whole will likely fail. On the other hand, when well designed, decentralized systems are fairly robust to small failures. Small failures are contained such that the consequences are proportionally small. Similarly, a centralized decision process can require significant time to collect state data, calculate a reaction, and implement the result. These delays result from communication delays between the operator and the physical devices, and from the computational time required to process raw state data and calculate a reaction. In large networks, the computational delays can be very large; merely estimating the state of a power network can require more than 30 seconds.¹ Delays have a particularly significant impact when the network state is changing rapidly with time, as is the case during a cascading failure. Finally, decentralized control is frequently an organizational necessity, particularly when infrastructure ownership is dispersed among organizations with diverse interests. The electricity networks in continental Europe and the United States illustrate this property well. In both cases the network infrastructure is owned and operated by many governmental and commercial entities, few of which are particularly eager to relinquish control to a single central authority. Because of these three factors, decentralized control can be a powerful tool in the operation of complex networks.

On the other hand, not all decentralized control schemes (or problem decompositions) are equally effective. When the actions of distributed controllers, or agents, do not align well with the global problem, the results can be disastrous. A good problem decomposition results in agents that, when acting optimally with respect to their local objectives and constraints, enable system performance that approaches global optimality. For example, given that the assumptions of perfect competition hold, competing agents buying and selling within an ideal, perfectly competitive, market jointly maximize global social welfare. However, when markets are imperfect, the

¹This datum comes from personal remarks by officials from large power system operators in the U.S.

aggregate actions of competing agents result in disastrously sub-optimal outcomes (see for example the California Energy crisis of 2000).

This chapter describes the problem decomposition method and presents some results that illustrate its effectiveness in managing stress in a power network. In addition, section 5.3 argues that the effectiveness of this method, and potentially of problem decomposition in general, depends largely upon the structure of the network that is to be controlled. More specifically, from a simplified analytical model of this problem, I show that the effectiveness of decentralized control depends greatly on the manner in which control variable effects propagate through the network. This effect is illustrated using a fairly generic model of network dynamics applied to several common network structures.

5.1. Decomposition method

A problem decomposition divides a large problem into a set of sub-tasks. Problem decomposition is necessary when the full problem is too difficult (expensive, time-consuming, politically infeasible, etc) for solution by a single agent. In a good problem decomposition, each of the sub-tasks is in some way preferable to the full problem and the results from each sub-task combine to form a nearly optimal solution to the global problem.

This thesis is particularly focused on decomposing the time-critical aspects of a network problem such that exactly one agent has responsibility to measure and control the variables at each node in a network. Since there is no overlap in control authority this approach is a disjoint decomposition scheme, and because there is one sub-problem for each node in the network it can be considered a complete decomposition. A disjoint-complete decomposition has numerous advantages with respect to execution speed and robustness. When each agent is co-located with the devices being measured and controlled, there are virtually no delays in measurement or control execution. Avoiding overlapping authority increases agent autonomy, which can

have benefits with respect to reliability and execution speed. For example, consider a hierarchy in which each agent shares responsibility for some control variables with a supervisor such that the agent must ask permission to take local actions. If the supervisor is unavailable, the agent is quite restricted in its action (reducing its autonomy). If the agent's action is critical to the operation of the system, the agent's actions can be delayed, with potentially disastrous consequences.

On the other hand, agents that are excessively autonomous have the potential to act in a way that is far from optimal with respect to the system as a whole if their local goals conflict with the global goals, or if they operate according to incomplete or inaccurate information. With biological agents the problem of conflicting objectives is particularly difficult as they tend to act according to very localized objective functions. While altruistic action is observed in biological systems, private utility maximization tends to be a better model of agent behavior in most species. With software agents this is less of a problem because the agents can be designed to operate altruistically. The problem of incomplete or inaccurate information, however, is less easy to overcome. This is true for both biological and engineered multi-agent systems. In tightly interconnected systems, small information and decision errors can have disastrous consequences. For example the East Asian economic crisis of 1997 was, at least to some extent, exacerbated by information and prediction errors made by the Thai government as it sought to defend the value of its currency against the actions of speculative investors. Because of the tightly interconnected nature of international currency markets, what might have otherwise been a localized economic problem quickly became an international disaster.

5.1.1. Decomposition process. To address the above challenges, we use a problem decomposition that is based upon reciprocal altruism. The agents within the system agree to share goals with sets of neighbors. The decomposition process can be summarized in the following four steps:

- (1) Assign agents to locations in the network. For the case of a power network we place one agent at each high voltage transmission substation.
- (2) Partition the decision variables such that each control variable is assigned to exactly one agent. Agent n is responsible for the control vector \mathbf{u}_{N_n} , and the combination of all \mathbf{u}_{N_n} gives the complete decision vector \mathbf{u} .
- (3) Break the goals from the global problem, including terms of the objective function and constraints, such that each constraint or function is assigned to exactly one agent. The result is a set of disjoint agent sub-problems.
- (4) Allow the agents to choose partners for reciprocal altruism, and incorporate the partner's goals into local problems (see section 5.1.2).
- (5) Use a very simple, default network model to approximate the effects of constraints that fall outside of the agent's neighborhoods.

Thus this problem decomposition is disjoint with respect to the decision space (decision variables are assigned to only one agent), and overlapping with respect to the goals (objectives and constraints) of the problem. Because the local problems will differ from the global problem, the optimal solutions of the sub-problems are not going to be optimal with respect to the global problem. But, we can move the result arbitrarily close to the global optimum by increasing the size of the reciprocal sets used by the decomposition. If the reciprocal sets are small, the solutions will differ substantially from the global optimum, but the agents will not need to exchange much information to maintain their network models that represent shared goals. If the sets are large, the information exchange requirements will be large, but the results will approach the globally optimal results. Results found later in this chapter, and in Chapter 6, illustrate this design trade-off.

5.1.2. Neighbors and reciprocal sets. Once agents are located within the network and are assigned local variables, objectives and constraints (steps 1-3), they must begin to build their local optimization problems. When the agents are RA agents, this includes the selection of a set of external goals (reciprocal set), which

will be incorporated into the agent's local problem. There are many mechanisms by which this could be done. In the method employed here, the agents select reciprocal partners based upon the graph distance to those partners within the network. Those agents that can be reached by crossing no more than r links in the graph become reciprocal partners; others are excluded from this set.

In actual implementation, the agents described here actually use two reciprocal sets. To choose these reciprocal sets, each agent divides its surrounding network into four regions. The first region (N) includes only the agent's local node, along with a set of associated goals and variables. The second region is known as agent n 's local neighbors (M_n), and includes all of the nodes that can be reached by traveling over no more than r_l branches. The third region includes all of the nodes that are not in M_n or n , and can be reached by traveling over no more than r_e branches. The fourth region includes all of the external nodes, variables and goals. See figure 5.1 for an illustration of these models. Agent n will use all of the variables and goals that are contained within N_n , M_n and R_n to build its local problem. The set $M_n \cup R_n$ comprise agent n 's reciprocal partners, because it will share goals with all of these agents.

5.1.3. Agent algorithm. What follows is a more detailed description of the process by which software agents can solve the SMP, or any other linear permutation of the OOP, through the proposed RA-based problem decomposition. During normal operation an agent must take the information that it has collected about the network and turn this into a control action. The agent performs this task by solving its local problem. For an RA agent, this problem is a combination of local goals and goals that are shared with other agents in the network.

When an agent's reciprocal set is large, it will need quite a bit of information about the network to solve its local problem. For this purpose each agent maintains a rough model of the entire network, and populates this model with data that it obtains by exchanging information with other agents. At each time step, each agent

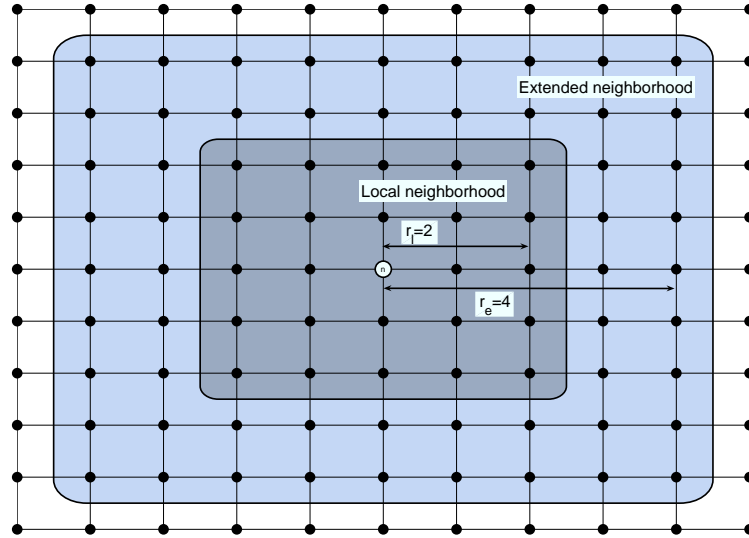


Figure 5.1: An illustration of agent n and its neighborhoods/sub-models within the network. For the sake of simplicity, this figure shows the neighborhoods for a regular square grid with agent n in the center. In this case M includes the 24 nodes in the “local neighborhood,” and R includes the 55 nodes in the “extended neighborhood.” (Note that the neighborhoods on this graph are drawn assuming that links also exist in the diagonal directions.)

essentially estimates the entire network state vector. If the current time step is t_0 (t_0 is generally used to refer to the current time in a rolling time horizon), each agent builds an estimate of \mathbf{x}_0 .

In order to solve for local control actions (\mathbf{u}_N), each agent must simultaneously anticipate the actions of other agents (\mathbf{u}_M and \mathbf{u}_R). Agents anticipate by assuming that all of the agents in the problem act optimally with respect to their local problems, and using locally available data about the network to estimate what these actions will be.

The following is an outline of the process by which the agents maintain their network models, and then use these model to calculate local control actions:

- (1) Agents are initialized by an operator with some very basic data about the structure of the network.
- (2) Agents exchange data and estimate the state of the network ($\mathbf{u}_0, \mathbf{x}_0$).

- (3) Agents use measurements to calculate a set of linear equations that represent the network's dynamics ($\mathbf{A}\Delta\mathbf{x} = \mathbf{B}\Delta\mathbf{u}$). These equations are used to build estimate the goals that are included within the agent's reciprocal set.
- (4) Agents predict neighbors' control actions and calculate local control actions by solving their local problem formulation.
- (5) Depending on the cooperation method employed, agents exchange information with neighbors to improve the above predictions and calculations.
- (6) Agents implement control actions, advance the time horizon and repeat from 1.

The following sections describe each step in this process in some detail.

5.1.3.1. *Initialization.* Because it is not generally possible for software agents to come to exist autonomously, some operator intervention is needed to set the control agents in motion. In this case, the role of the operator is to provide each agent with the form of its operating objectives and constraints, and the basic data and instructions it will need to operate with relative autonomy. The most important data that the operator provides to the agent is a skeleton network model. Included in this model are the following:

- The physical structure of the network, including the properties of the links and nodes.
- The locations of other control agents in the system.
- A default network state vector that the agent can use when it does not have measurements ($\bar{\mathbf{x}}$).
- A default network control vector $\bar{\mathbf{u}}$, and a set of limits ($\mathbf{u}_{\min}, \mathbf{u}_{\max}, \Delta\mathbf{u}_{\min}, \Delta\mathbf{u}_{\max}$) and costs (\mathbf{c}_u) associated with that vector.
- A default output matrix \mathbf{C} and a set of limits ($\mathbf{y}_{\min}, \mathbf{y}_{\max}$) and costs (\mathbf{c}_y) associated with the stress / output variables.
- A vector of costs associated with changes that the agent makes to the network state (\mathbf{c}_x).

In addition to the above, the operator will need to provide the agent with the basic form of the objectives and constraints that the agent will use in its decision process. Some of these data can be collected from other agents once the agent knows the physical structure (nodes, links, and agent locations) of the network. In the simulations described here this data is initially provided to the agent by the operator in one data package at the beginning of the simulation.

After collecting these data, the agents divide the network into sub-networks, essentially arranged in rings surrounding the agent. The first ring contains only the local agent (agent n) and its local variables, \mathbf{z}_{N_n} . The second ring (agent n 's local neighborhood) contains all of the agents and nodes that can be reached by traversing no more than r_l links. In a minor abuse of notation, this set of agents is referred as M_n , and the all variables in this section of the network is \mathbf{z}_{M_n} . The third ring (agent n 's extended neighborhood) contains all of the agents and nodes that can be reached by traversing no more than r_e links. This set of agents will be referred to as R_n and the variables \mathbf{z}_{R_n} . The final ring includes the remaining nodes and variables in the network. Since one agent is located at each node, the symbols for agent sets (R_n and M_n) will be used also to refer to sets of nodes. Agents use these subsets to choose the type of information exchange that will occur, and the fidelity of the agent's models.

5.1.3.2. *Exchange information.* While in operation agents constantly exchange information. Once per time step agents collect their local state measurements and control set points ($\mathbf{x}_N, \mathbf{u}_N$) and bundle them in a time-stamped message. It then sends this message to each agent in its local neighborhood (M_n). In addition to this regular message, agent n finds any members of \mathbf{y}_N that exceed local stress thresholds. These it passes to some or all members of its extended neighbors (R_n).

The receiving agent's role is to use this information to build a model with which it can accurately predict neighbor actions and enact local actions. The first step in building this model is to approximate the current state of the network. Given the measurements that the agent collects, there are a number of ways that agent's could

do this. One approach is to use statistical estimation methods, such as a Kalman filter, to produce a high probability estimate of the network state variables. What is used here is a simpler approach. When recent measurements are not available, the agents use default values for the state and control variables (for example the mean values $\bar{\mathbf{x}}$ and $\bar{\mathbf{u}}$), which is provided by the operator with the initial network model. Since each data point is time stamped, the agent replaces old data in its model with new data as it comes in from neighbors.

5.1.3.3. *Build a network model.* Once agent n has built a local estimate of the network state vector $\mathbf{x}_0^{[n]}$ and control vector $\mathbf{u}_0^{[n]}$, it can build a dynamic model of the network, which forms the basis for the equations in its local constraints and the shared constraints in agent n 's reciprocal set. To do this the agent builds the linear dynamic matrices \mathbf{A} and \mathbf{B} through a Taylor series expansion of the network equations. Given that the dynamic equations can be written as shown in 5.1, that the system is sufficiently close to linear to allow for a first order Taylor series approximation (that ξ_T is small), and that the error terms in eqs. 5.3 and 5.4 (ξ_x and ξ_u) are small, the following process can be used to calculate \mathbf{A} and \mathbf{B} .

$$(5.1) \quad \mathbf{0} = \mathbf{g}(\mathbf{u}_k, \mathbf{u}_{k+1}, \mathbf{x}_k, \mathbf{x}_{k+1})$$

$$(5.2) \quad \mathbf{0} = [\nabla_{\mathbf{u}_k} \mathbf{g}] \mathbf{u}_k + [\nabla_{\mathbf{u}_{k+1}} \mathbf{g}] \mathbf{u}_{k+1} + [\nabla_{\mathbf{x}_k} \mathbf{g}] \mathbf{x}_k + [\nabla_{\mathbf{x}_{k+1}} \mathbf{g}] \mathbf{x}_{k+1} + \xi_T$$

$$(5.3) \quad \mathbf{A} \triangleq -[\nabla_{\mathbf{x}_k} \mathbf{g}] = -[\nabla_{\mathbf{x}_{k+1}} \mathbf{g}] + \xi_x$$

$$(5.4) \quad \mathbf{B} \triangleq [\nabla_{\mathbf{u}_k} \mathbf{g}] = [\nabla_{\mathbf{u}_{k+1}} \mathbf{g}] + \xi_u$$

$$(5.5) \quad \mathbf{A}(\mathbf{x}_{k+1} - \mathbf{x}_k) = \mathbf{B}(\mathbf{u}_{k+1} - \mathbf{u}_k)$$

$$(5.6) \quad \mathbf{A} \Delta \mathbf{x}_k = \mathbf{B} \Delta \mathbf{u}_k$$

For most, if not all, large network problems \mathbf{A} and \mathbf{B} will be very sparse matrices (figure 5.3 shows the sparsity patterns of \mathbf{A} and \mathbf{B} for a test system). With these matrices and a few other bits of data the agent can build its control problem.

5.1.3.4. *Choose control actions.* After building a local control problem the agent calculates a set of control actions. Section 5.1.4 describes agent n 's control problem in detail. The outcome of this calculation is a vector of local control actions for the current time period, $\mathbf{u}_{N,0}$ along with estimates of its neighbors' control actions, $\mathbf{u}_{M,0}$ and $\mathbf{u}_{R,0}$. In some cases agents may exchange information (cooperate) after performing an initial calculation to improve the quality of the local solutions. Different approaches to cooperation, such as the negotiation protocol that was tested for this work, are described in Chapter 4.

5.1.3.5. *Implement control actions.* When the current time reaches an agreed upon deadline for implementing the control actions for the current time step (t_c , which will lie somewhere between t_0 and t_1), agent n implements its local set of control actions, $\mathbf{u}_{N,0}$, using its connections to local actuators. During normal conditions (at least in the case of the power system problem, SMP) the new set point will be exactly the same as the current set point ($\mathbf{u}_{N,0} = \mathbf{u}_{N,-1}$), thus the agent effectively takes no action. When the agent finds that it is excessively costly to keep its control variables at their current set point (given its local objectives and constraints), it will make adjustments. After implementing its locally calculated control actions, it continues to collect measured data from other agents until the end of the time horizon, at which time it advances its time horizon and restarts the control process.

5.1.4. Agent n 's control problem. Given a generic objective function that minimizes the discounted costs associated with the predicted trajectory of the network over the time horizon, the resulting control problem for agent n has the form given

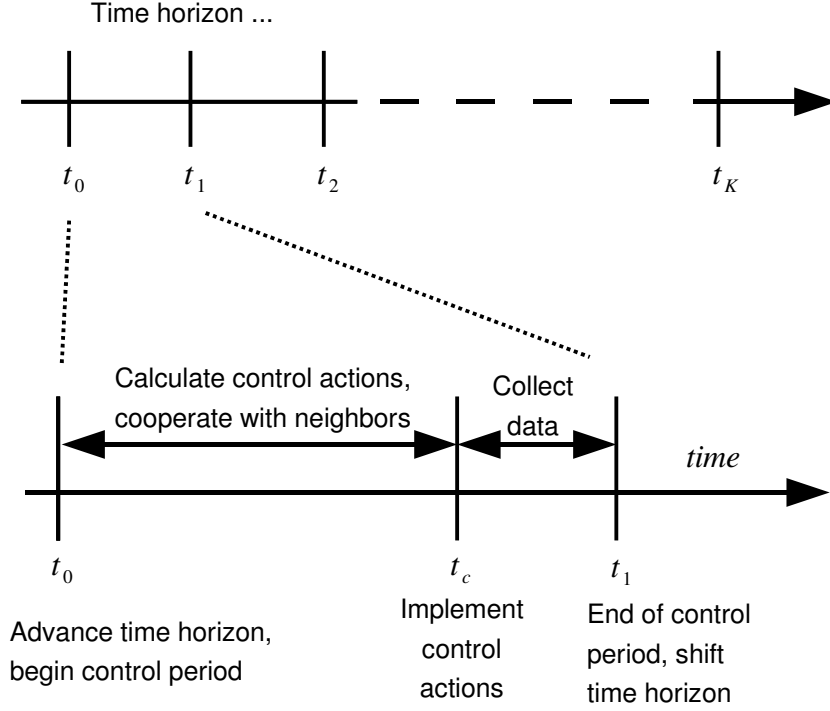


Figure 5.2: A time-line, showing agent activities during a time horizon, and within a single time step. During the first part a the time step agents estimate the state of the network and calculate control actions. After implementing control decisions agents exchange data with other agents until the end of the time step (t_1), at which time the agent advances the time horizon and restarts the process.

in the Agent Control Problem (ACP).

$$\begin{aligned}
 \text{ACP} \quad & \underset{\mathbf{U}}{\text{Minimize}} && \sum_{k=0}^{K-1} \rho^k f(\mathbf{z}_k, \mathbf{z}_{k+1}) \\
 \text{s.t.} \quad & && \mathbf{A}\Delta\mathbf{x}_k = \mathbf{B}\Delta\mathbf{u}_k \\
 & && \mathbf{y}_k = \mathbf{C}\mathbf{x}_k \\
 & && \Delta\mathbf{u}_{\min} \leq \Delta\mathbf{u}_k \leq \Delta\mathbf{u}_{\max} \\
 & && \mathbf{u}_{\min} \leq \mathbf{u}_k \leq \mathbf{u}_{\max}.
 \end{aligned}$$

Unfortunately this problem is difficult to solve in a timely manner for large networks and/or long time horizons. For this scheme to be practical with a one second time step, the solution time must be much less than one second for moderately sized

network problems. Table 5.1 shows the result of several experiments showing changes in solution time given different approaches to this problem. However, if some of the state variables are unlikely to significantly affect the objective function, the sparse nature of \mathbf{A} and \mathbf{B} can be used to substantially reduce the size of the problem. By re-writing the dynamic equation as $\mathbf{x}_{k+1} = \mathbf{x}_k + \mathbf{A}^{-1}\mathbf{B}\Delta\mathbf{u}_k$ it becomes possible to isolate and eliminate the unimportant equations and variables from the problem. If S is the subset of all problem variables that have a significant effect on the problem from agent n 's perspective, with S_u and S_x representing the portions of S for control and state variables respectively, and defining $\hat{\mathbf{A}} \triangleq \mathbf{A}^{-1}\mathbf{B}$, the agent's simplified problem is the following:

$$\begin{aligned} \text{RAP} \quad & \underset{\mathbf{U}}{\text{Minimize}} && \sum_{k=0}^{K-1} \rho^k f(\mathbf{z}_{S,k}) \\ & \text{s.t.} && \Delta\mathbf{x}_{S,k} = \widehat{\mathbf{A}}_{S_x, S_u} \Delta\mathbf{u}_{S,k} \\ & && \mathbf{y}_{S,k} = \mathbf{C}_S \mathbf{x}_{S,k} \\ & && \Delta\mathbf{u}_{S,\min} \leq \Delta\mathbf{u}_{S,k} \leq \Delta\mathbf{u}_{S,\max} \\ & && \mathbf{u}_{S,\min} \leq \mathbf{u}_{S,k} \leq \mathbf{u}_{S,\max}. \end{aligned}$$

This problem can have substantially fewer variables and constraints, but because the $\hat{\mathbf{A}}$ matrix is generally dense, the problem may still be time consuming to solve. Fortunately in at least some large network systems, the structure of $\hat{\mathbf{A}}$ is such that many of its elements are nearly zero. Some of these elements can be set to zero without significantly changing the outcome of the problem. This effect is described in some detail in section 5.3. Every agent uses the following set of rules to decide which entries in $\hat{\mathbf{A}}$ it will set to zero.

- (1) Look at each row of $\hat{\mathbf{A}}$: $\hat{\mathbf{a}}_i = \left[\hat{a}_{i0} \quad \hat{a}_{i1} \quad \dots \quad \hat{a}_{i, n_u} \right]$
- (2) Build another row vector that indicates the distance between the state variable x_i and each control variable u_j . This results in another matrix with

the same dimensions as $\hat{\mathbf{A}}$. Let \mathbf{D} represent this distance matrix, with rows

$$\mathbf{d}_i = \begin{bmatrix} d_{i,0} & d_{i,1} & \dots & d_{i,n_u} \end{bmatrix}.$$

- (3) Set each \hat{a}_{ij} to zero where $d_{ij} \geq r_c$. r_c is a control radius that indicates how many control variables that will act to affect each state variable. r_c is an exogenous variable that can be set by operators.

This procedure has two advantages with respect to the problem decomposition. Firstly, it increases the sparsity of the $\hat{\mathbf{A}}$ matrix. Secondly, it restricts the set of control variables that act in response to a given stress variable problem. If a state variable has exceeded its threshold, increasing the objective function, a limited set of control variables will act to mitigate the problem. The side effect of this action is that agents will not consider the more remote effects of changes to their local control actions. So long as these remote effects are small, this assumption is not particularly problematic. Small errors caused by this assumption can be overcome through feedback and iteration.

5.2. Adaptation to power networks

The adaptation of this algorithm to the optimal stress mitigation problem for power networks (SMP) is relatively straight forward. The linear formulation LSMP (eqs. 3.19-3.24), differs from RAP only in that the objective function has a somewhat more specific format. In the case of a power network, one agent is assigned to each bus (or transmission substation) such that agent n is located at bus n in the power network. If bus n has one block of load and one generator, the agent's set of control variables will include the voltage set point for the local generator, the real power output of the generator and the load scaling variable (Λ_n) that determines the amount of demand that is served from the substation. These three variables comprise \mathbf{u}_N , agent n 's control vector.

In the simulations described here, the time step size is assumed to be 1 second. Each agent chooses the length of the time horizon dynamically according to the rules

$$\begin{bmatrix} \mathbf{A} \\ \mathbf{A} \\ \mathbf{A} \end{bmatrix} \mathbf{x}_{k+1} = \begin{bmatrix} \mathbf{A} \\ \mathbf{A} \\ \mathbf{A} \end{bmatrix} \mathbf{x}_k + \begin{bmatrix} \mathbf{B} \\ \mathbf{B} \\ \mathbf{B} \end{bmatrix} \Delta \mathbf{u}_k \quad (1)$$

$$\mathbf{x}_{k+1} = \mathbf{x}_k + \begin{bmatrix} \hat{\mathbf{A}} \\ \hat{\mathbf{A}} \\ \hat{\mathbf{A}} \end{bmatrix} \Delta \mathbf{u}_k \quad (2)$$

$$\mathbf{x}_{S,k+1} = \begin{bmatrix} \widehat{\mathbf{A}}_{S_x, S_u} \\ \widehat{\mathbf{A}}_{S_x, S_u} \\ \widehat{\mathbf{A}}_{S_x, S_u} \end{bmatrix} \mathbf{x}_{S,k} + \Delta \mathbf{u}_{S,k} \quad (3)$$

Figure 5.3: An illustration of the dynamic constraints in the MPC problem, as they would be represented in the linear programming problem. (1) shows the equation without any reduction. The equation matrices are sparse, but the equations are fairly difficult to solve. (2) shows the equation after making the transformation: $\hat{\mathbf{A}} = \mathbf{A}^{-1}\mathbf{B}$. This equation is simpler, but requires enormous memory due to the dense structure of $\hat{\mathbf{A}}$. (3) shows the equation after removing constraints that were not likely to be binding and setting small values in the $\hat{\mathbf{A}}$ matrix to zero. This reduction makes the LP solution process much faster.

explained previously for the SMP. In the simulations described here the time horizon is set to no more than 6 time steps.

5.2.1. Sample results. Chapter 6 provides a detailed description of the simulation model and presents the results from extensive simulation of this method under a wide variety of conditions. This section describes the results from a few simulations

Table 5.1: Computational requirements for case300-1-1, test #2 from table 5.2 with perfect information. The results show the CPU time required to solve the SMP for this case on an AMD Athlon64 computer, using a MATLAB interface to the Coin-OR LP solver [100]. The LP size is shown in the form: (# of variables)-(# of constraints)-(# of non-zero values in the constraint matrix). These data illustrate the computational advantages of the reduced form of the MPC problem.

<i>Problem</i>	<i>Step number</i>	<i>Time steps</i>	<i>LP size</i> $n-m-nnz(\mathbf{A})$	<i>Solution time</i>	
				<i>LP only</i>	<i>Build & solve</i>
Un-reduced problem	1	7	4530-6030-41676	10.140	12.330
	2	5	4530-6030-41676	5.700	6.850
	3	3	2709-3612-23372	1.780	2.400
	4	1	901-1202-5091	0.130	0.360
	5	1	899-1201-5090	0.140	0.370
Reduced problem with full $\hat{\mathbf{A}}$	1	7	2709-4788-40809	0.294	0.322
	2	5	1895-3390-24482	0.083	0.110
	3	3	1128-2028-14546	0.049	0.076
	4	1	374-674-4337	0.008	0.034
	5	1	372-673-4632	0.007	0.033
Reduced problem with sparse $\hat{\mathbf{A}}$	1	7	1274-2170-8484	0.049	0.051
	2	4	696-1216-4252	0.017	0.019
	3	3	522-912-3245	0.013	0.015
	4	1	172-302-981	0.003	0.011

to demonstrate that the problem decomposition can effectively produce good solutions to the global problem, and to show the effect of some of the parameters in the model. All of the results are for test case “case300-1-1,” which is the same as that used in Chapter 3. Table 5.3 describes the control actions enacted by the agents over the time horizon. Table 5.2 describes the results of these experiments in terms of the following five measures:

- (1) Amount of generation lost (MW)
- (2) Amount of demand that was mechanically shed (MW)
- (3) Number of time steps required to eliminate the initial stress violations (seconds)
- (4) Costs associated with generator and demand reduction (\$)
- (5) The average communication burden over all 300 agents, during the active portion of the simulation (output kbytes/sec/agent)

Measures 1-4 are the same as what was used in Chapter 3. The communication burden measure indicates the amount of inter-agent communication that occurs during the simulation. The more inter-agent communication, the more sophisticated the communication infrastructure required to support this design.

Several important observations should be made from table 5.2. The first group of experiments shows that the interruption costs, due to generation and demand reduction, increases as the voltage control cost increases. This is roughly the same effect that appears in table 3.4. The second group of experiments show the effect of varying the size of the local neighborhood. Increasing this variable causes a clear increase on the communication burden. The effect on the overall quality of the control results is negligible for this particular case, though the average effect over many cases (see Chapter 6) is more clear. In the third group of experiments, the size of the extended neighborhood (r_e) is varied. These tests show a fairly clear decrease in demand lost/cost, and a fairly clear increase in communication burden, as r_e increases. The final set of experiments show the effect of changes to the control radius (r_c). While a linear relationship is not apparent, in general a large control radius results in improved quality, at the cost of making the problem more difficult to solve, and occasionally resulting in more disagreement among agents with respect to what actions to take to respond to a particular problem. A control radius of 4 was used for most of the experiments described in this thesis as this tends to give sufficiently good results.

5.3. Properties of the network operations problem

The OOP describes a time-domain MPC problem with a general objective function and an unspecified set of non-linear constraints representing the network dynamics. Starting with the linearized agent control problem (ACP), one can derive several interesting properties about the challenges associated with the control of complex networks with only local information.

Table 5.2: Test results that show the effects of changes to various parameters in the agent MPC problems

<i>Test #</i>	r_l	r_e	r_c	$c_{\Delta V_G }$	<i>Time Steps</i>	P_G lost	P_D lost	<i>Cost</i>	<i>Comm. Burden</i>
1	3	10	6	10000	5	142.8	110.5	\$66,581	10.99
2	3	10	6	20000	5	142.8	110.7	\$66,785	10.95
3	3	10	6	100000	4	173.6	112.3	\$70,019	14.1
4	1	10	6	20000	5	135.8	110.1	\$63,403	5.34
5	2	10	6	20000	5	140.3	109.7	\$64,873	7.43
6	3	10	6	20000	5	142.8	110.7	\$66,785	10.95
7	4	10	6	20000	5	133.0	110.7	\$65,391	15.79
8	5	10	6	20000	5	133.9	110.5	\$65,276	21.97
9	6	10	6	20000	7	154.9	114.8	\$68,443	22.35
10	3	7	6	20000	6	612.6	126.7	\$141,753	8.17
11	3	8	6	20000	4	237.2	128.4	\$80,068	12.24
12	3	9	6	20000	5	324.2	111.8	\$91,354	10.44
13	3	10	6	20000	5	142.8	110.7	\$66,785	10.95
14	3	11	6	20000	4	131.6	101.5	\$50,512	15.18
15	3	12	6	20000	5	131.5	101.4	\$50,433	12.37
16	3	10	3	20000	5	153.3	120.6	\$102,103	10.79
17	3	10	4	20000	4	153.5	112.0	\$67,122	14.96
18	3	10	5	20000	5	263.9	113.4	\$80,403	12.37
19	3	10	6	20000	5	142.8	110.7	\$66,785	10.95
20	3	10	7	20000	5	156.8	140.2	\$75,806	10.95
21	3	10	8	20000	5	197.0	141.8	\$80,669	10.96

In order to simplify the analysis somewhat, it is necessary to make several reasonable assumptions about the ACP. Firstly, I assume that the objective can be written such that the Hessian has non-zero elements only along the diagonal. In other words, the objective function does not include interaction terms among variables. Most practical MPC problems can be written in this form. Typically, a control objective is a sum of costs that come from a simple function of each individual control and state variable. For example, a common control objective is to minimize the sum of individual control action costs plus a function of the distance between the expected trajectory, and a goal trajectory (x_g); eg:

$$\text{Minimize}_U \quad c_u^T \mathbf{u} + \sum_{i=1}^n \varsigma_i (\|x - x_g\|_2^2).$$

Table 5.3: Detailed agent control actions from case300-1-1, test 3. The control actions column shows the location and amount of change in generator bus voltage (dVg), generator power output (dPg), or load (dPd) at each time step.

<i>Time</i>	<i>Control actions</i>	$\max(I / I _{\max})$	<i>Worst</i> $ V $	$ V _{\min}$
5	[Pre-disturbance condition]	0.7786	0.9290	0.92
6	[Post-disturbance condition]	1.6252	0.8548	0.92
7	dPd_141=-42.9 dPg_7=-36.5 dPg_8=-10.2 dVg_7=0.0080 dVg_8=0.0080 dVg_10=0.0061 dVg_32=0.0160 dVg_34=0.0075	1.3363	0.8749	0.92
8	dPd_141=-24.7 dPg_7=-13.4 dPg_8=-9.9 dVg_10=0.0018 dVg_34=0.0160	1.2073	0.8976	0.92
9	dPd_141=-24.7 dPg_8=-3.0 dPg_33=-28.9 dVg_30=0.0049 dVg_34=0.0077 dVg_41=0.0160	1.0312	0.9124	0.92
10	dPd_141=-8.1 dPg_30=-5.8 dPg_41=-1.8 dVg_34=0.0053 dVg_41=0.0036 dVg_43=0.0100	1.0003	0.9201	0.92
11	dPg_42=-0.0 dVg_41=0.0000	0.9992	0.9201	0.92
12	[Final condition]	0.9992	0.9201	0.92

Even where interaction terms do exist in the problem's natural objective function, they can be moved to the constraints through the creation of dummy variables, without making any substantive change to the formulation.

Secondly, as is done in the formulation of the ACP, I assume that the linearized dynamic equations are a reasonable approximation to the actual dynamics of the system, at least for small control steps. If this is true, the dynamics can be represented by an equation of the form:

$$\mathbf{A}(\mathbf{x}_{k+1} - \mathbf{x}_k) = \mathbf{B}(\mathbf{u}_{k+1} - \mathbf{u}_k)$$

$$\mathbf{A}\Delta\mathbf{x}_k = \mathbf{B}\mathbf{u}_k,$$

where \mathbf{A} and \mathbf{B} are very sparse matrices that describe interactions between control and state variables in the problem. While few networks actually have linear dynamics, it is often the case that linear models provide good approximations so long as the time steps are fairly small. It is important to note that unlike the standard state-space model, which in its discrete form is typically written as $\mathbf{x}_{k+1} = \mathbf{A}\mathbf{x}_k + \mathbf{B}\mathbf{u}_k$, \mathbf{A} affects

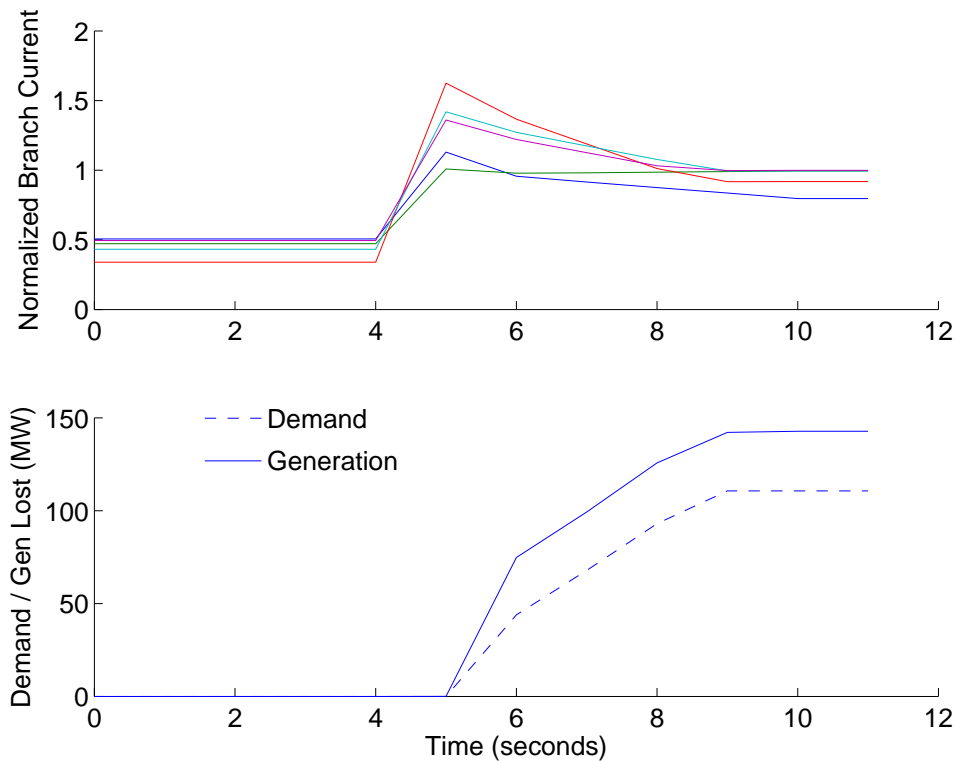


Figure 5.4: Time series trajectory of branch current magnitudes (normalized such that 1.0 is the limit for all branches) and total generation and demand lost during case300-1-1, test #2 (see table 5.2). This plot shows the similarity between the agent actions and the actions of the global algorithm, as shown in figure 3.5. As shown, the disturbance occurs at 5 secs. causing an initial set of current violations, which are incrementally mitigated over a period of 5 seconds.

both the current and next time step, making the model an algebraic equation that requires a linear system solution to solve. If \mathbf{x} is a true set of linearly independent state variables, \mathbf{A} will be a square matrix. If the problem has n state variables, and m control variables, $\mathbf{A} \in \mathfrak{R}^{n \times n}$ and $\mathbf{B} \in \mathfrak{R}^{n \times m}$. Some variant of this property is common to many network problems, particularly those with non-linear flows that are difficult to control individually. Networks that show these properties include electrical systems that operate according to Kirchhoff's laws and fluid piped systems that operate according to Bernoulli's equations.

Finally, in order to more explicitly show the effect of constraints on the output variables, instead of including these in the objective function, they show up in the constraints. If the stress/output variables have hard constraints (instead of the soft

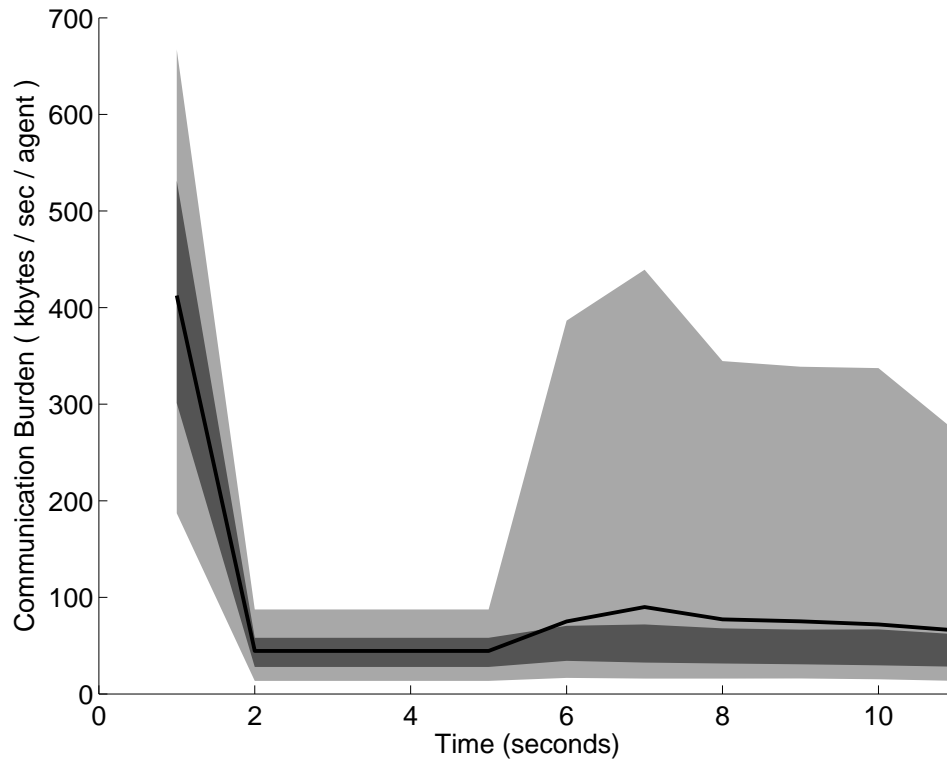


Figure 5.5: Time series plot showing the amount of data exchange (in KB sent/agent/second) required by the agent algorithm for the 300 bus system. The results shown here are for case300-1-1, test #2 from table 5.2, with a 1 second step size in the simulation. The light gray area shows the inner 90 percentile region, the dark gray shows the inner 50 percentile region, and the black line shows the mean. The Initially large communication burden (at $t = 1.0$) comes from the agents' exchanging their initial state data during the first time period. During normal operation, this exchange would be spread out over a long time period. The communication burden increases again (for a subset of the agents) after the initial violations occur, and the agents begin to exchange data about their stress variables.

constraints described in Chapter 3), it is also reasonable to assume that the objective function is continuously differentiable.

Thus our network MPC problem, with a discrete time horizon that spans $\{t_0, t_1, \dots, t_K\}$, has the form:

$$\begin{aligned}
& \underset{\mathbf{U}}{\text{Minimize}} && \sum_{k=0}^K \rho^k \sum_i f_i(\mathbf{z}_{ik}) \\
& \text{s.t.} && \mathbf{A}\mathbf{x}_{k+1} = \mathbf{A}\mathbf{x}_k + \mathbf{B}\Delta\mathbf{u}_k \\
& && \mathbf{y}_{\min} \leq \mathbf{C}\mathbf{x}_k \leq \mathbf{y}_{\max} \\
& && \Delta\mathbf{u}_{\min} \leq \Delta\mathbf{u}_k \leq \Delta\mathbf{u}_{\max} \\
& && \mathbf{u}_{\min} \leq \mathbf{u}_k \leq \mathbf{u}_{\max}.
\end{aligned}$$

Limiting our focus to a two period (t_0 and t_1) MPC problem, assuming that \mathbf{C} is an identity matrix, and applying the reduction used in RAP, one gets the formulation below:

$$\begin{aligned}
& \underset{\mathbf{u}_1}{\text{Minimize}} && C(\mathbf{z}_0, \mathbf{z}_1) = \sum_{k=0}^1 \rho^k \sum_i f_i(\mathbf{z}_{ik}) \\
& \text{s.t.} && \mathbf{y}_{\min} \leq \mathbf{x}_0 + \mathbf{A}^{-1}\mathbf{B}(\mathbf{u}_1 - \mathbf{u}_0) \leq \mathbf{y}_{\max} \\
& && \mathbf{u}_{\min} \leq \mathbf{u}_1 \leq \mathbf{u}_{\max}.
\end{aligned}$$

Defining multipliers $\lambda_{(+)}$, $\lambda_{(-)}$, $\mu_{(+)}$, and $\mu_{(-)}$ to reflect the shadow costs of the inequality constraints, the Lagrangian function for this formulation can be written as:

$$\begin{aligned}
\mathcal{L} &= C(\mathbf{z}_0, \mathbf{z}_1) - \lambda_{(-)}^T (\mathbf{y}_{\min} - \mathbf{x}_0 - \mathbf{A}^{-1}\mathbf{B}(\mathbf{u}_1 - \mathbf{u}_0)) \\
&\quad - \lambda_{(+)}^T (\mathbf{x}_0 + \mathbf{A}^{-1}\mathbf{B}(\mathbf{u}_1 - \mathbf{u}_0) - \mathbf{y}_{\max}) \\
&\quad - \mu_{(-)}^T (\mathbf{u}_{\min} - \mathbf{u}_1) - \mu_{(+)}^T (\mathbf{u}_1 - \mathbf{u}_{\max}).
\end{aligned}$$

If $\lambda = \lambda_{(-)} - \lambda_{(+)}$ and $\mu = \mu_{(-)} - \mu_{(+)}$, the first-order optimality conditions include the following:

$$(5.7) \quad \nabla_{u_1} \mathcal{L} = \nabla_{u_1} C(\mathbf{z}_0, \mathbf{z}_1) + \lambda^T \mathbf{A}^{-1} \mathbf{B} + \mu \odot \mathbf{u}_1 = 0$$

$$(5.8) \quad \nabla_{x_0} \mathcal{L} = \nabla_{x_0} C(\mathbf{z}_0, \mathbf{z}_1) - \lambda \odot \mathbf{x}_0 = 0.$$

Defining the matrix $\hat{\mathbf{A}}$ as:

$$\hat{A} = A^{-1}B = \begin{bmatrix} \hat{a}_{1,1} & \cdots & \hat{a}_{1,n} \\ \vdots & \hat{a}_{i,j} & \vdots \\ \hat{a}_{m,n} & \cdots & \hat{a}_{m,n} \end{bmatrix},$$

gives the following set of conditions:

$$(5.9) \quad \frac{\partial C_i}{\partial u_i} + \lambda_1 \hat{a}_{1,i} + \dots + \lambda_m \hat{a}_{m,i} + \mu_1 u_1 + \dots + \mu_n u_n = 0 \quad \forall i = 1 \dots n$$

$$(5.10) \quad \frac{\partial C_j}{\partial x_{0,j}} + \lambda_j x_{0,j} = 0 \quad \forall j = 1 \dots m$$

As in all optimization problems the inequality multipliers, λ and μ , are non-zero when the constraints are binding, and indicate the cost of the binding constraint when the constraint is binding. Eq. 5.10 indicates that measurement and estimation errors (errors in \mathbf{x}_0) will result in the optimization algorithm giving a proportionally erroneous estimates of λ . Errors in λ will in turn affect control variable choices according to 5.10, but only when the relevant elements of $\hat{\mathbf{A}}$ are significantly different from zero. This is an important result for network problems because the elements of $\hat{\mathbf{A}}$ tend to decay with the distance between the control and state variables. If the problem is decomposed such that agent i has responsibility for variable u_i , and can accurately measure \mathbf{x}_0 in its local neighborhood, errors in the calculation of λ will also decay with distance. If the problem decomposition is a good one, and if both measurement errors and the elements of $\hat{\mathbf{A}}$ decay sufficiently with distance, the

agent's local decisions are likely to align well with the global problem, even in the midst of remote measurement errors.

5.3.1. Sensitivity decay. The conditions given in 5.9 indicate that errors in Lagrange multiplier estimates will affect a given control variable choice in proportion to the corresponding row of the matrix $\hat{\mathbf{A}} = \mathbf{A}^{-1}\mathbf{B}$, which has rows $\hat{\mathbf{a}}_i = [\hat{a}_{i,1} \ \dots \ \hat{a}_{i,m}]$. Due to the sparsity of \mathbf{A} and \mathbf{B} in most network problems, the magnitudes of the elements of $\hat{\mathbf{a}}_i$ decay with distance between the node corresponding to associated control and state variables. Due to the matrix inversion, $\hat{\mathbf{A}}$ is a nearly full matrix. If \mathbf{D} ($\mathbf{D} \in \mathfrak{R}^{n \times m}$) is a matrix with each d_{ij} indicating the distance between x_i and u_j , the sensitivity decay rule can be written:

$$(5.11) \quad |\hat{a}_{ij}| \propto d_{ij}^{-1}.$$

In words, the magnitude of $|\hat{a}_{ij}|$ is roughly proportional to the inverse of the distance between i and j .

5.3.2. Illustrating sensitivity decay. To illustrate the sensitivity decay effect, the results that follow show that (a) sensitivity decay exists in simple network problems, and that (b) local changes propagate through a network differently depending upon the structure of the network. Specifically, the results show how the terms of $\hat{\mathbf{a}}_i$ decay with distance given a simple set of network constraints and several different network structures. The network constraints used here simulate a set of nodes connected by resistors in a simple DC electricity network. The control variable at each node is the amount of current injected by a current source at that node. The state variable at each node is the amount of current that flows from the node, through a $1 \ \Omega$ resistor, to ground, which will be equal to the voltage at that node. The links in each graph are $1 \ \Omega$ resistors that connect node pairs. Figure 5.6 shows a diagram of this system. In this simple system \mathbf{B} is an identity matrix, and \mathbf{A} implements Kirchhoff's laws for each node in the DC circuit. The dynamic constraints (\mathbf{A} and \mathbf{B})

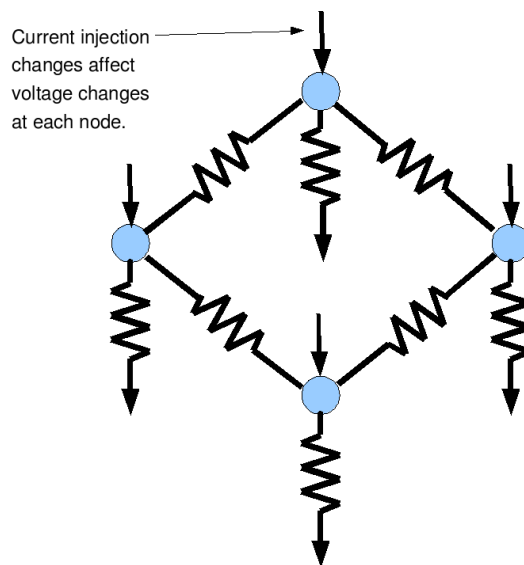


Figure 5.6: Illustration of the simple resistor circuit used for testing network structures. The state variables are the currents that flow to ground, and the control variables are current injections at each node. Because all of the resistors are 1Ω , the currents flowing to ground and the voltages at each node are equivalent ($I_{a0} = V_{a0} \forall a$).

consist of equations of the form:

$$(5.12) \quad \sum_{j \in M_i} (x_{1i} - x_{1j}) = \sum_{j \in M_i} (x_{0i} - x_{0j}) + u_{1i} - u_{0i}$$

where M_i gives the set of nodes connected to node i , at which u_i and x_i are located. While eq. 5.12 represents a simple DC electricity network fairly well, it also has some relationship to the equations that would represent other network flow problems such as gas pipeline flows (where the state variables give pressure, and control variables are gas injections at nodes), sewage flows, or traffic in a congested road system.

Applying this simple model to an unconnected set of nodes, two circular graphs, a random graph, a scale-free network and a power network provides some insights into the properties of these graph structures (see fig. 5.7 for pictures of these structures). The parameters for the scale free and random networks were chosen to give graphs that have the same number of vertexes and edges as the IEEE 300 bus network (300

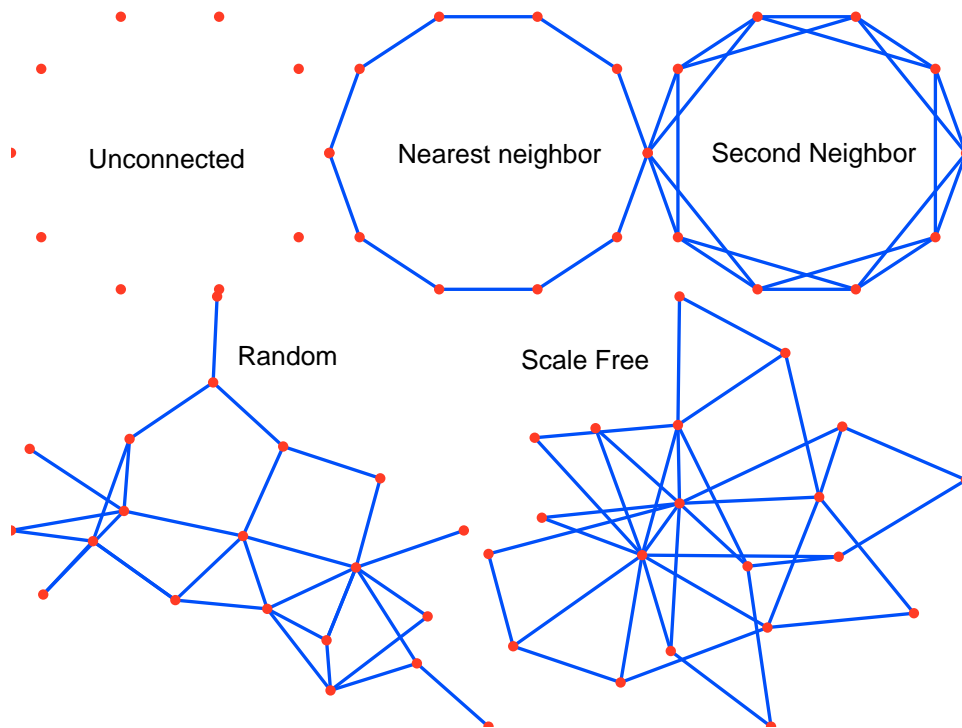


Figure 5.7: Example graphs for network structures 1–unconnected, 2–nearest neighbor, 3–second neighbor, 4–random [26], 5–scale free [101].

nodes, 411 branches²). Thus we have six networks with similar sizes, whose properties we can compare to learn about the potential for decentralized control of each network.

To do so, it is useful to define a measure of relative sensitivity ($s_{i,j}$), which is defined as the magnitude of the change in x_j given a change in u_i that produces a one unit change in x_i . Since $\hat{\mathbf{A}}$ gives the partial derivatives of each x_i with respect to all u_j , $s_{i,j}$ is:

$$s_{i,j} = |\hat{a}_{i,j}/\hat{a}_{i,i}|.$$

Figure 5.8 shows how $s_{i,j}$ decays with graph distance in the six 300 node networks. In each network, except for the scale-free graph, $s_{i,j}$ decays exponentially (linearly in log-space) with the distance between i and j . The sub-linear decay in the scale-free network likely comes from the way that its hubs allow remote changes to propagate through the network more easily. While all six networks show a similar decay with

²Due to the random generation of branches, the scale-free graph only had 410 branches, not 411.

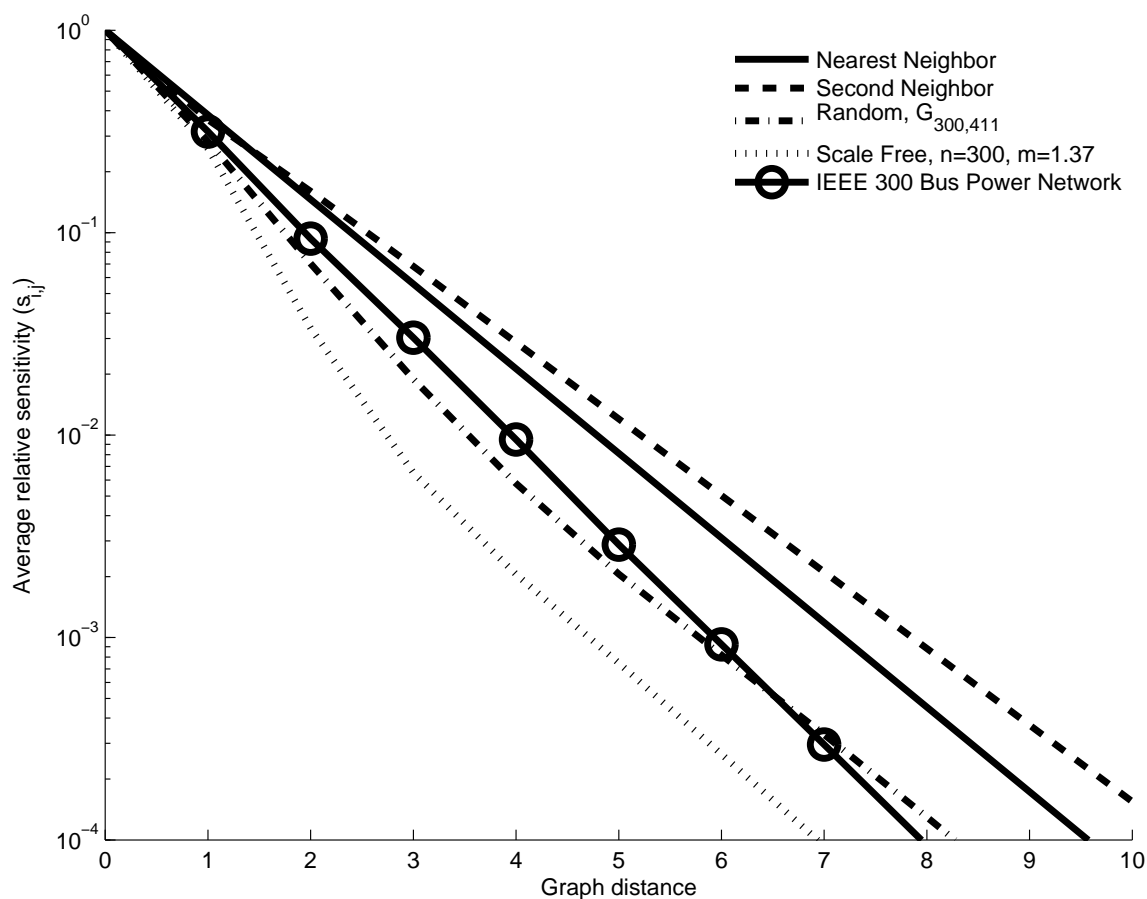


Figure 5.8: As the distance between a control variable and a state variable increases, the extent to which control changes will effect the state variable decrease. This figure shows how $s_{i,j}$ (a measure of sensitivity between control variables and state variables in the resistor networks) changes with distance ($d_{i,j}$) for several network structures. Each point shows the average of all $s_{i,j}$, where $d_{i,j}$ is the graph distance shown on the horizontal axis. In all of the networks $s_{i,j}$ decays roughly exponentially with the graph distance between the two variables.

distance, the networks differ substantially in the spacial dispersion of a given control variable change. By counting the number of nodes that are affected by a 1 V change at nodes in the network, figure 5.9 shows how disturbances or control changes propagate differently through the various networks. The structure of a network can significantly change the way that changes propagate through the network.

This result is particularly important if one wants to design a decentralized control algorithm for these networks. In the case of the unconnected graph (not shown on figures 5.8 or 5.9) control variable changes only affect the local state variable, so

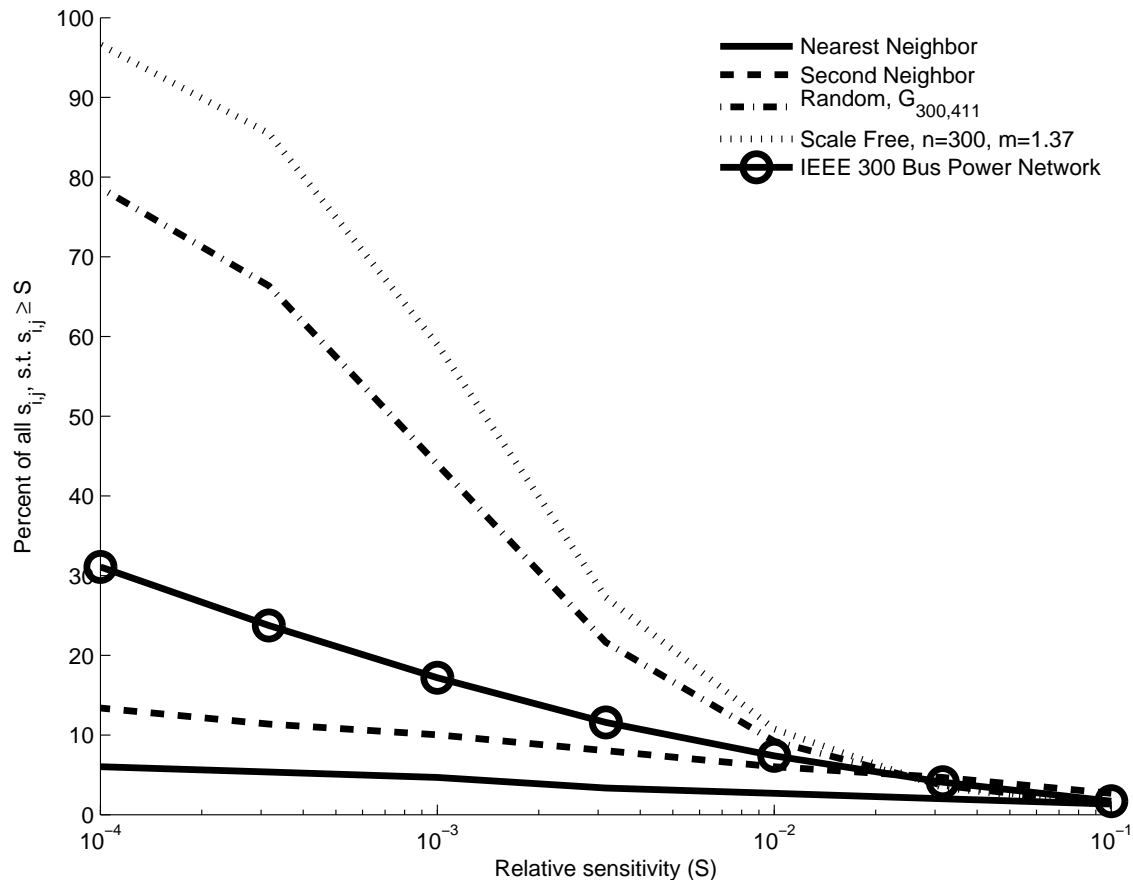


Figure 5.9: The percent of all node pairs in each network (i, j) for which have a substantial influence $(s_{i,j})$ upon each other, given different influence/sensitivity thresholds, S . This figure shows that the effects of a change at one location will disperse more broadly through the networks that show up higher on the vertical axis (namely the scale free and random graphs). When relative sensitivity $s_{i,j}$ is consistently high throughout a network, the network may be more difficult to control using decentralized methods, because more information is needed to consider these effects.

sensitivity falls off with distance as a step function. The decomposition of a control problem for the unconnected network is trivial—allow each agent to measure and control only its local variables. Since in an unconnected network, all of off-diagonal $s_{i,j}$ are zero, this type of decentralized control will work well as long as the objective is separable. For the simple nearest neighbor and second neighbor graphs, control changes only have significant effects on a small percentage of the whole network (with a sensitivity threshold of 0.0001, less than 15% of the network would be affected in both cases). If an agent can obtain good measurements for 15% of the state variables

Table 5.4: Descriptive statistics for the 6 example networks tested in Chapter 4

Network	Vertexes	Edges	Avg. Degree	Diameter
1. Unconnected	300	0	0.00	∞
2. Nearest neighbor	300	300	2.00	151
3. Second neighbor	300	600	4.00	76
4. Random graph	300	411	2.96	13
5. Scale free network	300	411	2.71	10
6. IEEE 300 bus network	300	410	2.74	25

closest to its local node and control variable (u_i), it can approximately calculate the optimal u_i^* , by ignoring all of the variables outside of this 15% of the network. On the other hand the random graph and the scale-free network, present a different story. In both cases more than 75% of each network lies within the 0.0001 sensitivity threshold, and over 40% is within the 0.01 threshold, indicating that any control variable change will have a significant effect on almost the entire network. The power network, on the other hand, shows a moderate level of sensitivity propagation (only slightly more than that of the second-neighbor network), indicating that problem decomposition is challenging, but, as indicated by examples described in this thesis, feasible. The structure of power networks makes decentralized control feasible in a way that is common to some, but not all, other network structures.

5.4. Discussion

This chapter describes a method by which the Optimal Operations Problem (or at least some permutations of the OOP) can be decomposed and solved by agents located at nodes scattered throughout a large network system. Apart from a set of initial settings provided by an operator, the agent-based control system can operate without the help of centrally located facilities. Results from application of this method to an AC electrical power network indicates that the method is both effective, and that the inter-agent communications required by the method are well within the capabilities of standard communications hardware. This result is further verified in Chapter 6.

The proposed approach exploits the fact that the dynamic equations for network problems can often be represented by sparse matrices. This structure results in control-to-state variable sensitivities that decay with the distance between the respective control and state variables. This effect has been demonstrated through experiments with simple resistor networks. These experiments indicate that the structure of a network dramatically affects the extent to which decentralized control methods will be effective.

CHAPTER 6

Verification

This section describes the data, methods and results used to verify that the proposed algorithm can meet the primary objective of this work—reducing the costs associated with cascading failures in electrical power networks. The primary mode of verification is the simulation of the control scheme on randomly sampled perturbations of the IEEE 300 bus network. As with any verification method for a large, complex system, the results hold only given a set of model-reducing assumptions. The simulation model used in the verification process is based upon the AC power flow equations, but captures the most important components of power system dynamics, particularly focusing on the discrete dynamics which are important to cascading failures.

It is important to note that the simulation/verification model described here differs substantially from the simple network models that the agents use while solving their MPC problems. The simulation model is a moderately sophisticated representation of the power system dynamics. The agents use very simple predictive models with linear equations to calculate how they will interact with the more accurate network model. The agents compensate for modeling inaccuracies through feedback from the non-linear power system model.

By simulating the proposed multi-agent control scheme over a wide variety of operating conditions, and under many different stress conditions I show that the method can dramatically reduce the costs associated with the vast majority of large cascading failures.

6.1. Simulated network data

In order to demonstrate that this method can effectively control cascading failures in a moderately sized power network, the IEEE 300 bus network was chosen as a test case. While smaller than most industry models of US power networks, the IEEE 300 bus system is sufficiently large to capture many of the features of larger networks. Unfortunately for the purpose of this work, the base case system is fairly robust to failures, and does not include flow limits for the transmission lines or transformers. Also, some portions of the network are connected to the whole by only one transmission line, in violation of the “N-1” rule commonly used in power system operations.

In order to build a set of test cases that reflect a variety of operating conditions, ten versions of the 300 bus network were designed, each with a distinct set of operating parameters. For each of the ten cases, ten disturbances were randomly selected to create a set of stressed conditions for each case. The process for creating the test cases follows:

- (1) Randomly assign values (in the range \$100-\$10,000 / MW interrupted) to each load in the system to indicate the relative costs associated with interrupting load at each bus.
- (2) Add a parallel, duplicate branch (transmission line or transformer) at each location (node-pair) where removing the existing branch would separate the network into 2 sub-networks.
- (3) Randomly perturb the demand (\mathbf{P}_D and \mathbf{Q}_D) and generation (\mathbf{P}_G) to obtain a new operating state, scaling the generation as needed to get a system for which the AC power-flow equations converge.
- (4) Iteratively remove each branch in the system, recording the maximum current flow on each branch, and the minimum and maximum voltages in the network.
- (5) Select branch current and bus voltage limits such that no single branch outage causes a voltage or current violation.

- (6) Randomly choose a set of branch outages through draws from a Bernoulli trial with probability 0.01 (each branch fails with probability 0.01). Discard any disturbances that do not create voltage or current violations, or that result in a case for which the power flow does not converge.
- (7) Repeat step 5 to obtain 10 disturbances that cause voltage and current violations.
- (8) Repeat steps 1-7 to obtain 10 cases, each with 10 disturbances.

The result is 100 test cases to which various control methods can be applied. The cases are numbered from “case300-1-1” (the first case, with the first disturbance) through “case300-10-10” (the tenth case with the tenth disturbance). The disturbances are generally severe with between 3 (case300-3-4) and 14 (case300-1-8) branch outages that result in many current and voltage violations dispersed throughout the network. Given the simulation method below, about 30% of these events result in system-wide cascading failures, where all the load is lost (see figure 6.2).

6.2. Power system simulation

Cascading failures in power networks are a consequence of interactions between the continuous and discrete dynamics in the system. The discrete dynamics largely result from relays designed to protect equipment from damage. The continuous dynamics result from interactions between rotating machines via electrical energy flowing over the transmission network. In the later stages of most cascading failures, the voltages and currents will oscillate with wavelengths of several seconds. In order to simulate such a late stage failure, one needs a dynamic power system model that accurately represents the parameters of each machine (inertia, damping, control settings, governors, etc). However, in the vast majority of cascading failures, the network does not begin rapid oscillation until the final seconds of the event. For example according to [10], the Western Interconnect on Aug. 10, 1996 did not experience any major oscillation between the time of the initial disturbance (15:42:37) and 5 minutes later

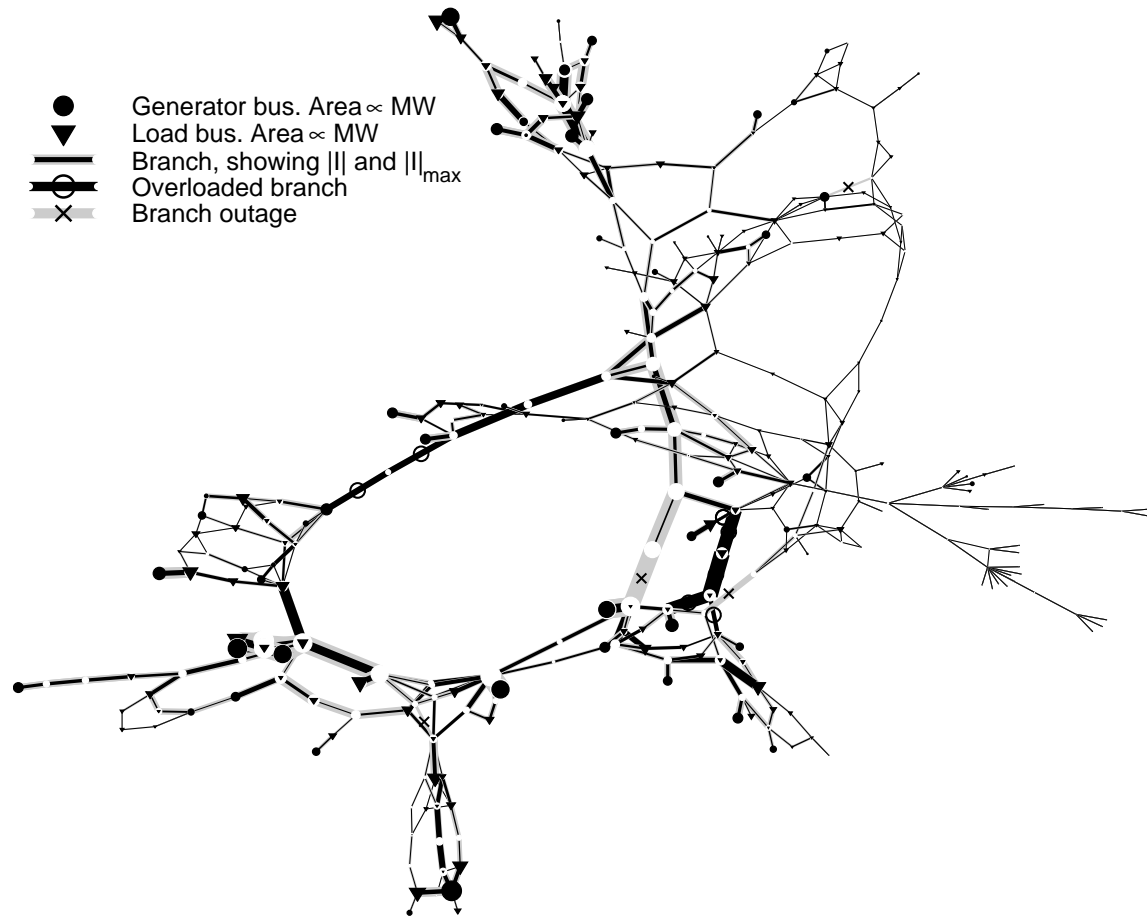


Figure 6.1: A depiction of “case300-10-3,” one of the more severe cases in this set. The initial disturbance of 4 branch outages (marked with an X) results in 7 branches with over-current violations (marked with an O).

(15:47:37) when 5 major hydroelectric machines failed. Between these two points the cascading failure propagated through the sequential overloading of transmission lines, with relays removing them from service. Even after 15:47:37, the oscillations remained small until 15:48:45 at which point the network rapidly broke into four islands.

With this in mind, the cascading failure simulator captures the discrete dynamics associated with branch relays, but largely neglects the machine rotor dynamics, which are important only during later stages of an event. The simulator uses an AC power-flow model to calculate voltages and currents at each time step, within each connected portion of the network. To ensure that all generators participate equally in load

balancing, the output power of each generator is scaled such that the slack bus does not change disproportionately. The generator maximum output limits are neglected by this portion of the algorithm, since most of these adjustments are small. When the AC power-flow fails to find a feasible solution, the load and generation are reduced in 25% blocks to approximately simulate the actions of under-frequency load shedding relays. Finally time over-current relays at each branch remove overloaded branches from service.

The time over-current relays operate by updating an overload memory variable at each time step. The over-current relays operate when overload (the integral of the current above the limit) exceeds a threshold value. The threshold value is set such that the branch can remain at its emergency rating (which is about 30% higher than the over-current limits) for 5 seconds before resulting in a relay operation. If o_{ik} represents the overload memory variable for branch i at time t_k , and $|I_{ik}|$ is the corresponding current magnitude, the following expression holds:

$$o_{ik} = \begin{cases} o_{i,k-1} + \Delta t \left(\frac{|I_{ik}| + |I_{i,k-1}|}{2} - |I_i|_{\max} \right), & |I_{ik}| > |I_i|_{\max}, |I_{i,k-1}| > |I_i|_{\max} \\ o_{i,k-1} + \Delta t \frac{(|I_{ik}| - |I_i|_{\max})^2}{|I_{ik}| - |I_{i,k-1}|}, & |I_{ik}| > |I_i|_{\max}, |I_{i,k-1}| \leq |I_i|_{\max} \\ 0, & |I_{ik}| < |I_i|_{\max} \end{cases}$$

This expression adds the excess current to the memory variable at each time step, or zeros out o_{ik} if the current dips below the threshold. This is roughly equivalent to the actions of actual time-over-current relays, as would be used in a power system. The simulated relays will trip fairly quickly if the overload is extreme. If the overload is smaller, the relays allow it to persist for tens of seconds, simulating the action of a transmission line sagging into a tree.

In the results presented here, each simulation lasts for 60 seconds/time steps (each time step approximately simulates one second). The disturbance (branch outages) occurs after 5 seconds; thus the network does not change during the initial 5 steps of a simulation. At the end of the simulation the blackout size is recorded in terms of

the MW of demand interrupted, the number of transmission lines tripped by relays and the overall interruption cost of the event, given the costs assigned to individual loads and system components. The following are the three components of the cost measure:

- the cost-weighted sum of the demand lost during the cascading outage,
- the cost-weighted sum of changes to generator output power (\$30/MW increase + \$60/MW decrease), and
- a penalty (\$1000/violation) for voltage or current violations that remain at the end the simulation.

The simulation algorithm thus includes the following steps:

- (1) Calculate voltages and currents using an AC power-flow.
- (2) Depending on the type of simulation, calculate control actions. In a cascading failure simulation no controls are calculated. In a global-MPC simulation the system uses the SMP to calculate controls for the entire network. In a sequential agent-based MPC simulation (see simulation method 1 below), each agent calculates its controls independently.
- (3) Implement control actions calculated above (if any).
- (4) Implement disturbances that occur at this time period (only occurs at $t = 5$ sec.).
- (5) Update the relays in the network, and remove branches corresponding to tripped relays.
- (6) Advance the simulation time ($t = t + 1$), and repeat from 1.

Figure 6.2 shows the blackout sizes that result from applying this method to all 100 cases. The results labeled “Base” show the cascading failure sizes in terms of the amount of demand interrupted and the overall interruption cost. The results labeled “MPC” show the change in outcome after applying the global MPC/SMP algorithm to the cascading failure simulation.

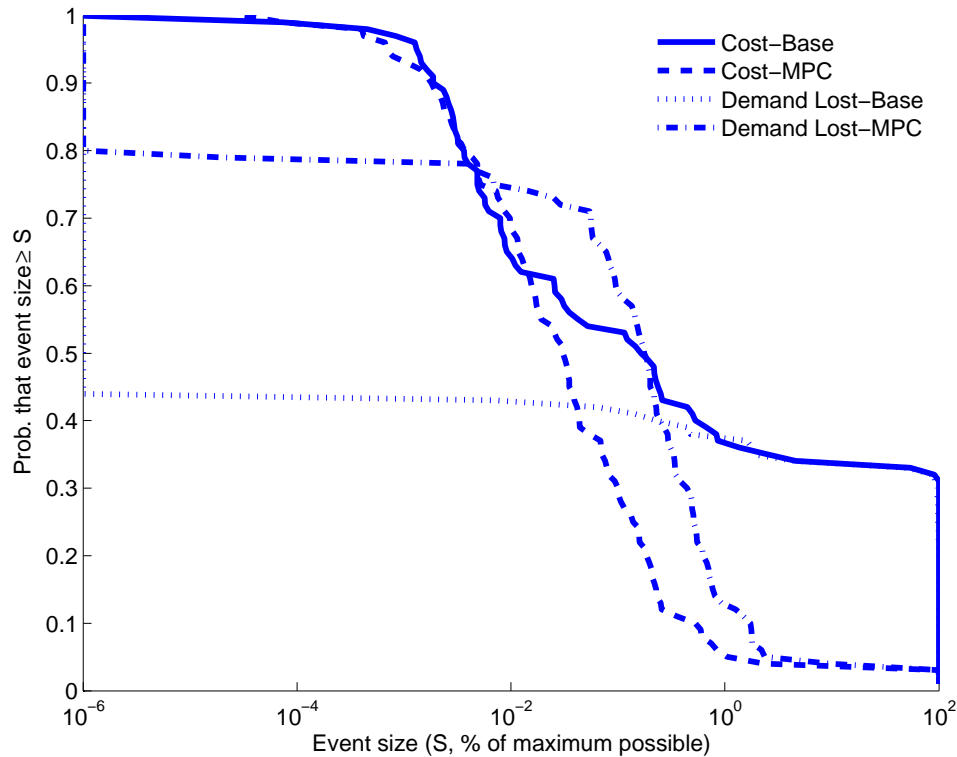


Figure 6.2: The cumulative probability (frequency) distribution of simulated blackout sizes for the 100 test cases. The “Base” results show the event sizes without mitigating control actions. The “MPC” results show event sizes after applying the SMP method to each event sequence. This figure shows that the MPC approach dramatically reduces the probability and size of large cascading failures. It also shows that the method is not stochastically dominant over the base case—the probability of some small blackouts increases slightly.

6.3. Simulation Method 1: Sequential code

In simulation method 1, each agent is designed to perform its calculations sequentially, though in such a way that all of the agents’ control actions are enacted simultaneously at the beginning of each time step. While it is an imperfect representation of agent actions, this method is a close approximation so long as the calculations and communications that occur are small relative to the capabilities of current computational and communications technology. As described in Chapter 5, the time required for an agent to calculate its control actions is small (generally about 0.01 second), so the computational aspect of this assumption is reasonable. The inter-agent communication requirements for various versions of the simulated multi-agent

system are shown in figure 6.5. While the quantity of inter-agent communication is significant, in most cases it is not beyond the capabilities of current communications technology.

The results shown in Figures 6.3-6.5 show the relationship between the size of the agents' local neighborhoods (essentially their inner reciprocal sets) and the control outcomes. Figure 6.3 shows the results from experiments with agents using the “simple reciprocal altruism” algorithm. Figure 6.4 shows the results from experiments with the “simple reciprocal altruism with negotiation” algorithm. In the former case, as the size of the local radius increases, at least for $r_l \in \{1, 2, 3\}$, the quality of the outcome increases. In terms of the measures shown, the average cost over all 100 blackouts decreases. In Figure 6.4, the quality of the outcome is constant across the different neighborhood sizes, indicating that the negotiation can overcome data errors that result from incomplete information in the cases with small inner neighborhoods. Figure 6.5 essentially shows the communications bandwidth requirements for the various methods. Finally, Figure 6.6 shows the change in cost for all 100 cases between the “No Control” and agent-based control cases. This figure shows a potential risk associated with this method—that there may exist some conditions under which the control method would cause a larger cascading failure, rather than decreasing the size. While these cases are not common, the simulation results indicate that they do exist. Future work will look for ways to reduce the likelihood that the control agents will take actions that are worse than what would result without remedial control actions.

6.4. Simulation method 2: Parallel code

To confirm that this algorithm can operate within the constraints of existing communications technology, simulation method 2 allows the control-agents to operate as separate software processes on a parallel computer cluster. The power system is simulated in one process on the cluster, and each software agent is launched as a separate process. The agents communicate via the MPICH2 implementation of the

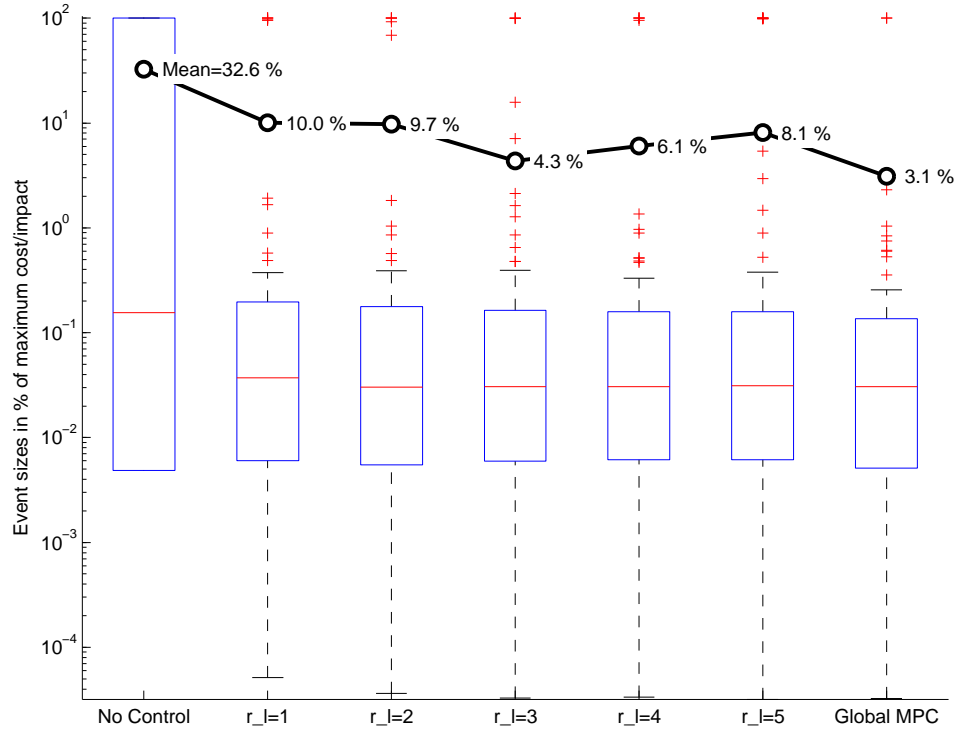


Figure 6.3: Box-plots showing the distribution of blackout sizes for five versions of the “simple” cooperation method. Here size is measured in the percent of the costs associated with a complete blackout. On the left is the distribution of sizes without any control. On the right is the distribution of sizes for SMP control with perfect information. The distributions in the middle show agent-based control for the “simple RA” cooperation scheme, while varying the size of the local (inner) communication radius r_l .

Message Passing Interface (MPI), which is commonly used on large computer clusters for inter-process communication.

The simulation runs at a rate of 1 second of power-system time per 1 second of computer time (i.e. real-time). Several times (typically 5) during each 1-second time step the power system simulator process recalculates voltages and currents in the network using the AC power-flow method described above. After calculating new voltages and currents, the simulator sends these data to the agents according to the agents’ locations. No single voltage or current data point is sent to any two agents, thus simulating the fact that an agent located at a substation can only measure local voltages and currents. During the simulation the agents perform the following actions:

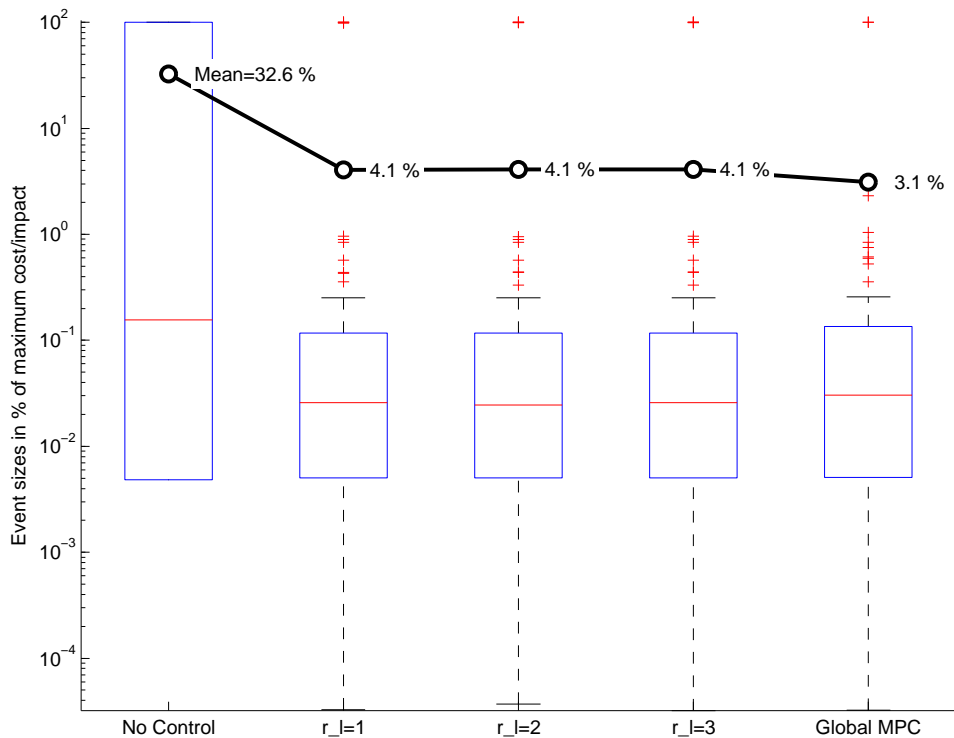


Figure 6.4: Box-plots showing the distribution of blackout sizes for three versions of the “negotiate” cooperation method. Here size is measured in the percent of the costs associated with a complete blackout. On the left is the distribution of sizes without any control. On the right is the distribution for SMP control with perfect information. The distributions in the middle show agent-based control for the “negotiate” cooperation scheme, while varying the size of the local (inner) communication radius r_l . The inner radius does not have a large effect on the control quality in these cases.

- When measurements arrive from the network simulator process, update the local power network model and forward the data to members of the local neighborhood. If some of the variables are stressed, also pass these data to members of the agent’s extended neighborhood.
- When measurements arrive from another agent, incorporate these data into the local network model, so long as the time stamps on the data are not less than what is contained in the local model.
- At the top of each second (time $t.00$) begin to calculate control actions which will be implemented at an agreed upon control deadline (I used 0.80 seconds

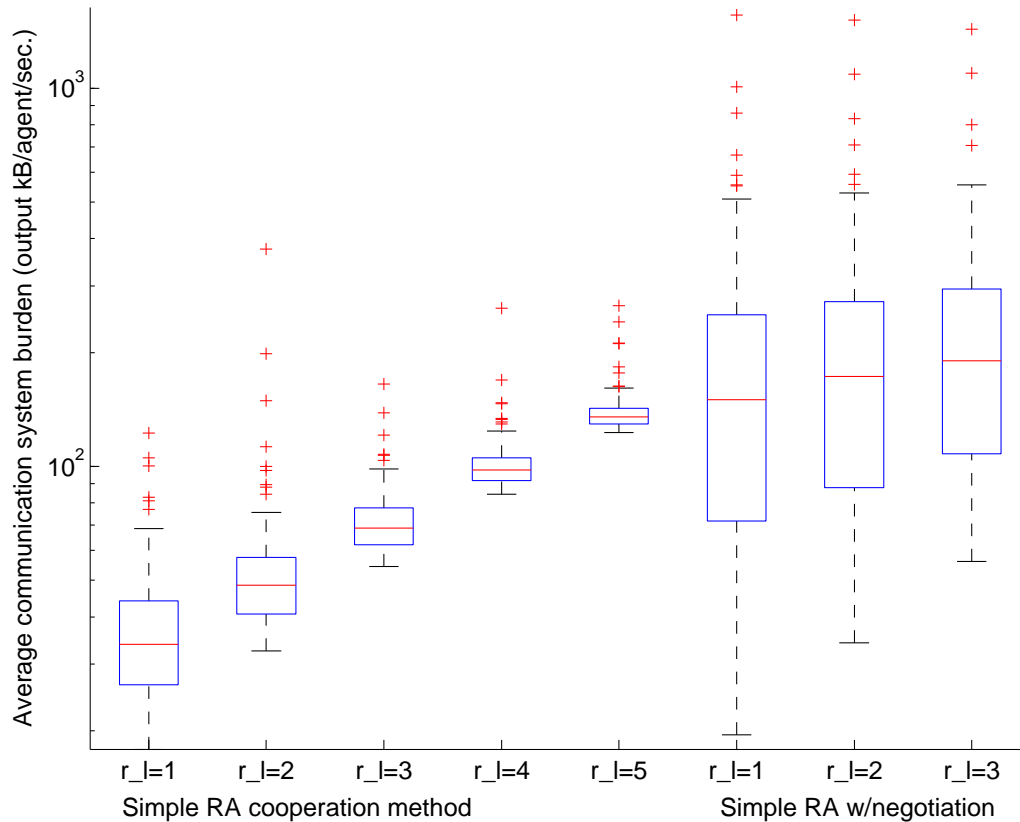


Figure 6.5: Box-plots showing the amount of data exchanged by the agents for eight versions of the agent control method. The data on the left show the results from simulations with the “simple” cooperation scheme, with the local neighborhood size (r_l) varied between 1 and 5. The data on the right show the results from simulations for the “negotiate” (share-data) cooperation scheme with r_l varied between 1 and 3. For the “Simple RA” scheme, communications increase exponentially with r_l . Clearly the negotiation scheme requires more bandwidth.

after the beginning of the time step—time $t.80$). Exchange information with neighbors to improve the calculated control actions until the control deadline.

- When the control deadline arrives (time $t.80$), if the local control variables need to change given the agent’s local calculation the agent implements these actions by sending a message to the simulator process.
- Whenever the simulator process receives a control action message it immediately implements the action (changes the generator or load variables) in the global power system model.

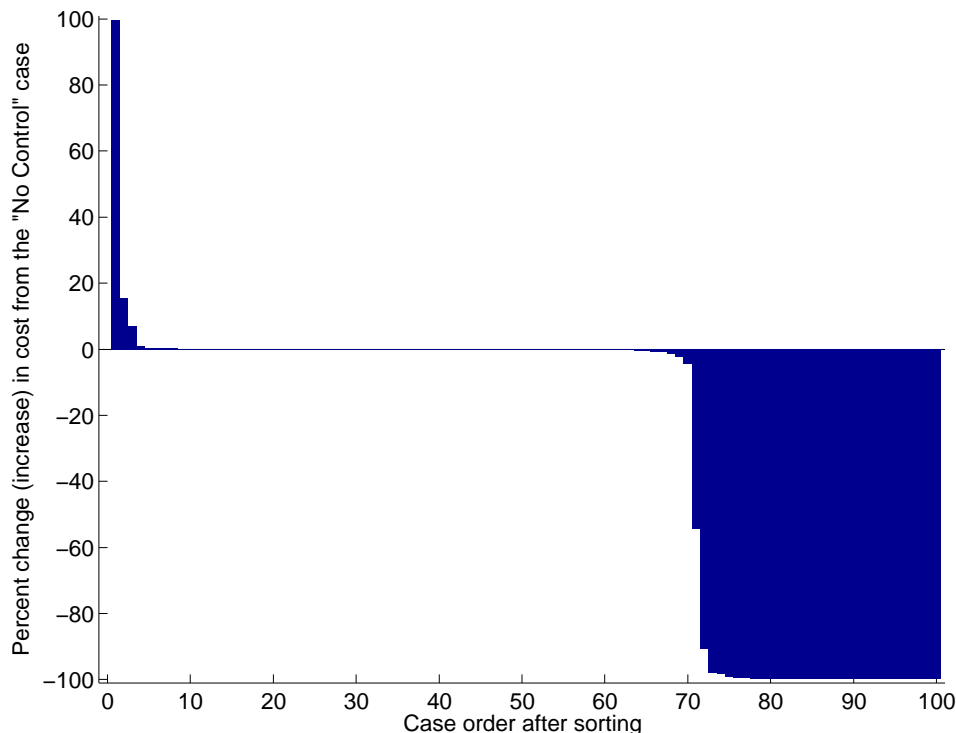


Figure 6.6: The cost difference between the “no control” and agent-based control test cases. Positive values indicate that the agent-based control was more costly than the “no control” case. On the left, the figure shows that in a few cases the control agents cause a large blackout that would not have otherwise occurred. On the right, the figure shows the cases in which the agents prevent large blackouts.

This process roughly approximates the way that this method would operate in a real power network. If the communication system becomes bogged down through excessive inter-agent message passing, agents will not be able to collect good data, and their control decisions will be far from optimal.

6.5. Discussion

The results presented in this chapter illustrate that at least in many cases, it is possible to dramatically reduce the size, and thus costs, associated with cascading failures. Over the 100 random test cases, the average cost of the cascading failure events was reduced by as much as 87% (nearly an order of magnitude reduction in event cost). On the other hand, some of the results indicate that the method can, under highly stressed conditions, increase the size of the resulting blackout, relative

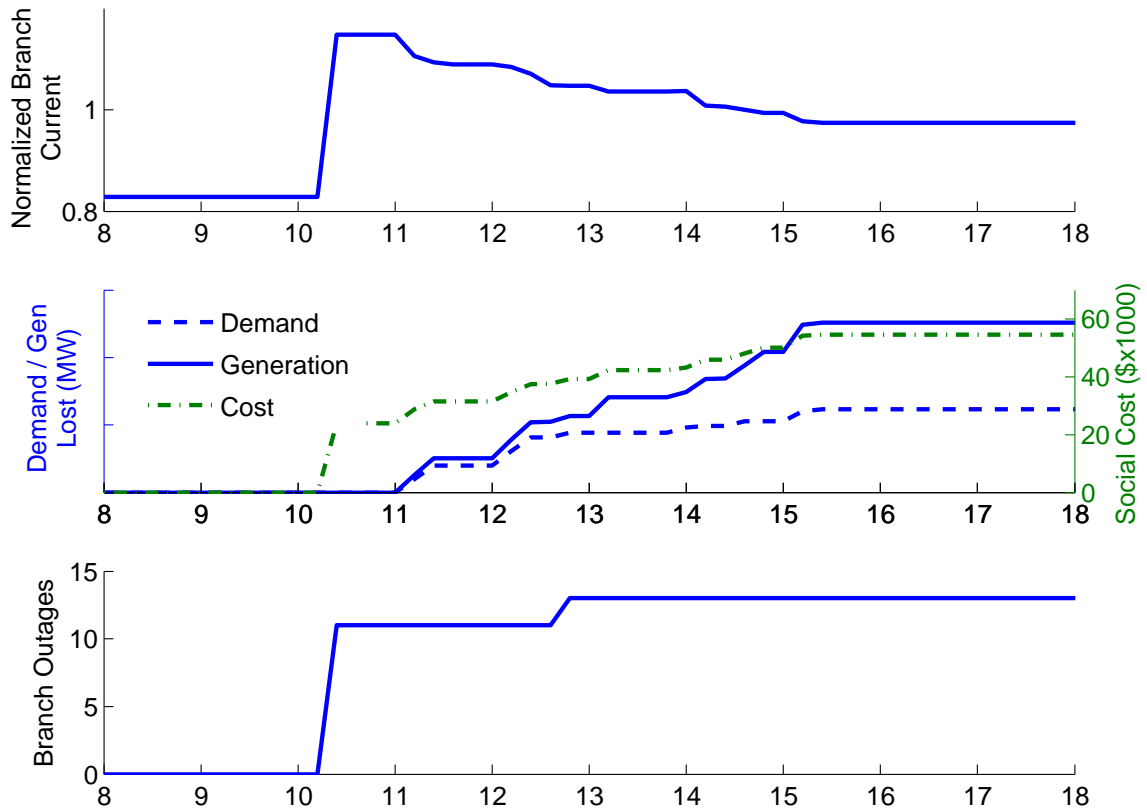


Figure 6.7: Results from the simulation of case300-2-5 on a parallel computer cluster. The top trajectory shows the change in the worst branch current over time during the simulation. The second set of trajectories show the load and generation losses, and costs resulting from this event. The final plot shows the branch outages during the simulation. Two over-current relay operations occur after the initial disturbance at around time 12.7 in the simulation. The simulation used a cluster of 40 four processor Intel Xeon computers, networked via standard gigabit Ethernet cards. While the violations are eliminated, the results are not quite as good as that given by the Global MPC simulations.

to a case without remedial actions. This effect will need to be studied further in future work.

While the methods used to simulate agent behavior and power system dynamics do not perfectly represent the actions of control agents interacting with a physical power network, the models used provide a sufficiently accurate picture of the method to illustrate its utility. In future work the simulation methods will be refined to confirm that the cost reductions shown here would remain under more sophisticated simulation environments.

CHAPTER 7

Conclusions

The real-time management of stress within large interconnected systems, such as an electrical power network, is an important and challenging problem. Cascading failures in electrical power networks illustrate both the importance and challenge of this problem. Because the problem is important, extensive academic and industry research has focused on improving the way in which power networks react to stress. Because the problem is challenging, these efforts have not significantly reduced the frequency or size of large cascading failures.

The problem is important because bulk power system control failures can inflict large social costs. These costs come from two sources: indirect costs that result from cascading failures, and indirect costs that come from actions required to mitigate the risk of direct costs. Chapter 2 infers that the direct costs in the United States, given existing data on large blackouts, are on the order of \$230 million per year. The indirect costs of control failures are likely to be much larger. Indirect costs come from inefficiencies due to stability margins that operators use when dispatching energy sources, new transmission technology built to improve reliability and the overhead associated with coordinating the efforts of the human operators who manage the reliability of a complex network. While there will always be some need for stability margins, transmission construction and skilled human operators, a grid that could react to stress nearly optimally could reduce these indirect reliability costs in addition to reducing the direct costs associated with cascading failures.

The problem is challenging because of the enormous number of components in the system, each of which has unique discrete and continuous dynamic properties. Because power networks have millions of components and are geographically dispersed

with many loosely connected operators, solutions that require extensive centrally located information processing are not generally practical. On the other hand decentralized control methods produce results that are sub-optimal with respect to the mission of the network as a whole. The role that protective relays play in the cascading failure process illustrates the potential consequences of a decentralized control scheme that can act in opposition to global network goals. The decentralized control scheme described in this thesis attempts to reconcile these two problems through the use of software agents that act with reciprocal altruism. The proposed control agents think and act with respect to the goals of the system as a whole, while assuming that their neighbors will do likewise. Experimental results show that the use reciprocal-altruism agents can dramatically reduce the costs associated with cascading failures.

The following sections describe the technical contributions of this thesis in some detail, outline some of the policy and implementation challenges related to this technology, and describe some issues to be resolved in future research.

7.1. Technical contributions

The primary contributions of this thesis are in the areas of decentralized control in general and the control of cascading failures in power systems in particular. With respect to decentralized control, this thesis provides a new control algorithm that combines Reciprocal Altruism with Model Predictive Control. The result is a multi-agent system that can cooperatively control a tightly interconnected network with reasonable communications requirements. With respect to cascading failures in power systems, this thesis provides evidence that the size of large cascading failures can be dramatically reduced through the use of the proposed decentralized control scheme. The following is a more detailed discussion of these contributions.

7.1.1. Decentralized control in general. The focus of this thesis is on the design of a decentralized control scheme for mitigating the costs associated with cascading failures. The resulting method, which uses both Model Predictive Control

and a form of Reciprocal Altruism, was shown to effectively solve this specific power systems problem. While the method is somewhat specialized to this particular problem, the conceptual design is sufficiently general that it has at least some potential to be useful for other large network problems. If the method can be effectively applied to other network problems, it may result in a significant contribution to the more general problem of operating complex networked systems in a decentralized manner. This would be a particularly important result because few methods currently exist for the cooperative, decentralized control of tightly interconnected systems.

A related result from Chapter 5 is that the effectiveness of decentralized control, for flow-based networks¹, will depend at least to some extent on the structure of the network. An unconnected set of nodes is easy to control with decentralized methods. Scale-free, flow-based networks appear to be particularly difficult to control with a decentralized approach, as very small changes can propagate through the entire network. Electrical power networks fall somewhere between these two cases, making decentralized methods feasible, but not without some difficulty.

7.1.2. Controlling cascading failures and special protection schemes.

While substantial research efforts have contributed to the development of SPS technology, many of the more sophisticated approaches to SPS have not widely penetrated the electricity industry. The history of this technology suggests two reasons for this effect—insufficient SPS reliability and centralized architectures. I argue that the insufficient reliability is at least somewhat a product of the way that most SPS designs are very specifically tuned to a particular system and a particular set of apparently dangerous conditions, and the centralized architecture is unnatural to the structure of power networks. What follows is a short discussion of these two conditions.

¹A flow-based network is one in which a product flows between nodes over branches in the network, and does not include large amounts of storage at the nodes. Water, traffic, sewer, and natural gas systems are among the networks that fall into this category. Some networks that do have substantial product storage at the nodes (such as Internet communications and social networks) will share many properties with flow-based networks.

Firstly, SPS tend to be very specifically tuned to particular events and systems and act according to coarse predictive network models, which are developed from off-line system studies. Systems that require this type of tuning tend to react poorly to events outside of the set of operating parameters to which the method was tuned. Since cascading failures are by their very nature extreme events and difficult to predict this approach can lead to unpredictable behavior. Anderson et al. [57] report that many operators have had mis-operation problems with SPS. In response to this problem, some new approaches to SPS use feedback and more general purpose network models (see for example [63, 96, 65]). The optimal stress mitigation problem (SMP) described in Chapter 3 is an incremental improvement over these methods because it combines feedback-based control and predictive models (via MPC) with a problem formulation that is directly related to the overall problem of power network operations.

Secondly, SPSs tend to rely on centrally located communications and computational resources. There are a number of problems with a centralized approach to this problem. For one, the amount of time required to collect measured power network data, process the data through a state estimation algorithm, calculate control actions and dispatch the results to control devices, is prohibitively large. The state estimation step alone can require 30 seconds or more. If control actions need to be calculated and dispatched within seconds in order to avoid a massive failure, the centralized approach is not practical. It is in part for this reason that existing SPS (the BPA RAS for example) operate using a fairly simple rules, thus avoiding the need for state estimation and sophisticated calculations. Another problem with centralized systems is their inherent vulnerability to a small set of device failures. This vulnerability adds to the risk associated with both directed attacks and random failures. Finally, a centralized approach to power network control can be impractical within large networks that have many operators. In much of the world's electricity markets, local operators guard their ability to manage their own network infrastructure.

Where wide-area control schemes have been widely adopted (for example, in the US western interconnect), large government agencies (e.g., BPA) have often played a vital role in coordinating the implementation process. In systems without a dominant public-sector industry member (for example, the US Eastern Interconnect and to a lesser extent continental Europe²), the implementation of a single coordinated control scheme has been difficult. Localized schemes are generally insufficient to arrest the spread of large cascading failures. A decentralized approach, such as that proposed here, could provide a more natural fit with the structure of a synchronous system with many disjoint control areas, and could lead to wider market penetration.

7.2. Implementation and policy challenges

The implementation of large wide-area power system control schemes is challenging largely because the benefits of these schemes (improved system reliability and efficiency) have the properties of public goods. The benefits of improved control spread broadly throughout a network such that it is impractical to exclude specific consumers, thus making system control a non-excludable good. Similarly if a customer consumes one increment of system-wide control (by getting better reliability), this will have little to no effect on other customers' ability to take part in these benefits. This essentially makes system-wide control a non-rival good.³ Non-rival, non-excludable goods are public goods, which will generally be under-provided by profit-maximizing private entities.

If wide-area control is a public good, some government intervention is required to produce sufficient investment in this area. It is natural then to ask what actions government entities should take to facilitate an appropriate quantity and type of investment.

²Électricité de France (EDF) is a possible exception in Europe

³It is potentially more straight forward to think of the problem in terms of economies of scale. There are enormous economies of scale in system-wide control in that the benefit of an integrated scheme for the entire network is much greater than the benefit of n separate schemes for n regions in a given system. Regional schemes may fix localized problems, but probably will not fix problems that rapidly spread across the regional boundaries.

The Remedial Action Scheme (RAS) operated by the Bonneville Power Administration [61], and other operators in the US Western Interconnect, provides a useful example. To build the western interconnect RAS, BPA developed a partnership with the major private and public utilities whose customers would benefit from improved control. Being a federal agency, they had the ability to invest in the scheme despite enormous uncertainty in the return on investment.

In the US Eastern Interconnect the Tennessee Valley Authority (TVA) has played, and continues to play, an important role in coordinating efforts to improve system control. TVA plays a major role in the Eastern Interconnect's phasor measurement unit (PMU) project. TVA could likewise play an important role in advancing the adoption of a control scheme like what is proposed here. Programs like EPRI's Intelligrid and DOE's Modern Grid Initiative can also play a role in implementation by facilitating demonstration projects that make use of decentralized grid control technology within portions of the US grid.

An important role for coordinating entities like NERC, EPRI, DOE and the UTCE in Europe, during the implementation of agent-based control technologies, will be to establish standards that ensure the interoperability of differing technologies. If competing technologies do emerge, it will be essential that the agent-based technologies adhere to standards for inter-agent communication (such as KQML [102]) and data formats (such as XML/CIM [103]). Similarly, standards for data security will need to be established and enforced to ensure that the control scheme cannot be altered by an intruder.

7.3. Future work

While this thesis provides evidence that the proposed control scheme can control cascading failures, a number of questions and design problems remain for future work.

Currently there is no way to guarantee the proposed method will perform optimally (or even nearly optimally) with respect to the global operations problem. In

fact, Figure 6.6 indicates that there are some conditions under which the proposed control algorithm performs worse than the case without any control. Certainly, before this technology could be adopted, one would need to develop a method to ensure that the risk of causing new cascading failures is negligible. There are three steps to this process. (1) Run further tests to understand why these cases perform worse than the base case, (2) modify the control scheme to provide some assurance that the method will not perform worse than the base case, and (3) develop some theoretical proof, or at least very strong evidence, that the method will not perform worse than the base case.

Theoretical evidence for the quality of this method would certainly facilitate the acceptance of this technology by many in the engineering community. Similarly, a method for calculating probabilistic performance guarantees would allow operators to estimate the overall benefit of the method given their system conditions. Both measures will be difficult to obtain through theory, due to the enormous number of variables in the problem, and because it is difficult to statistically characterize the output of a mathematical programming problem with highly uncertain input variables. When the control outputs come from many mathematical programming problems, such results are particularly challenging. Still, some related decentralized control methods include performance guarantees [15, 104], so this may be an area for future development.

The simulation model that was used to evaluate this work was based upon repeated solutions of the non-linear power-flow problem. The model did not explicitly model machine rotor dynamics or generator controls like real-power governors or excitation controls. It would be helpful to model this control method interacting with a full dynamic power system model. A well respected industry model, such as Siemens's PSS/E package or the GE PSLF package, would likely be most valuable for this purpose, as the use of an existing tool would reduce the uncertainty associated with modeling errors.

Finally, the use of better cooperation methods and agent-based machine learning has the potential to substantially improve the performance of this technology. The two information exchange methods described in Chapter 4 are very simple. Future work will include a more thorough comparison of different methods of data exchange, and explore the design of more sophisticated cooperation schemes. Also, in this work, the problems that the agents solve, and the methods that they use to solve them are essentially fixed in time. Machine learning could be used in the future to allow the agents to improve the methods that agents use to solve their problems, moving their solutions closer to global optimality.

7.3.1. Commercialization. Given that the proposed method can be improved somewhat to give reliably high performance characteristics, it could prove to be a viable commercial technology. Before this technology can be deployed numerous design details need to be clarified. One of the most important is the communications protocols that the agents will use to exchange information. Since much of the data that the agents exchange is useless if delayed, it might be beneficial for the communications protocol to discard delayed messages. This would differ from TCP/IP in which delayed messages are repeatedly resent at lower data rates until the message gets through. As mentioned earlier, the agent language is likely to be more effective in the long run if it is based upon standards that will facilitate interoperability with other technologies.

Once the initial design details are completed, and a prototype set of devices has been demonstrated with simulators, it would be valuable to develop a pilot project with a transmission system operator. This would require several steps. Firstly, one would want to install the agent-devices at a small set of substations, without connecting them to actuation system (generator controls, circuit breakers, etc.). Instead of implementing their actions, the agents would choose control actions and record them to a database. Data from agent negotiations and decisions could be used to identify risks and refine the design. This would not allow one to test the effects of feedback,

but it could give some insights into the effects of the agents on the network. After a period of initial testing, one could deploy a set of the agents with a limited mandate, perhaps only allowing them to take one or two control iterations after an initially detected stress variable. If successful, this process could lead to a larger deployment.

Bibliography

- [1] “Power Systems Test Case Archive, University of Washington, Electrical Engineering.” online: <http://www.ee.washington.edu/research/pstca/>, 2007.
- [2] “Final Report on the August 14, 2003 Blackout in the United States and Canada,” tech. rep., US-Canada Power System Outage Task Force, 2004.
- [3] “Final Report of the Investigation Committee on the 28 September 2003 Blackout in Italy,” tech. rep., Union for the Co-ordination of Transmission of Electricity, 2004.
- [4] “A Review of System Operations Leading up to the Blackout of August 14, 2003,” tech. rep., North American Electric Reliability Council, 2004.
- [5] J. C. Swidler, “Report to the President by the Federal Power Commission on the Power Failure in the Northeastern United States and the Province of Ontario on Nov. 9-10, 1965,” tech. rep., US Federal Power Commission, 1965.
- [6] G. D. Friedlander, “What went wrong VIII: The Great Blackout of '65,” *IEEE Spectrum*, 1976.
- [7] FERC, “The Con Edison Power Failure of July 13 and 14, 1977,” tech. rep., U.S. Dept. of Energy Federal Energy Regulatory Commission, 1978.
- [8] “DAWG Database: Disturbances, Load Reductions, and Unusual Occurrences,” tech. rep., North American Electric Reliability Council, Disturbance Analysis Working Group, online: <http://www.nerc.com/dawg/>, 2006.
- [9] WSCC Operations Committee, “Western Systems Coordinating Council Disturbance Report For the Power System Outages that Occurred on the Western Interconnection on August 10, 1996,” tech. rep., Western Systems Coordinating Council, 1996.
- [10] D. Kosterev, C. Taylor, and W. Mittelstadt, “Model validation for the August 10, 1996 WSCC system outage,” *IEEE Transactions on Power Systems*, vol. 14, pp. 967 – 979, 1999.
- [11] “Report on the Events of September 28th, 2003 Culminating in the Separation of the Italian Power System from the Other UCTE Networks,” tech. rep., Commission de Regulation de L’Energie and Autorita per l’energia elettrica e il gas, 2004.
- [12] UTCE, “Final Report System Disturbance on 4 November 2006,” tech. rep., Union for the Co-ordination of Transmission of Electricity, 2007.

- [13] A. Wood and B. Wollenberg, *Power Generation Operation and Control*. Wiley & Sons, 1996.
- [14] P. Hines and S. Talukdar, "Controlling cascading failures with cooperative autonomous agents," *International Journal of Critical Infrastructures*, vol. 3, pp. 192 – 220, 2007.
- [15] E. Camponogara, *Controlling Networks with Collaborative Nets*. PhD thesis, Carnegie Mellon University, 2000.
- [16] S. Talukdar, "Unpublished lecture notes from Carnegie Mellon Univ. course 18-879 / 19-615: Multi-Agent Systems," January 2007.
- [17] M. Wooldridge and N. R. Jennings, "Intelligent agents: theory and practice," *The Knowledge Engineering Review*, vol. 10, pp. 115–152, 1995.
- [18] T. Aquinas, "*Summa Theologica, 1.14.1*" in *The Pocket Aquinas*, ch. A Description of Cognitive Agents, p. 8. New York: Washington Square, 1960.
- [19] V. R. Lesser, "Multiagent systems: An emerging subdiscipline of ai," *ACM Computing Surveys*, vol. 27, pp. 340–342, 1995.
- [20] B. Hoelldobler and E. O. Wilson, *The Ants*. Cambridge: Harvard University Press, 1990.
- [21] R. L. Trivers, "The evolution of reciprocal altruism," *Quarterly Review of Biology*, vol. 46, pp. 35–57, 1971.
- [22] R. Gallagher and T. Appenzeller, "Beyond Reductionism," *Science*, vol. 284, no. 5411, p. 79, 1999.
- [23] P. Bak, C. Tang, and K. Wiesenfeld, "Self-organized criticality," *Physical Review A*, vol. 38, pp. 364–374, 1988.
- [24] B. A. Carreras, D. E. Newman, I. Dobson, and A. B. Poole, "Evidence for Self-Organized Criticality in a Time Series of Electric Power System Blackouts," *IEEE Transactions on Circuits and Systems-I: Regular Papers*, vol. 51, pp. 1733–1740, 2004.
- [25] H. Liao, J. Apt, and S. Talukdar, "Phase Transitions in the Probability of Cascading Failures," in *Proc. of the First Annual Carnegie Mellon Conf. on the Electricity Industry, Electricity Transmission in Deregulated Markets: Challenges, Opportunities, and Necessary R&D Agenda*, 2004.
- [26] P. Erdos and A. Renyi, "On random graphs," *Publ. Math. Debrecen*, vol. 6, pp. 290–297, 1959.
- [27] D. J. Watts and S. H. Strogatz, "Collective dynamics of 'small-world' networks," *Nature*, vol. 393, pp. 440–442, 1998.
- [28] A.-L. Barabasi and R. Albert, "Emergence of scaling in random networks," *Science*, vol. 286, pp. 509–512, 1999.

- [29] S. Blumsack and P. Hines, "The topological and electrical structure of electrical power networks," tech. rep., "Carnegie Mellon University Electricity Industry Center", 2007.
- [30] X. Cheng and B. H. Krogh, "Stability-Constrained Model Predictive Control," *IEEE Transactions on Automatic Control*, vol. 46, pp. 1816 – 1820, 2001.
- [31] E. Camacho and C. Bordons, *Model Predictive Control*. London: Springer, 2004.
- [32] J. Rawlings, "Tutorial Overview of Model Predictive Control," *IEEE Control Systems Magazine*, vol. 20, pp. 38–52, 2000.
- [33] S. J. Qin and T. A. Badgwell, "An overview of industrial model predictive control technology," in *Proceedings of Chemical Process Control - V (American Institute of Chemical Engineers)*, 1997.
- [34] E. Camponogara, D. Jia, B. H. Krogh, and S. Talukdar, "Distributed model predictive control," *IEEE Control Systems Magazine*, vol. 22, pp. 44–52, Feb. 2002.
- [35] T. Keviczky, F. Borrelli, and G. J. Balas, "Decentralized Receding Horizon Control for Large Scale Dynamically Decoupled Systems," *Automatica*, vol. 42, pp. 2105–2115, 2006.
- [36] F. Borrelli, T. Keviczky, and G. E. Stewart, "Decentralized Constrained Optimal Control Approach to Distributed Paper Machine Control," in *Proc. of the 44th IEEE Conf. on Decision and Control*, 2005.
- [37] F. Borrelli, T. Keviczky, K. Fregene, and G. Balas, "Decentralized Receding Horizon Control of Cooperative Vehicle Formations," in *Proc. of the 44th IEEE Conference on Decision and Control*, 2005.
- [38] A. N. Venkat, J. B. Rawlings, and S. J. Wright, "Stability and optimality of distributed model predictive control," in *Proceedings of the 44th IEEE Conference on Decision and Control, and the European Control Conference*, 2005.
- [39] I. Hiskens and B. Gong, "MPC-Based Load Shedding for Voltage Stability Enhancement," in *Proceedings of the 44th IEEE Conference on Decision and Control*, 2005.
- [40] M. Zima and G. Andersson, "Model Predictive Control Employing Trajectory Sensitivities for Power Systems Applications," in *Proceedings of the 44th IEEE Conference on Decision and Control*, 2005.
- [41] M. Larsson, "An Adaptive Predictive Approach to Emergency Frequency Control in Electric Power Systems," in *Proceedings of the 44th IEEE Conference on Decision and Control*, 2005.
- [42] E. H. Durfee, "Practically coordinating," *AI MAGAZINE*, vol. 20, no. 1, pp. 99–116, 1999.
- [43] S. Talukdar, L. Baerentzen, A. Gove, and P. D. Souza, "Asynchronous Teams: Cooperation Schemes for Autonomous Agents," *Journal of Heuristics*, vol. 4, pp. 295 – 321, 1998.

- [44] P. J. Modi, W.-M. Shen, M. Tambe, and M. Yokoo, "ADOPT: Asynchronous Distributed Constraint Optimization with Quality Guarantees," *Artificial Intelligence Journal*, vol. 161, pp. 149–180, 2005.
- [45] K.-S. Hwang, S.-W. Tan, and C.-C. Chen, "Cooperative Strategy Based on Adaptive-Learning for Robot Soccer Systems," *IEEE Transactions on Fuzzy Systems*, vol. 12, pp. 569–576, 2004.
- [46] A. Ollero, S. Lacroix, L. Merino, J. Gancet, J. Wiklund, V. Remuss, I. Perez, L. Gutierrez, D. Viegas, M. Benitez, A. Mallet, R. Alami, G. Chatila, R. and Hommel, F. Lechuga, B. Arrue, J. Ferruz, J. Martinez-De Dios, and F. Caballero, "Multiple Eyes in the Skies: Architecture and Perception Issues in the COMETS Unmanned Air Vehicles Project," *IEEE Robotics & Automation Magazine*, vol. 12, pp. 46–57, 2005.
- [47] T. Keviczky, F. Borrelli, K. C. Fregene, D. Godbole, and G. J. Balas, "Decentralized Receding Horizon Control and Coordination of Autonomous Vehicle Formations," *IEEE Transactions on Control Systems Technology*, 2006.
- [48] B. E. Bishop, "On the use of redundant manipulator techniques for control of platoons of cooperating robotic vehicles," *IEEE Transactions on Systems, Man, and Cybernetics—Part A: Systems and Humans*, vol. 33, pp. 608–615, 2003.
- [49] J. Blackburn, *Protective Relaying: Principles and Applications*. Marcel Dekker, 1998.
- [50] D. V. Coury, J. S. Thorp, K. M. Hopkinson, and K. R. Birman, "An agent-based current differential relay for use with a utility intranet," *IEEE Transactions on Power Delivery*, vol. 17, pp. 47–53, Jan. 2002.
- [51] D. P. Bertsekas and J. N. Tsitsiklis, *Parallel and Distributed Computation: Numerical Methods*. Athena Scientific, 1997.
- [52] S. Nash and A. Sofer, *Linear and Nonlinear Programming*, ch. Penalty and Barrier Methods, pp. 527–566. McGraw-Hill, 1996.
- [53] G. Cohen and D. L. Zhu, *Advances in Large Scale Systems*, vol. 1, ch. Decomposition Coordination Methods in Large Scale Optimization Problems: The Nondifferentiable Case and the Use of Augmented Lagrangians, pp. 203–266. Greenwich: JAI Press, 1984.
- [54] A. Losi and M. Russo, "On the Application of the Auxiliary Problem Principle," *Journal of Optimization Theory and Applications*, vol. 117, pp. 377–396, 2003.
- [55] B. H. Kim and R. Baldick, "A Comparison of Distributed Optimal Power Flow Algorithms," *IEEE Transactions on Power Systems*, vol. 15, pp. 599–604, 2000.
- [56] P. Hines and S. Talukdar, "Reducing the costs of disturbances to the electric power network." Presented at the Int. Assn. for Energy Economics Meeting, Washington, DC, June 2004.

- [57] P. M. Anderson and B. K. LeReverend, "Industry experience with special protection schemes," *IEEE Transactions on Power Systems*, vol. 11, pp. 1166–1176, Aug. 1996.
- [58] Y. Makarov, V. Reshetov, V. Stroeve, and N. Voropai, "Blackout Prevention in the United States, Europe, and Russia," *Proceedings of the IEEE*, vol. 93, pp. 1942–1955, 2005.
- [59] M. Zima, "Special Protection Schemes in Electric Power Systems," tech. rep., ETH Power Systems Laboratory, 2002.
- [60] M. Amin, ed., *Proceedings of the IEEE: Special Issue on Energy Infrastructure Defense Systems*, vol. 93. IEEE, May 2005.
- [61] C. Taylor, D. Erickson, K. Martin, R. Wilson, and V. Venkatasubramanian, "WACS-wide-area stability and voltage control system: R&D and online demonstration," *Proceedings of the IEEE*, vol. 93, pp. 892–906, 2005.
- [62] M. Zima, M. Larsson, P. Korba, C. Rehtanz, and G. Andersson, "Design Aspects for Wide-Area Monitoring and Control Systems," *Proceedings of the IEEE*, vol. 93, pp. 980–996, 2005.
- [63] W. Shao and V. Vittal, "Corrective switching algorithm for relieving overloads and voltage violations," *IEEE Transactions on Power Systems*, vol. 20, pp. 1877 – 1885, 2005.
- [64] H. You, V. Vittal, and X. Wang, "Slow coherency-based islanding," *IEEE Transactions on Power Systems*, vol. 19, pp. 483–491, 2004.
- [65] H. Li, G. Rosenwald, J. Jung, and C. ching Liu, "Strategic Power Infrastructure Defense," *Proceedings of the IEEE*, vol. 93, pp. 918–933, 2005.
- [66] NETL-MGI, "Modern Grid v2.0 Powering Our 21st-Century Economy: The Modern Grid Initiative," tech. rep., U.S. Department of Energy Office of Electricity Delivery and Energy Reliability, 2007.
- [67] J. Hughes, "The Integrated Energy and Communication Systems Architecture, Volume III: Models," tech. rep., Electric Power Research Institute, 2004.
- [68] P. Joskow and J. Tirole, "Reliability and competitive electricity markets," *RAND Journal of Economics*, vol. 38, 2007.
- [69] J. Hughes, "The Integrated Energy and Communication Systems Architecture, Volume I: User Guidelines and Recommendations," tech. rep., Electric Power Research Institute: Electricity Innovation Institute Consortium for Electric Infrastructure to Support a Digital Society (CEIDS), 2004.
- [70] J. B. Treaster, "The blackout: Business losses; insurers say most policies do not cover power failure," *The New York Times*, p. 6, August 16, 2003.

- [71] K. LaCommare and J. Eto, "Understanding the cost of power interruptions to U.S. electricity consumers," Tech. Rep. Report No. LBNL-55718, Ernest Orlando Lawrence Berkeley National Laboratory, 2004.
- [72] B. A. Carreras, D. E. Newman, I. Dobson, and A. B. Poole, "Initial evidence for self-organized criticality in electric power system blackouts," in *Proceedings of Hawaii International Conference on System Sciences*, 2000.
- [73] S. Talukdar, J. Apt, M. Ilic, L. Lave, and M. Morgan, "Cascading failures: survival versus prevention," *The Electricity Journal*, 2003.
- [74] R. Weron and I. Simonsen, "Blackouts, risk, and fat-tailed distributions," in *Proceedings of the 3rd Nikkei Econophysics Symposium*, 2005.
- [75] I. Dobson, B. A. Carreras, and D. E. Newman, "A loading-dependent model of probabilistic cascading failure," *Probability in the Engineering and Informational Sciences*, vol. 19, pp. 15–32, 2005.
- [76] Q. Qiu, *Risk Assessment of Power System Catastrophic Failures and Hidden Failure Monitoring & Control System*. PhD thesis, Virginia Polytechnic Institute and State University, 2003.
- [77] "Form OE-417, Electric emergency incident and disturbance report." U.S. Dept. of Energy, Office of Electricity Delivery and Energy Reliability, online: <http://www.eia.doe.gov/oss/forms.html>, 2005.
- [78] U.S. Census Bureau, "U.S. Census Bureau Population Estimates (1980-2000 and 2000-2006)." online: <http://www.census.gov/>, 2006.
- [79] US-EIA, "Net Generation by Energy Source by Type of Producer."
- [80] "Net Internal Demand, Capacity Resources, and Capacity Margins by North American Electric Reliability Council Region for 2005," tech. rep., US Dept. of Energy, Energy Information Agency, 2007.
- [81] B. Saha and B. Moody, "The economic cost of the blackout: An issue paper on the northeastern blackout, august 14, 2003," tech. rep., ICF Consulting, 2003.
- [82] J. Bowring, *Electricity Market Reform: An International Perspective*, ch. The PJM Market, pp. 451–478. Elsevier, 2006.
- [83] J. Casazza, "Electric power deregulation – a bad idea?." In "Today's Engineer," IEEE Press, May 2005.
- [84] S. Abraham, "National transmission grid study," tech. rep., U.S. Dept. of Energy, May 2002.

- [85] E. Hirst, "U.S. Transmission Capacity: Present Status and Future Prospects," tech. rep., Edison Electric Institute and Office of Electric Transmission and Distribution, U.S. Department of Energy, Aug. 2004.
- [86] S. Vajjhala and P. Fischbeck, "Quantifying Siting Difficulty: A Case Study of U.S. Transmission Line Siting," *Energy Policy*, vol. 35, pp. 650–671, 2007.
- [87] S. A. Blumsack, *Network Topologies and Transmission Investment Under Electric-Industry Restructuring*. PhD thesis, Carnegie Mellon University, 2006.
- [88] J. Apt, L. B. Lave, S. Talukdar, M. G. Morgan, and M. Ilic, "Electrical blackouts: A systemic problem," *Issues in Science and Technology*, vol. 20, no. 4, pp. 55–61, 2004.
- [89] P. Hines, J. Apt, H. Liao, and S. Talukdar, "The frequency of large blackouts in the United States electrical transmission system: an empirical study," in *Proc. of the Second Carnegie Mellon Conference in Electric Power Systems: Monitoring, Sensing, Software and Its Valuation for the Changing Electric Power Industry*, 2006.
- [90] M. D. Ilic, E. H. Allen, J. W. Chapman, C. A. King, J. H. Lang, and E. Litvinov, "Preventing Future Blackouts by Means of Enhanced Electric Power Systems Control: From Complexity to Order," *Proceedings of the IEEE*, vol. 93, pp. 1920–1941, 2005.
- [91] J. Momoh, R. Adapa, and M. El-Hawary, "A review of selected optimal power flow literature to 1993. I. Nonlinear and quadratic programming approaches," *IEEE Transactions on Power Systems*, vol. 14, pp. 96 – 104, 1999.
- [92] J. Momoh, M. El-Hawary, and R. Adapa, "A review of selected optimal power flow literature to 1993. II. Newton, linear programming and interior point methods," *IEEE Transactions on Power Systems*, vol. 14, pp. 105 – 111, 1999.
- [93] A. Bergson, "A Reformulation of Certain Aspects of Welfare Economics," *The Quarterly Journal of Economics*, vol. 52, pp. 310–334, 1938.
- [94] A. R. Bergen, *Power Systems Analysis*. Prentice-Hall, 1986.
- [95] S. Borenstein, M. Jaske, and A. Rosenfeld, "Dynamic Pricing, Advanced Metering and Demand Response in Electricity Markets," tech. rep., Center for the Study of Energy Markets (CSEM WP 105), 2002.
- [96] W. Shao and V. Vittal, "LP-Based OPF for Corrective FACTS Control to Relieve Overloads and Voltage Violations," *IEEE Transactions on Power Systems*, vol. 21, pp. 1832–1839, 2006.
- [97] R. D. Zimmerman, C. E. Murillo-Sánchez, and D. D. Gan, "MATPOWER: A MATLAB Power System Simulation Package, Version 3.1b2, User's Manual," tech. rep., Power Systems Engineering Research Center, 2006.

- [98] K. J. Arrow, "A difficulty in the concept of social welfare," *The Journal of Political Economy*, vol. 58, pp. 328–346, 1950.
- [99] G. S. Wilkinson, "Reciprocal food sharing in the vampire bat," *Nature*, vol. 308, pp. 181–184, 1984.
- [100] R. Lougee-Heimer, "The Common Optimization INterface for Operations Research: Promoting open-source software in the operations research community," *IBM Journal of Research and Development*, vol. 47, p. 57, 2003.
- [101] R. Albert and A. Barabasi, "Statistical mecahnics of complex networks," *Reviews of Modern Physics*, vol. 74, 2002.
- [102] T. Finin, Y. Labrou, and J. Mayfield, "Kqml as an agent communication language," in *Proceedings of the 3rd International Conference on Information and Knowledge Management (CIKM'94)*, 1995.
- [103] A. de Vos, S. Widergren, and J. Zhu, "Xml for cim model exchange," in *Proc. of the IEEE Power Engineering Society International Conference on Power Industry Computer Applications*, 2001.
- [104] D. Jia, *Distributed coordination in multi-agent control systems through model predictive control*. PhD thesis, Carnegie Mellon University, 2003.

APPENDIX A

Blackout data

This appendix shows the actual blackout data studied in Chapter 2. The data come from the NERC Disturbance Analysis Working Group (DAWG) database [8].

Date	Location	Customers	MW	Notes
01/03/84	WSCC	126,000	190	Transmission trip
02/26/84	SERC	382,939	1,755	Auxiliary power system being revised
02/26/84	SPP	26,161	127	Failure of lightning arrester
02/28/84	SERC	998,350	2,519	Failure of lightning arrester
02/29/84	WSCC	3,159,559	7,901	One Pacific AC intertie circuit tripped due to relay misoperation
03/05/84	MAIN	35,000	150	Severe ice storm.
03/18/84	SPP	120,000	145	Severe ice storm.
03/29/84	NPCC	327,000	650	Storm and high winds caused outage of transmission circuits
06/25/84	NPCC	0	183	Fire beneath the Celilo-Sylmar DC line
06/28/84	WSCC	532,134	2,369	Fire beneath the Celilo-Sylmar DC line
06/30/84	WSCC	86,272	698	Thunderstorm with lightning and winds to 59 MPH
07/23/84	SPP	60,000	300	Lightning caused xfmr overload (cascade)
07/28/84	SERC	50,000	164	Tap changer arced (cascade)
08/06/84	NPCC	20,000	50	
09/11/84	WSCC	170,000	350	Disturbance confined to local area (not specified)
10/02/84	WSCC	732,473	3,868	Mis-operation of a phase comparison relay
01/01/85	ECAR	285,000	366	Ice Storm
01/21/85	SPP	150,000	870	Circuit breaker failed to clear phase-to-ground fault
01/21/85	SPP	75,000	650	Loss of generation caused by freezing weather.
01/21/85	ECAR	10	137	
01/21/85	ECAR	0	100	
02/01/85	WSCC	100,000	150	Transformer fault/fire
02/12/85	WSCC	90,000	400	Breaker failure, gen loss, cascade
02/13/85	SPP	16,800	255	DC control bus in substation caused cascade
02/26/85	WSCC	103,800	240	DC control bus in substation caused cascade
03/03/85	MAIN	150,000	200	Ice Storm
03/11/85	WSCC	30,000	170	
03/17/85	WSCC	0	115	
03/20/85	SPP	4,600	0	Woodpecker damaged 230kV line, cascade
03/26/85	SERC	170,000	255	Woodpecker damaged 230kV line, cascade
04/03/85	WSCC	29,000	80	Ground wire broke, faulted 230kV line, cascade
04/06/85	NPCC	55,600	214	Ground wire broke, faulted 230kV line, cascade
05/01/85	SPP	0	650	Line fault
05/03/85	WSCC	90,000	90	Lightning
05/17/85	SERC	1,500,000	4,300	Fire near substation
05/31/85	NPCC ECAR MACC	576,000	1,900	Tornado
07/02/85	WSCC	145,000	394	Wind storm blew tent, which caused cascade
07/02/85	WSCC	40,000	200	Wind storm blew tent, which caused cascade
07/06/85	WSCC	300,000	1,400	Fault + relay failure, caused cascade
07/06/85	WSCC	0	300	Lightning + lines out for maintenance, caused cascade
09/02/85	SERC	461,260	760	Hurricane Elena
09/27/85	SERC NPCC	2,991,139	0	Hurricane Gloria
01/05/86	WSCC	25,000	150	Snow storm caused line outage, cascade
04/03/86	WSCC	356,856	1,500	Snow storm caused line outage, cascade
05/05/86	WSCC	200,000	400	Relay operation in substation. Loss of 43 subs. resulted
05/13/86	WSCC	0	600	Snow storm.
05/15/86	SERC	32,000	100	Line fault from maintenance crew. Cascade.
05/22/86	SERC	345,000	1,000	Line fault from maintenance crew. Cascade.
06/06/86	SERC	31,000	175	
06/07/86	SERC	31,000	120	
06/22/86	NPCC	0	158	Earthquake, 6.0 magnitude
07/08/86	WSCC	88,500	110	Earthquake, 6.0 magnitude
07/17/86	MAPP	30,000	20	
08/17/86	SERC	187,000	500	Hurricane Charlie
10/27/86	WSCC	550	200	
11/19/86	NPCC	210,000	38	Storm
12/23/86	MAIN	200,000	200	Heavy fog caused subs. fault. Interrupted 3 dist. subs.
02/11/87	NPCC	50,000	100	Flag caused line fault, resulted in 6 transformer trips
02/22/87	MAAC	100,000	400	Snow storm
02/23/87	MAAC	250,000	0	Snow storm
04/03/87	SERC	85,000	340	Snow storm
04/13/87	WSCC	0	144	
05/06/87	WSCC	46,000	110	
06/11/87	SERC	0	444	Transformer (CT) explosion caused transformer explosion.
07/10/87	MAIN	120,000	300	Lightning, cascade
07/20/87	MAPP	0	269	
07/20/87	ECAR	150,000	0	Wind and lightning damage
07/26/87	SERC	36,000	170	CT Failure, xfmr outage, line overloading
07/30/87	SERC	18	400	CT Failure, xfmr outage, line overloading
07/31/87	SERC	0	450	CT failure
07/31/87	WSCC	22,000	350	Tornados
08/17/87	NPCC	0	500	Capacity shortage, forced demand reduction
08/17/87	MAIN	50,000	50	Rain storm caused distribution outages near Chicago
08/18/87	NPCC	0	500	Capacity shortage, forced demand reduction
08/23/87	SERC	0	990	Fault in subs. caused cascade
10/01/87	WSCC	593,800	1,000	Earthquake, 6.0 magnitude

Date	Location	Customers	MW	Notes
10/06/87	WSCC	90,000	273	Transformer fire (merged 2 events)
10/06/87	WSCC	37,000	123	Lines opened, cascade
11/03/87	SERC	701,373	2,192	Lines opened, cascade
12/06/87	WSCC	134	800	Line fault, cascade (SPS/RAS activated)
12/15/87	MAIN	165,000	300	Winter storm caused distribution system outages
01/07/88	SERC	61,350	265	Storm damaged distribution circuits.
01/14/88	NPCC	0	335	Voltage reduction and load curtailment due to shortage
01/15/88	NPCC	0	335	Voltage reduction and load curtailment due to shortage
03/03/88	ECAR	60,650	60	Ice Storm
03/09/88	WSCC	108,000	408	Wind, subs. fault, line outages
04/04/88	WSCC	6,225	38	Line fault, cascade
04/13/88	WSCC	100,000	400	Line fault, cascade
04/18/88	NPCC	2,800,000	18,500	Ice Storm
06/26/88	NPCC	149,500	155	Lightning, cascade
08/02/88	NPCC	10,000	615	Area being fed by single line, which tripped (Canada, removed)
08/02/88	MAIN	0	120	
08/03/88	NPCC	2,300,000	0	Voltage reduction and load curtailment due to shortage
08/03/88	WSCC	35,000	100	Voltage reduction and load curtailment due to shortage
08/04/88	NPCC	2,300,000	0	Voltage reduction and load curtailment due to shortage
08/10/88	NPCC	0	400	Voltage reduction and load curtailment due to shortage
08/17/88	NPCC	0	144	
11/16/88	NPCC	500,000	4,200	Circuit breaker fault, cascade
11/20/88	NPCC	420,000	730	Voltage reduction and load curtailment due to shortage
12/15/88	NPCC	0	500	Tower collapsed, cascade
01/25/89	WSCC	135,428	474	PT failed + fault, cascade
01/29/89	WSCC	57	240	
02/01/89	WSCC	70,000	265	Line trip + gen trip, cascade
03/13/89	NPCC	0	19,400	Solar flare caused 5 lines to trip, cascade
04/04/89	SERC	95,000	275	Thunderstorms
06/01/89	MAAC	47,500	305	Bushing failure, fire, cascade
06/14/89	SERC	51,000	200	Thunderstorm mostly affected distribution system.
07/10/89	NPCC	95,000	100	Thunderstorm damaged distribution system
07/14/89	NPCC	22,000	28	
07/30/89	WSCC	20,000	430	Lightning, fault, cascade
08/04/89	WSCC	70,000	148	Maintenance, trip, cascade
08/16/89	NPCC	0	1,000	Fault, cascade
08/20/89	SERC	0	2,970	Switch failure at power station, cascade
09/06/89	NPCC	0	450	Lightning, cascade?
10/17/89	WSCC	1,400,000	2,000	Earthquake, 6.9 magnitude
11/08/89	WSCC	0	360	500kV line faults, cascade
11/16/89	NPCC	5	524	CT fault, loss of subs.
11/20/89	WSCC	30,000	320	Cold weather, xfmr out of service, 2 xfms trip, cascade
12/02/89	NPCC	30,000	320	Cold weather, xfmr out of service, 2 xfms trip, cascade
12/04/89	NPCC	0	600	Voltage reduction and load curtailment due to shortage
12/06/89	NPCC	86,600	200	XFMR service, fire, strange fault, lines trip, cascade
12/14/89	NPCC	0	240	7 gens lost (1275 MW). Dispatchers cut 500 MW of load.
12/21/89	ERCOT	0	500	7 gens lost (1275 MW). Dispatchers cut 500 MW of load.
12/23/89	SERC	0	3,100	Supply shortage due to unexpected high demand
12/31/89	NPCC	0	518	Some ice, fault on 3 lines, cascade?
12/31/89	NPCC	90,000	240	Switch failure, cascade?
01/16/90	WSCC	2	100	
01/26/90	WSCC	26,334	133	Tornados
02/10/90	SERC	598,000	1,800	Tornados
02/16/90	WSCC	160,000	650	Snow storm, miscommunication, cascade
03/07/90	MAPP	91,000	150	Ice storm, mostly distribution problems.
03/29/90	NPCC	33,000	250	Faulty lightning arrester cause transformer trip.
04/09/90	NPCC	53,000	260	Faulty lightning arrester cause transformer trip.
04/25/90	NPCC	300,000	740	PT failed, cascade
04/27/90	WSCC	60,000	142	Snow storm, loss of several feeders
05/04/90	NPCC	55,000	450	Unauthorized switching, cascade
06/07/90	NPCC	20	1,100	Lightning, line fault, industrial plants tripped.
06/10/90	NPCC	600	236	
06/19/90	SPP	60,000	500	No details listed
07/05/90	MAAC	0	400	Voltage reduction and load curtailment due to shortage
07/28/90	MAIN	66,005	310	Fire in distribution system (Chicago)
08/06/90	WSCC	56,000	200	Fire, 2 500kV lines trip, RAS initiated (200 MW firm 614 MW other)
08/13/90	NPCC	4,150	300	Fire in NYC distribution system
08/29/90	SERC	320,831	30	XFMR bushing failure then gen failure
09/07/90	WSCC	30,001	1,113	Lightning, line fault, CB failure, subs. fault, ...
09/19/90	NPCC	200,000	4,000	Deliberate transformer failure by employee, 7 735 lines lost
09/28/90	MAIN	40,000	350	Tornado
01/25/91	NPCC	25,000	350	Transformer cascade
01/28/91	NPCC	35,000	570	CT fault, loss of subs.
03/03/91	NPCC	315,000	0	Ice Storm
03/04/91	WSCC	176	993	Wind caused tower failure, RAS initiated, relay failure (no firm load lost)
03/12/91	ECAR MAIN	500,000	0	Ice Storm

Date	Location	Customers	MW	Notes
03/27/91	ECAR	404,000	300	Wind storm. MW probably half actual loss, as data point missing.
04/09/91	HI	246,000	950	Maintenance, plant trip, cascade
04/13/91	SERC	43,696	300	Pole fire
04/25/91	SERC	71,000	213	Wind storm caused distribution system damage
04/29/91	SPP	65,000	300	Tornadoes.
04/30/91	SPP	29,900	150	
05/21/91	NPCC	30,000	327	CT failure, under-frequency relays interrupt load
05/23/91	NPCC	20,000	230	
07/07/91	ECAR	899,000	1,000	Storms
07/22/91	NPCC	10,300	240	
08/08/91	SERC	115,000	1,061	CB failure after cap. fault, backup relay failure, 3rd backups cleared fault
08/19/91	NPCC	2,085,000	4,400	Hurricane Bob
09/12/91	WSCC	206,000	335	Lightning, line fault, relay failure, cascade
11/16/91	WSCC	400,000	0	Storm caused transmission outages.
01/06/92	MAAC	18,819	335	Underground cables tripped, cascade
04/27/92	WSCC	0	383	Line fault.
06/17/92	ECAR	875,000	0	Severe weather, mostly distribution
06/19/92	SPP	100,000	75	Thunderstorm, cascade
07/01/92	MAAC	0	105	
07/22/92	SERC	0	586	Transformer trip, under-voltage load shedding,
08/10/92	WSCC	50,000	380	Fault, distance relay trips on overload, cascade (mostly Canada)
08/24/92	SERC	1,500,000	0	Hurricane Andrew
08/26/92	SPP	650,000	0	Hurricane Andrew
08/27/92	SERC	58,000	200	Tornadoes
08/28/92	WSCC	142,000	739	Fire, breaker failure, cascade
10/05/92	NPCC	350,000	850	CT failure, SPS shed 850 MW
10/30/92	WSCC	71,000	300	Line fault, bus lockout, cascade
11/25/92	WSCC	312,000	530	Line trips. Cause unknown
01/04/93	WSCC	0	514	Line fault, fire, cascade
02/26/93	NPCC	40,000	1,200	Switching error, fault, cascade
05/27/93	WSCC	0	230	
06/04/93	WSCC	0	730	Lines tripped, load in Vancouver interrupted (Canada only)
07/14/93	WSCC	100,000	300	Tree fell, lines tripped, load/gen trips
07/20/93	SPP	0	300	35 transmission interruptions. 300MW is probably low
07/28/93	ECAR	300,000	1,000	Severe storm
10/04/93	WSCC	1,800	11	
10/10/93	WSCC	0	713	Ground wire broke, fault, cascade
10/21/93	NPCC	300,000	1,400	XFMR trip, gen loss, relay failure?
11/01/93	NPCC	70,000	715	CT failure, overload, cascade
11/02/93	NPCC	70,000	677	Ice block caused fault, parallel line trips on overload.
12/26/93	WSCC	29,000	30	
01/04/94	ECAR	122,000	0	Storm, mostly distribution losses, some transmission
01/06/94	WSCC	0	205	
01/17/94	WSCC	0	4,235	Earthquake, 6.6 magnitude
01/19/94	MAAC SERC	0	2,800	Shortage due to unexpectedly high demand
02/10/94	SERC	660,000	0	Ice Storm
02/10/94	ECAR	145,000	400	Ice Storm
02/10/94	SPP	50,000	300	Ice Storm
02/10/94	SERC	92,000	0	Ice Storm
02/22/94	MAIN	0	200	
02/23/94	WSCC	60,000	300	Line fault, failure of transfer scheme
03/14/94	NPCC	173,000	530	Explosives on transmission line.
05/13/94	WSCC	106,850	132	XFMR failure, 3 lines tripped, cascade
06/07/94	SERC	0	400	Lightning, breaker failure, load loss.
06/16/94	ECAR	25,000	133	
07/01/94	SPP	146,000	0	Line fault, cascade
08/15/94	WSCC	158,000	350	Brush fire, gen failures,
11/04/94	WSCC	0	350	CB failure, subs. faults, cascade
11/30/94	MAIN	0	1,000	Maintenance crew error
12/14/94	WSCC	1,500,000	5,020	Cascading failure
02/22/95	SERC	0	121	
02/28/95	NPCC	0	4,500	Line faults, overload, gen loss, cascade
05/07/95	NPCC	80,000	300	Line fault, overload, load shedding
07/18/95	WSCC	7,500	170	
07/29/95	WSCC	0	1,600	High demand, maintenance failure, cascade
08/12/95	WSCC	82,500	162	Switching error, under-frequency load shedding
09/19/95	WSCC	0	1,477	Fault, relay error, RAS operations
10/05/95	WSCC	272,000	1,048	Line fault, other lines open, gens fail, cascade
10/20/95	NPCC	0	520	Maintenance staff trip XFMRs, cascade
10/21/95	WSCC	272,000	637	Line fault, overload, gen loss, cascade
03/12/96	SERC-FL	0	3,440	Transmission problems, cascade
03/29/96	WSCC	0	1,116	Line fault, relay actions, RAS sheds load,
04/15/96	WSCC	0	290	
04/16/96	SPP	207,200	2,070	Maintenance, gen failure, cascade
05/06/96	NPCC_OH	39,500	450	Conductor broke, fault, cascade
05/14/96	MAAC	363,476	819	Maintenance error, 15 CB's open.

Date	Location	Customers	MW	Notes
05/21/96	NPCC-NYPP	113,200	280	Voltage reduction and load curtailment due to shortage
06/24/96	WSCC	0	520	Bird caused 8 lines to trip. Pump loads lost
07/02/96	WSCC	1,500,000	2,500	Cascading failure
07/03/96	WSCC	0	1,200	Line fault (same initiating event as 7/2), manual load shedding
08/07/96	ECAR	15,000	258	
08/10/96	WSCC	7,500,000	0	High demand/temperature, cascading failure
08/26/96	NPCC-NYPP	0	240	
08/26/96	WSCC-RM	8,000	60	
09/03/96	WSCC-AZ/NM	56,000	118	Bulldozer caused line to trip. Near line tripped after 2 hours
09/25/96	WSCC-CA/SNV	88,000	168	Maintenance and relay problems
10/21/96	WSCC-CA/SNV	60,000	150	Switch failure, cascade?
11/05/96	MAAC	29,000	88	
12/25/96	WSCC-NWPP	75,000	480	Line failure, gen outage, cascade
01/09/97	SERC-VACAR	95,000	325	Winter Storm
03/13/97	ECAR	725,000	550	Ice Storm
04/04/97	MAPP	128,000	564	Ice storm, affected transmission lines.
04/06/97	ECAR	148,000	100	Wind storm, mostly distribution
05/18/97	ECAR	100,000	150	Thunderstorm, public appeal, 3 tx lines out.
06/03/97	WSCC	2,000	3	
06/06/97	WSCC-AZ/NM	48,000	373	2 lines trip (lightning, relay problem), RAS shed load
06/20/97	MAAC	18,000	350	CB failure, cascade.
06/23/97	MAIN	5,300	800	XFMR failure, demand dropped by 800MW from low voltage,
06/29/97	WSCC-AZ/NM	32,000	257	
07/02/97	ECAR	250,000	2,000	Storm, tornado
08/05/97	WSCC-CA/SNV	0	3,525	Plane hit line, demand tripped on low voltage,
08/13/97	FRCC	45,000	280	
10/23/97	WSCC-CA/SNV	1,260,000	110	Operator error in subs.
10/26/97	ECAR	284,000	250	Snow storm, mostly distribution
10/26/97	MAPP	70,000	145	Snow storm, some transmission
12/04/97	NPCC-H-Q	0	1,170	Ice storm.
12/07/97	NPCC-H-Q	400,000	1,816	Ice storm, cascade
01/06/98	NPCC - HQ	1,300,000	0	Severe Ice Storm
01/27/98	SERC-VACAR	80,000	150	Snow storm, primarily distribution
02/02/98	FRCC	500,000	400	Severe weather, tornados
03/09/98	MAIN	290,000	900	Winter Storm
12/08/98	WSCC-Calif	375,000	600	Human error, some cascade?
01/02/99	SERC-VACAR	240,000	850	Ice Storm
01/14/99	MAAC	870,000	900	Ice Storm
01/17/99	MAAC	70,000	90	CB failure, fire, cascade
01/17/99	SERC-TVA	50,000	0	Severe Weather, tornados
01/29/99	SPP	50,000	0	Snow/ice storm, wind, etc
03/04/99	NPCC-Ontario	0	640	Wind, line fault, voltage drop, load shed
03/17/99	MAPP	18,000	60	Equipment failure
05/03/99	SPP	51,000	300	Severe Weather & Tornados
05/10/99	ERCOT	51,000	300	Severe weather, mostly distribution
05/17/99	ECAR	145,000	150	Severe weather, mostly distribution
06/17/99	WSCC-PNW	0	300	Lightning, line fault, UFLS
07/23/99	ECAR	219,000	1,700	Storm damage, mostly distribution
07/23/99	SERC - Entergy	557,354	900	Generation forced out of service.
07/23/99	MAIN	68	125	Generation forced out of service.
07/31/99	ECAR	191,000	2,000	Storm damage, mostly distribution
08/12/99	MAIN	2,900	110	Equipment failure.
08/24/99	WSCC - Rocky Mouni	163,000	425	XFMR fault, gen outage, SPS shed load
08/26/99	NPCC - Qu?bec	1	255	Sabotage.
08/31/99	NPCC - Qu?bec	0	698	CB failure, backup PS (SPS?) shed load
08/31/99	WSCC - CA/SNV	257,718	470	Substation cleaning, fault, SPS actions
08/31/99	ERCOT	176,000	0	Severe weather.
09/14/99	FRCC SERC - VACA	1,660,000	0	Hurricane Floyd.
10/14/99	WSCC - NWPP	0	1,200	Relay problem, SPS removed line, cascade
10/15/99	FRCC	1,600,000	0	Hurricane Irene.
12/06/99	MAPP	0	1,150	Gen failure. Perhaps no customer losses.
12/25/99	WSCC - AZ/NM	0	1,926	Same as above
01/03/00	NPCC	60,000	326	Storm, SPS removed demand
01/23/00	SERC	133,000	0	Storm
01/24/00	SERC	173,000	960	Storm, 4 tx lines out.
01/24/00	SERC	62,000	0	Winter storm, SPS removed 3 tx lines,
01/29/00	SERC	81,000	0	Storm, mostly distribution
02/02/00	MAPP	20,000	100	
02/26/00	WECC-CAMX	112,000	300	Maintenance error, SPS operated (perhaps in error)
03/18/00	WECC-AZNMSNV	600,000	1,590	Line out of service, brush fire, UVLS and and manual LS, SPS, etc
04/01/00	SERC	37,000	143	
04/01/00	FRCC	24,000	46	
05/02/00	ERCOT	238,000	0	Thunderstorms
05/18/00	ECAR	50,000	0	Thunderstorm damaged distribution system
05/20/00	SERC	50,000	200	Thunderstorm
05/25/00	SERC	147,000	500	Thunderstorms

Date	Location	Customers	MW	Notes
06/14/00	ERCOT	0	294	
06/14/00	WECC-AZNMSNV	40,911	138	
06/14/00	WECC-CAMX	32,000	130	
06/28/00	SERC	30,500	175	
06/29/00	NPCC-HQ	1	1,630	SPS opened gen, HVDC line opened
07/03/00	MAIN	14,273	35	
07/05/00	WECC-NWPP	0	325	Maintenance, 2 XFMRs tripped, cascade
07/20/00	SERC	160,000	0	Thunderstorms
08/04/00	WECC-NWPP	0	190	
08/06/00	MAIN	230,000	0	Weather
08/09/00	ECAR	92,000	0	Thunderstorm
08/10/00	SERC	75,000	0	Thunderstorm
08/18/00	SERC	130,000	500	Thunderstorm
08/22/00	NPCC	1	130	
08/28/00	ECAR	124,000	15	Supply shortage. Interruptible load curtailed
09/17/00	FRCC	120,000	0	Hurricane Gordan
11/02/00	WECC-CAMX	0	160	
12/07/00	WECC-CAMX	0	1,500	Supply shortage. 1350 MW int. 200 MW firm
12/13/00	SPP	235,000	1,400	Ice Storm
12/16/00	SERC	50,000	0	Tornado
12/20/00	NPCC	0	530	Storm, faults, minor cascade?
12/25/00	SPP	94,285	460	Ice Storm
01/03/01	NPCC-HQ	71,000	450	Switching error, xfmr removed, relay failure,
01/16/01	WECC-CAMX	0	1,146	Supply shortage
01/16/01	WECC-NWPP	100,000	430	Switch failure, SPS opened lines
01/17/01	WECC-CAMX	0	841	Supply shortage
01/17/01	NPCC-HQ	234,000	0	CB failure, SPS actions, UFLS,
01/18/01	WECC-CAMX	0	1,000	Supply shortage
01/21/01	WECC-CAMX	0	101	
01/31/01	WECC-AZNMSNV	0	116	
02/16/01	SERC	300,000	0	Weather, some transmission faults
02/28/01	WECC-NWPP	258,000	1,340	Earthquake, 7.0 magnitude
03/06/01	NPCC	130,000	340	Snow/ice storm (Emily), prot. sys. failures,
03/10/01	MAPP	246,000	1,250	Gen failure, SPS actions, UFLS,
03/14/01	ERCOT	114,000	0	Thunderstorms
03/19/01	WECC-CAMX	0	1,000	Supply shortage
03/20/01	WECC-CAMX	0	500	Supply shortage
04/06/01	WECC-NWPP	120,000	600	Bus diff. relay, cascade
05/07/01	WECC-CAMX	0	300	Supply shortage
05/08/01	WECC-CAMX	0	400	Supply shortage
06/06/01	ECAR	24,506	350	Maintenance error, cascade
06/11/01	NPCC-HQ	10	620	Lightning, loss of industrial demand (10 customers is a guess)
07/02/01	WECC-AZNMSNV	10,000	100	
07/08/01	NPCC	160,000	500	Relay opps, xfmr outage, load losses
07/24/01	NPCC-HQ	0	390	Lightning, gen/line losses
08/09/01	SERC	0	200	Voltage reduction reduced demand by 200MW, not cust. losses (removed 600k, changed 1000MW to 200MW)
08/09/01	MAAC	0	200	
09/11/01	NPCC	12,000	190	
09/14/01	FRCC	203,000	0	Tropical storm Gabrielle
09/18/01	WECC-CAMX	50,462	134	Relay opp, tx losses,
09/24/01	WECC-CAMX	40,000	150	
09/25/01	WECC-CAMX	59,000	138	Lightning, xfmr loss
09/25/01	FRCC	15,000	49	
10/02/01	MAAC	1,646	168	
11/14/01	MAIN	0	263	
11/24/01	WECC-CAMX	500,000	0	Storm
12/11/01	FRCC	0	1,200	SPS failure
01/30/02	SPP	570,000	1,310	Ice Storm
02/27/02	WECC-CAMX	210,882	340	Maintenance error, cascade
02/28/02	WECC-CAMX	0	850	Wind, line fault, SPS acted (correctly) to dump pump loads
03/09/02	NPCC	46,000	196	
03/09/02	ECAR	190,000	190	Storm, mostly distribution
03/10/02	WECC-NWPP	17,000	274	
04/29/02	FRCC	360,000	2,100	Line fault, relay failure, overload, cascade
05/13/02	SERC	74,000	250	Thunderstorm, mostly distribution losses
06/18/02	WECC-NWPP	19,000	334	Lightning, line fault, UFLS
06/26/02	WECC-CAMX	460,000	1,450	Fire, line fault, cascade
07/03/02	NPCC	65,000	210	Line fault, relay opps,
07/09/02	FRCC	25,000	48	
07/09/02	FRCC	18,351	33	
07/15/02	FRCC	25,000	83	
07/20/02	NPCC	63,500	278	Transformer fire, distribution losses
07/27/02	WECC-AZNMSNV	1,000	15	
07/29/02	NPCC	9,000	0	
07/31/02	WECC-NWPP	50,000	240	Software error in RTU caused UVLS (not cascade)
08/01/02	ECAR	114,500	100	Storms

Date	Location	Customers	MW	Notes
08/02/02	WECC-AZNMSNV	350,000	1,071	Dump truck hit tower, cascade
08/02/02	NPCC-HQ	10	848	Lightning, industrial demand interrupted (in Quebec)
08/09/02	FRCC	25,000	51	
08/14/02	NPCC-HQ	8	1,060	Lightning, voltage fluctuation, demand losses
08/26/02	WECC-AZNMSNV	50,000	270	SPS/maintenance errors.
08/28/02	FRCC	25,000	68	
10/03/02	SERC	242,910	0	Hurricane Lily
10/03/02	SPP	164,500		Hurricane Lily
10/03/02	SPP	55,000	212	Hurricane Lily
10/31/02	NPCC-HQ	0	250	
11/06/02	WECC-CAMX	877,000	0	Storm, gen. outages due to ocean waves, mostly distribution
11/07/02	NPCC-HQ	1	250	
12/03/02	SERC	43,000	0	
12/04/02	SERC	1,140,000	7,200	Snow/ice storm.
12/05/02	SERC	464,000	2,400	Snow/ice storm.
12/11/02	SERC	90,000	63	Ice storm, mostly distribution problems.
12/14/02	WECC-CAMX	2,100,000	0	Storm, mostly distribution losses, some transmission
12/19/02	WECC-CAMX	385,000	0	Storm, mostly distribution losses, some transmission
12/25/02	MAAC	166,000	250	Snow storm
12/25/02	MAAC	95,630	0	Storm, mostly distribution losses, some transmission
12/26/02	WECC-NWPP	0	862	Ice caused fault, UFLS reacted
02/13/03	WECC-NWPP	200,000	700	Third Party - Dump Truck contacting tower structure
02/27/03	SERC-VACAR	350,000	1,000	Weather - Ice Storm - Severe
03/21/03	WECC-CAMX	1	300	Equipment Failure -
03/22/03	WECC-NWPP	135,000	1,080	Sys. Prot. - Line Fault
04/04/03	ECAR	425,000	0	Weather - Ice Storm - Severe
04/07/03	WECC-CAMX	0	650	Sys. Prot. - Cause Unknown
04/15/03	ERCOT	68,530	212	Sys. Prot. - Erroneous Trip Signal
05/02/03	SERC-VACAR	139,000	1,500	Weather
05/04/03	SERC-TVA	14,825	0	Weather - Tornadoes
05/11/03	MAIN	65,000	0	Weather - Severe
05/15/03	ERCOT	419,863	1,549	Equipment Failure - Insulator Failure - Sys. Prot. Malfunction
05/15/03	MAIN	2	240	Flooding
05/15/03	MAIN	2	240	Weather - Flooding
06/24/03	NPCCQuebec		260	Smoke contamination
06/24/03	NPCC-Quebec	0	260	Equipment Failure - Smoke
07/01/03	WECC-AZNMSNV	48,000	1,000	Equipment Failure
07/17/03	MAIN	80,000	0	Weather
07/21/03	MAAC	185,000	1,000	Weather - Lightning and Thunderstorms - Severe
07/28/03	WECC-AZNMSNV	90,000	440	Human Error
08/12/03	WECC-NWPP	7,400	465	Equipment Failure
08/14/03	Eastern Interconnect	15,330,850	57,669	Major Blackout
08/17/03	SERC-Entergy	65,000	500	Equipment Failure
09/12/03	MAPP	4,090	22	Flashover and SPS misoperation
09/12/03	MAPP	4,090	22	SPS Misoperation - Flashover and SPS misoperation
09/15/03	MAAC	45,000	400	Weather - Lightning - Relay Misoperation
09/18/03	SERC-VACAR	1,800,000	6,512	Weather - Hurricane Isabel
09/18/03	SERC-VACAR	320,000	1,655	Weather - Hurricane Isabel
09/18/03	MAAC	350,000	1,300	Weather - Hurricane Isabel
09/18/03	MAAC	120,000	600	Weather - Hurricane Isabel
09/28/03	NPCC-Maritimes	300,000	412	Weather - Hurricane Juan
10/26/03	WECC-CAMX	90,000	0	Fires - Brush Fires
11/13/03	NPCC-NYISO	50,280	180	Weather - High Winds
11/13/03	SERC	67,000	0	Weather - High Winds
12/01/03	NPCC-ISO-NE	300,000	630	Off-Normal Operation
12/04/03	MAIN	36,000	500	Sys. Prot. - Cause Unkown
12/04/03	WECC-NWPP	175,000	175	Weather - High Winds
12/05/03	FRCC	16,500	27	Equipment failure and system protection misoperation
12/05/03	FRCC	16,500	27	Equipment Failure - Sys. Prot. Misoperation
12/23/03	MAAC	80,000	0	Human Error
12/26/03	NPCC-HQ	10	630	Weather
01/08/04	NPCC-NYISO	18,600	100	Public Appeal
01/23/04	NPCC-NYISO	18,600	100	Public Appeal
01/26/04	SERC	150,000	700	Weather - Ice Storm
01/26/04	SERC	92,000	475	Weather - Ice Storm
01/26/04	SERC-Southern	30,689	150	Weather - Ice Storm
01/26/04	NPCC-NYISO	18,600	100	Voltage Reduction
01/28/04	MAAC	65,000	300	Weather - Icing
02/26/04	WECC-NWPP	0	180	Weather - Fog and Hoarfrost
02/26/04	SERC-Southern	61,284	0	Weather - High Winds and Thunder
03/04/04	ERCOT	41,000	0	Weather - High Winds - Possible Tornado
03/08/04	WECC-CAMX	70,000	460	Human Error
03/17/04	WECC-AZNMSNV	100,000	300	Equipment Failure
03/18/04	WECC-NWPP	74,000	78	Equipment Failure
03/23/04	WECC-RMPA	0	135	Equipment Failure - Misoperation
04/12/04	FRCC	179,000	250	Weather - Lightning and High Winds

<i>Date</i>	<i>Location</i>	<i>Customers</i>	<i>MW</i>	<i>Notes</i>
04/28/04	NPCC-Maritimes	97,500	245	System Protection - Conductor Sagging
05/28/04	FRCC	50,000	0	Public Appeal - Inadequate Resources
06/01/04	ERCOT	500,000	0	Weather - Lightning and High Winds
06/12/04	MAPP	120,212	428	Weather
06/14/04	WECC-AZNMSNV	41,000	492	Equipment Failure - System Protection Malfunction
06/23/04	WECC-RMPA	35,000	157	System Protection - Unknown
06/23/04	SERC-Southern	50,595	50	Weather - Thunderstorm - Severe
07/05/04	NPCC-Quebec	175,000	1,778	Maintenance Error
07/07/04	SERC-VACAR	8,110	120	Weather - Thunderstorms - Severe
07/13/04	FRCC	42,122	283	System Protection
07/20/04	WECC-AZNMSNV	50,000	250	Equipment Failure
07/21/04	MAIN	200,000	0	Weather - Thunderstorm and High Winds
07/25/04	SERC-Southern	61,004	0	Weather
08/04/04	WECC-CAMX	171,600	480	Equipment Failure
08/13/04	FRCC	200,000	700	Weather - Hurricane Charley
08/13/04	FRCC	400,000	0	Weather - Hurricane Charley
08/14/04	SERC-VACAR	94,000	500	Weather - Hurricane Charley
08/18/04	ERCOT	2	178	Human Error
08/20/04	NPCC-ISO-NE	27,388	0	Weather - Lightning
08/29/04	SERC	125,000	0	Weather - Tropical Storm Gaston
08/30/04	SERC-VACAR	99,816	150	Weather - Tropical Storm Gaston
09/04/04	FRCC	1,807,881	0	Weather - Hurricane Frances
09/06/04	SERC-Southern	556,383	3,000	Weather - Hurricane Frances
09/15/04	SERC-Southern	1,536,433	1,364	Weather - Hurricane Ivan
09/16/04	SERC	75,000	0	Weather - Hurricane Ivan
09/18/04	SERC	112,000	400	Weather - Hurricane Ivan
09/25/04	FRCC	1,700,000	6,000	Weather - Hurricane Jeanne
09/27/04	SERC-Southern	85,455	854	Weather - Hurricane Jeanne
10/30/04	ECAR	117,842	60	Weather - High Winds
11/14/04	NPCC-Maritimes	132,000	600	Weather - Snow Storm - Severe
11/23/04	WECC-NWPP	88,775	370	Equipment Failure
11/24/04	SERC-Southern	83,450	100	Weather - Thunderstorms
01/29/05	SERC-Southern	150,000	100	Weather - Winter Storm - Severe
03/08/05	SERC	51,600	0	Weather - Wind Storm - Severe
04/20/05	WECC-CAMX	48,000	200	Human Error
04/21/05	WECC-CAMX	48,000	168	Human Error
04/22/05	WECC-CAMX	69,979	127	SPS Misoperation - RTU Malfunction
04/30/05	SERC-Southern	51,808	100	Weather - Thunderstorm - Severe
05/08/05	ERCOT	243,000	672	Weather - Thunderstorm - Severe
05/27/05	NPCC-Ontario	0	2,300	Human Error
05/29/05	ERCOT	123,000	0	Weather - Thunderstorm - Severe
06/02/05	NPCC-Quebec	415,000	1,500	Fires - Forrest Fires
06/15/05	SPP	150,000	1,100	Weather - High Winds
06/19/05	MAPP-Canada	15,000	0	Weather - Tornado
06/21/05	WECC-NWPP	0	200	Weather - Lightning and Winds - Severe
06/24/05	MAIN	51,500	0	Equipment Failure
07/01/05	ERCOT	0	100	Sys. Prot. - Unknown
07/09/05	WECC-RMPA	18,600	150	Equipment Failure
07/10/05	SERC-Southern	66,830	0	Weather - Hurricane Denis
07/10/05	SERC	50,000	0	Weather - Hurricane Dennis
07/17/05	NPCC-Quebec	361,166	1,173	Human Error
07/28/05	SERC	52,200	0	Weather - Thunderstorm - Severe
08/25/05	WECC-CAMX	0	1,700	Equipment Failure
08/26/05	FRCC	17,500	38	Weather - Hurricane Katrina
08/29/05	SERC-Southern	897,257	8,972	Weather - Hurricane Katrina
08/29/05	SERC	50,800	380	Weather - Hurricane Katrina
08/29/05	SPP	143,000	300	Weather - Hurricane Katrina
09/10/05	WECC-NWPP	8,000	8	Weather - Snow and High Wnds
09/12/05	WECC-CAMX	0	2,200	Human Error
09/12/05	WECC-CAMX	50,686	172	Human Error
09/12/05	WECC-CAMX	63,000	130	Human Error
09/13/05	MAIN	110,000	600	Weather - Winds - Severe
09/14/05	SERC	60,000	215	Weather - Hurricane Ophelia
09/23/05	SERC-Entergy	787,774	0	Weather - Hurricane Rita
09/23/05	ERCOT	715,000	0	Weather - Hurricane Rita
09/23/05	SERC	125,000	350	Weather - Hurricane Rita
09/24/05	ERCOT	100,000	0	Weather - Hurricane Rita
09/24/05	SERC	80,000	0	Weather - Hurricane Rita
10/23/05	FRCC	3,200,000	10,000	Weather - Hurricane Wilma
10/24/05	FRCC	17,500	33	Weather - Hurricane Wilma
11/02/05	WECC-NWPP	2,700	350	Weather - Lightning
11/25/05	WECC-NWPP	0	375	Weather - Snow Heavy Wet and Freezing Rain
12/15/05	SERC	600,000	3,000	Weather - Ice Storm
12/15/05	SERC	52,000	200	Weather - Ice storm
12/15/05	SERC-Southern	52,659	75	Weather - Ice storm
12/18/05	WECC-CAMX	60,000	0	Weather - Rain and High Winds

Date	Location	Customers	MW	Notes
12/31/05	WECC-CAMX	1,667,316	800	Weather - Rain and High Winds
01/14/06	RFC	155,879	0	Weather - High Winds
01/18/06	RFC	72,535	0	Weather - High Winds
01/28/06	WECC-CAMX	76,000	0	Equipment Failure - Transformer Failure
02/04/06	WECC-RMPA	3,827	150	Weather - Wind Storm
02/18/06	WECC-RMPA	323,000	428	Fuel - Natural Gas Supply and Pressure Limitations
02/27/06	WECC-CAMX	160,000	0	Weather - High Winds Rain
03/09/06	SERC-Entergy	73,000	0	Weather - Thunderstorms
03/12/06	RFC	61,750	200	Weather - Tornado
03/17/06	WECC-NWPP	0	650	Weather - Ice Fog
04/08/06	SERC-Southern	115,589	300	Weather - Tornados Thunderstorms
04/17/06	ERCOT	200,000	1,000	Weather - High Temperatures Limited Resources
04/17/06	ERCOT	0	380	Weather - High Temperatures Limited Resources
04/17/06	ERCOT	0	260	Rolling in 15 Min Weather - High Temperatures Limited Resources
04/17/06	ERCOT	51,404	58	Weather - High Temperatures Limited Resources
04/17/06	ERCOT	9,000	39	Weather - High Temperatures Limited Resources
05/03/06	WECC-CAMX	55,655	0	Equipment Failure - Transformer Failure
05/25/06	RFC	112,000	0	Weather - High Winds Storms Lightning
06/01/06	RFC	111,555	0	Weather - Thunderstorms Lightning
06/04/06	WECC-RMPA	31,076	130	Equipment Failure - Transmission Line Fault
07/04/06	SERC	67,000	335	Weather - Thunderstorms
07/18/06	RFC	380,000	0	Weather - High Winds Storms
07/19/06	SERC	600,000	0	Weather - Thunderstorms Lightning
07/19/06	SERC-Entergy	8,000	40	Equipment Failure - Transformer Failure
07/22/06	WECC-CAMX	1,271,893	200	Weather - High Temperatures
07/24/06	WECC-CAMX	0	855	Weather - High Temperatures
08/03/06	NPCC-ISO-NE	11,000	40	Equipment Failure - Transmission Vegetation
09/01/06	SERC-VACAR	150,520	225	Weather - Tropical Storm Ernesto
09/01/06	SERC-VACAR	61,000	0	Weather - Tropical Storm Ernesto
09/15/06	FRCC	26,894	81	Weather - Lightning Storm
10/02/06	RFC	269,322	0	Weather - Thunderstorms
10/02/06	WECC-CAMX	130,000	308	Equipment Failure - Breaker
10/03/06	ERCOT	100,308	185	Equipment Failure - CCVT
10/12/06	NPCC-ISO-NE	180,000	400	Weather - Snow Storm
10/15/06	NONE	291,000	1,170	Earthquake
10/20/06	RFC	92,300	0	Weather - Wind Storm and Rain
11/15/06	SERC-Southern	109,000	363	Weather - Wind Storm and Rain
11/15/06	WECC-RMPA	50,000	0	Weather - Wind Storm and Rain
11/30/06	SERC	550,000	0	Weather - Snow Storm and Ice Storm
12/13/06	WECC-RMPA	70,000	0	Weather - Wind Storm and Rain
12/14/06	WECC-CAMX	249,500	0	Weather - Wind Storm and Rain
12/14/06	WECC-NWPP	75,000	280	Weather - Wind Storm and Rain
12/14/06	WECC-RMPA	15	233	Weather - Wind Storm and Rain
12/14/06	WECC-NWPP	63,750	0	Weather - Wind Storm and Rain
12/15/06	WECC-RMPA	170,000	0	Weather - Wind Storm and Rain
12/16/06	WECC-CAMX	50,000		Equipment Failure - Transformer
12/22/06	ERCOT	0	1,037	Equipment Failure - Transformer
12/26/06	WECC-CAMX	850,000	0	Weather - Wind Storm and Rain
12/30/06	MRO	15,000	275	Weather - Snow Storm and Ice Storm

APPENDIX B

IEEE 300 bus network data

This appendix provides the complete power network data used in this thesis for simulations. Figure B.1 shows the original one-line diagram of the IEEE 300 bus network. Figure B.2 shows the bus numbers in this network, from which the other components can be located. The remaining tables show the bus, branch, generation, the load data, and the disturbances used for this work. These data are useful to look up the precise data for a given component, such as the rating of a particular branch, or the relative value of a particular load.

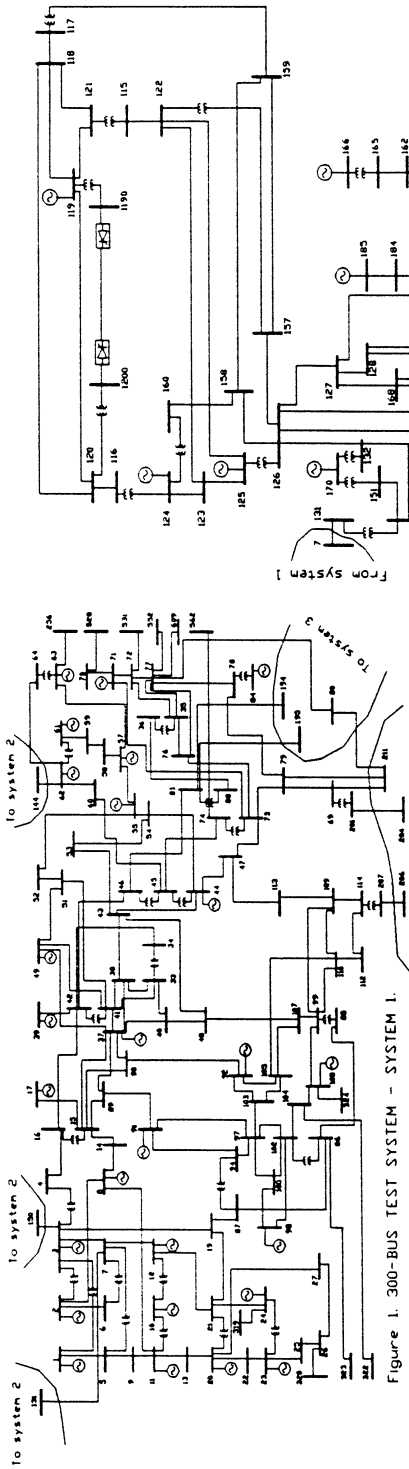


Figure 1. 300-BUS TEST SYSTEM - SYSTEM 1.

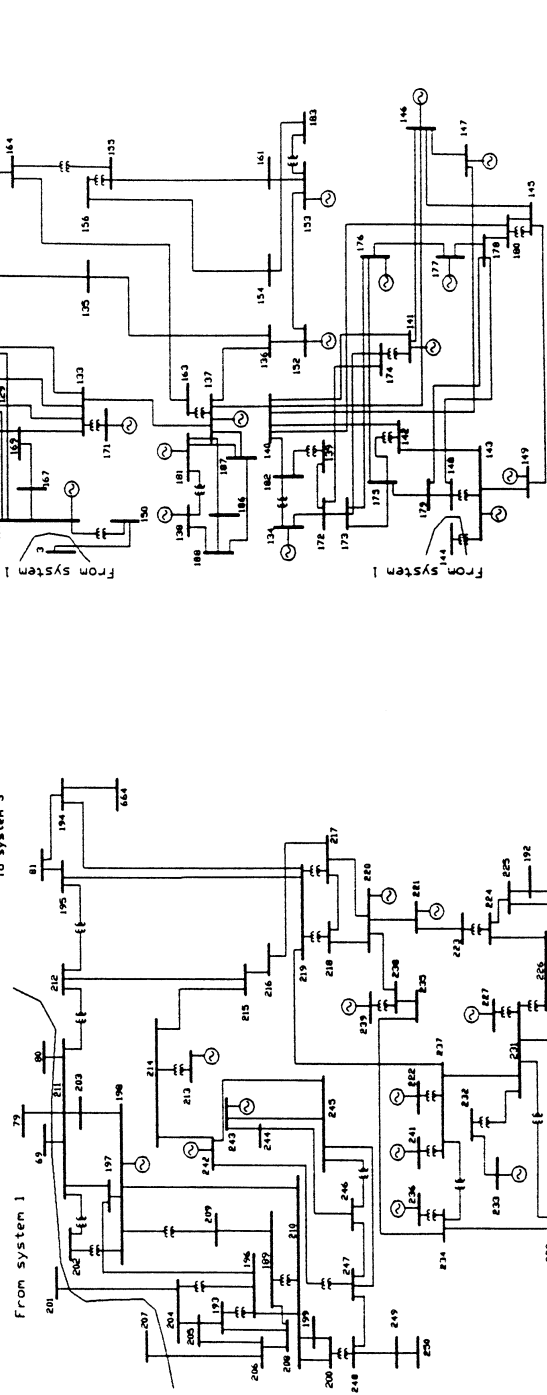


Figure 2. 300-BUS TEST SYSTEM - SYSTEM 2.

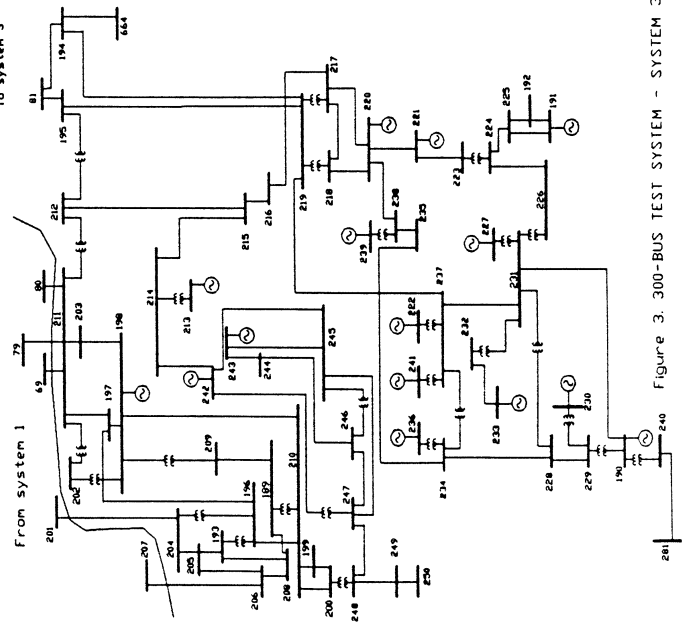


Figure 3. 300-BUS TEST SYSTEM - SYSTEM 3.

Figure B.1: One-line diagram of the IEEE 300 bus network [1]

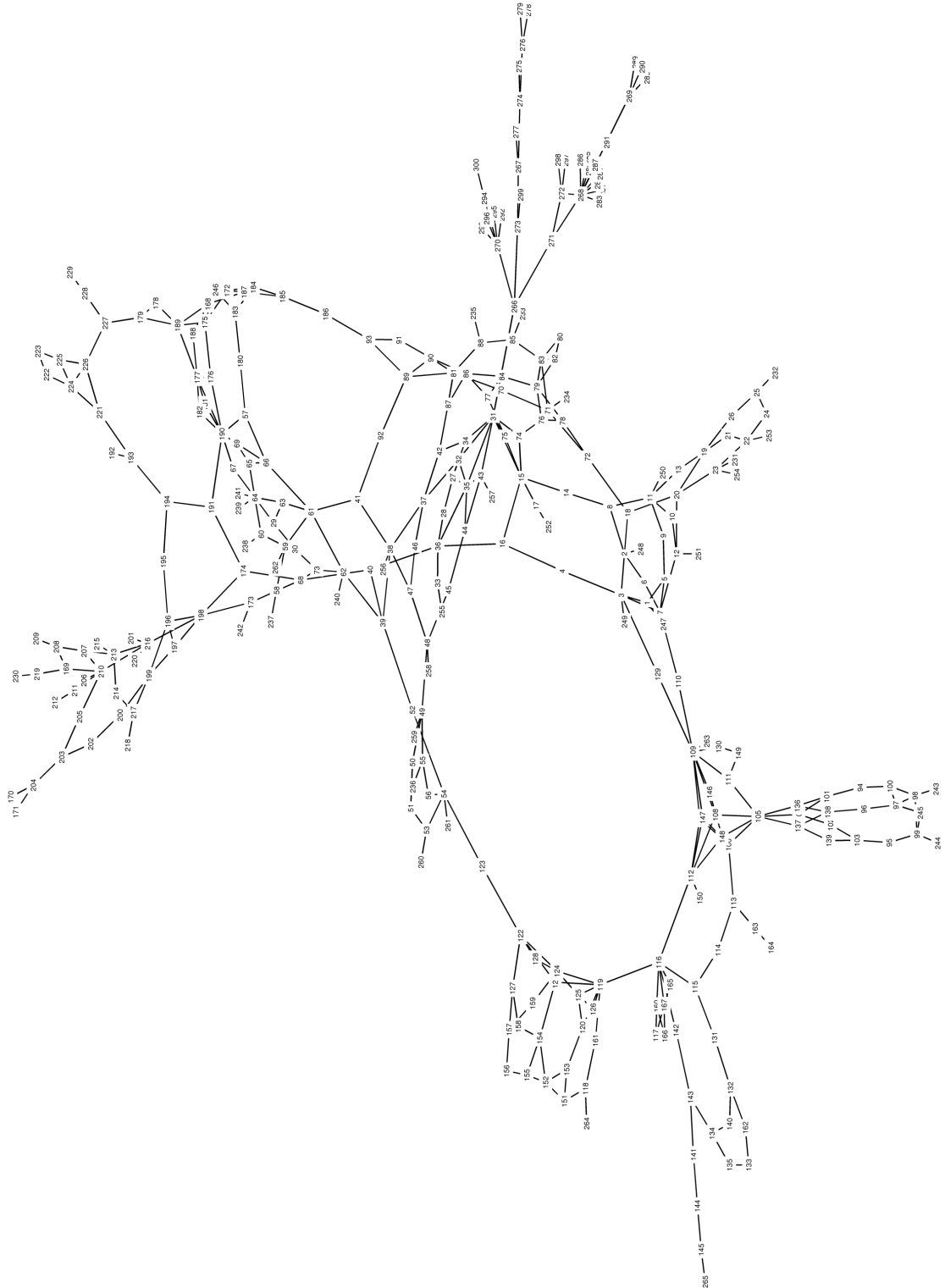


Figure B.2: Graph of the IEEE 300 bus network with bus numbers

Bus Numbers			Voltage magnitudes (p.u.) and phase angles (degrees)																			
Local	Original	Type	case300-1		case300-2		case300-3		case300-4		case300-5		case300-6		case300-7		case300-8		case300-9		case300-10	
296	9055	PV	1	-8.28	1.00	-8.71	1.00	-6.18	1.00	-6.02	1.00	-5.80	1.00	-6.00	1.00	-8.28	1.00	-5.89	1.00	-6.41	1.00	-7.30
297	9071	PQ	1.03	-14.89	1.03	-15.29	1.03	-12.38	1.03	-13.07	1.03	-12.19	1.03	-12.64	1.03	-14.94	1.03	-12.58	1.03	-13.23	1.03	-14.36
298	9072	PQ	1.03	-14.61	1.03	-15.39	1.03	-12.30	1.03	-12.89	1.04	-11.90	1.03	-12.32	1.03	-14.71	1.04	-12.22	1.03	-13.02	1.03	-14.28
299	9121	PQ	1.01	-13.52	1.00	-14.59	1.00	-11.88	1.00	-12.03	1.01	-11.26	1.01	-11.37	1.00	-13.91	1.01	-11.44	1.01	-11.87	1.01	-13.18
300	9533	PQ	1.04	-13.46	1.04	-13.86	1.04	-10.75	1.04	-12.14	1.04	-10.77	1.04	-10.84	1.04	-13.73	1.04	-10.82	1.04	-11.70	1.04	-13.13

Branch data for the IEEE 300 bus system.

Branches after #411 were added to the original data

Branch limits for each sub-case (amps—w/ all buses on the same voltage base)

Number	From	To	R	X	Bc	Tap ratio	phase	1	2	3	4	5	6	7	8	9	10
							shift										
484	227	228	0.03510	0.10040	0.0000	0.0000	0.00	55	55	55	55	55	55	55	55	55	55
485	228	229	0.06160	0.18570	0.0000	0.0000	0.00	55	55	55	55	55	55	55	55	55	55
486	15	17	0.01940	0.03110	0.0000	0.9561	0.00	198	341	198	242	231	176	352	220	231	198
487	55	56	0.00000	0.03800	0.0000	1.0170	0.00	220	253	231	220	264	242	253	242	242	286
488	121	154	0.00240	0.04980	-0.0870	1.0000	0.00	209	198	176	176	176	187	209	209	187	176
489	124	159	0.00050	0.01820	0.0000	1.0000	0.00	352	341	374	374	286	407	374	385	341	363
490	132	162	0.00270	0.06390	0.0000	1.0730	0.00	110	110	88	99	99	99	110	99	88	99
491	134	135	0.00080	0.02560	0.0000	1.0500	0.00	165	165	165	143	154	165	154	143	165	154
492	181	190	0.00000	0.12800	0.0000	1.0100	0.00	55	55	55	55	55	55	55	55	55	55
493	208	209	0.00100	0.03320	0.0000	1.0200	0.00	363	341	374	396	396	330	385	407	407	330
494	213	215	0.00050	0.01600	0.0000	1.0700	0.00	803	781	759	726	682	792	748	649	770	726
495	217	218	0.00050	0.01600	0.0000	1.0200	0.00	627	550	572	682	627	660	616	594	682	605
496	98	243	0.00100	0.02300	0.0000	1.0223	0.00	99	132	110	110	132	121	132	121	132	121
497	99	244	0.00000	0.02300	0.0000	0.9284	0.00	132	132	110	121	110	132	110	121	110	132
498	248	2	0.00100	0.01460	0.0000	1.0000	0.00	671	748	627	726	572	748	638	726	671	671
499	249	3	0.00000	0.01054	0.0000	1.0000	0.00	1144	1485	1353	1177	1155	1254	1463	1243	1122	1320
500	260	53	0.00000	0.02380	0.0000	1.0000	0.00	407	418	407	484	385	473	528	462	506	517
501	261	54	0.00000	0.03214	0.0000	0.9500	0.00	528	484	473	484	473	506	462	517	506	561
502	265	145	0.00000	0.01540	0.0000	1.0000	0.00	594	539	616	660	638	627	506	616	583	484
503	254	23	0.00000	0.02890	0.0000	1.0000	0.00	517	440	418	429	440	385	506	539	451	484
504	247	1	0.00000	0.01953	0.0000	1.0000	0.00	539	473	484	539	528	539	451	517	462	429
505	263	109	0.00000	0.01930	0.0000	1.0000	0.00	1133	1265	1463	1584	1375	1441	1452	1089	1474	1441
506	250	11	0.00000	0.01923	0.0000	1.0000	0.00	286	253	275	308	253	275	253	264	253	297
507	253	22	0.00000	0.02300	0.0000	1.0000	0.00	187	187	187	242	198	198	209	165	198	209
508	257	43	0.00000	0.01240	0.0000	1.0000	0.00	484	517	396	418	385	407	506	374	407	473
509	264	118	0.00000	0.01670	0.0000	1.0000	0.00	847	858	847	792	935	726	814	836	814	781
510	251	12	0.00000	0.03120	0.0000	1.0000	0.00	418	429	429	462	385	352	385	407	473	429
511	252	17	0.00000	0.01654	0.0000	0.9420	0.00	462	462	440	462	484	451	440	418	451	440
512	255	33	0.00000	0.03159	0.0000	0.9650	0.00	451	429	572	583	572	539	550	462	550	473
513	259	49	0.00000	0.05347	0.0000	0.9500	0.00	209	220	209	231	176	231	176	187	198	154
514	256	38	0.00000	0.18181	0.0000	0.9420	0.00	66	121	110	88	66	99	77	66	66	121
515	258	48	0.00000	0.19607	0.0000	0.9420	0.00	55	66	55	66	66	66	55	55	55	66
516	262	59	0.00000	0.06896	0.0000	0.9565	0.00	154	143	143	154	154	165	165	165	165	154

Disturbances applied to create the 100 individual cascading failure test cases

Case Name	Branch Outages												
case300-5-6	57	59	144	165	361	414	468						
case300-5-7	50	179	242	244	360	436	445						
case300-5-8	81	106	123	150	202	313	448	471	503				
case300-5-9	5	19	102	106	150	187	201	211	216	228	461	508	
case300-5-10	38	129	153	166	211	228	361	389	487				
case300-6-1	97	139	153	254	384								
case300-6-2	65	104	152	153	212	283	303	317	373	394	422		
case300-6-3	232	234	288	315	333	367	423						
case300-6-4	82	161	304	319	320	443	467						
case300-6-5	19	41	72	238	244	337	487						
case300-6-6	41	132	228	384									
case300-6-7	195	214	282	319	335	447	493						
case300-6-8	2	67	98	106	298	342	361	386	445	464	515	516	
case300-6-9	109	126	169	227	230	248	411	439	495	509			
case300-6-10	15	182	326	363	366	391	403	409	424	436	499	502	505
case300-7-1	105	115	284	326									
case300-7-2	34	90	336	348	395	399	458	473	485				
case300-7-3	25	89	185	287	337	387	396	493					
case300-7-4	57	66	163	226	278	363							
case300-7-5	93	173	367	456									
case300-7-6	112	211	238	287	304	391	393	463					
case300-7-7	39	54	64	163	296	328	345	407	514				
case300-7-8	79	125	241	310	350	413	482						
case300-7-9	11	150	193	254	269	281	328	356	442	478	483	486	501
case300-7-10	3	99	124	172	195	235	262	365	426	444	447		
case300-8-1	50	67	125	186	305	365	413	439	445	461			
case300-8-2	94	346	384										
case300-8-3	21	47	59	132	142	171	366	409	507				
case300-8-4	13	39	44	83	304	402							
case300-8-5	59	120	231	316	379	390	457	470					
case300-8-6	3	24	39	51	240	313							
case300-8-7	4	92	132	137	142	190	196	341	366	511			
case300-8-8	17	67	304	395	423								
case300-8-9	10	44	140	294	297								
case300-8-10	125	160	173	361	373	380							
case300-9-1	97	116	232	317	321								
case300-9-2	68	134	249	292	365	410							
case300-9-3	130	169	187	217	263	308	314	390	423	462			
case300-9-4	20	241	332	342	398	428	490	503					
case300-9-5	19	60	106	120	280	350							
case300-9-6	79	132	268	343	384	480							
case300-9-7	40	109	338	347									
case300-9-8	35	164	233	257	337	474	515						
case300-9-9	128	150	351	435	458								
case300-9-10	111	115	126	138	162	200	273	294	324	350	351	387	

Disturbances applied to create the 100 individual cascading failure test cases

Case Name	Branch Outages									
case300-10-1	9	38	40	91	198	205	238	363		
case300-10-2	55	120	173	280	324	383				
case300-10-3	61	193	281	337						
case300-10-4	131	261	278	332	335	346	385	443	489	
case300-10-5	175	317	371	508						
case300-10-6	73	101	131	166	172	214	301	345		
case300-10-7	22	37	49	85	280	284	380	506		
case300-10-8	90	99	115	150	157	218	302	439	443	456
case300-10-9	177	303	317	361	428					
case300-10-10	84	223	274	276	303	317	336	393	433	493

Cascading failure simulation results for all 100 test cases

Case	No. of branch outages	No. of over-currents	Worst $ I / I _{max}$	No. of under-voltages	Worst V	V min	Cascading failure sizes					
							No Control \$ x 1000	Centralized MPC \$ x 1000	Agent-based MPC \$ x 1000	MPC MW		
case300-1-1	7	5	1.63	4	0.855	0.920	123,303	23,456	50	103	123	142
case300-1-2	9	3	1.09	4	0.780	0.820	131,333	23,750	239	166	272	156
case300-1-3	7	1	1.07	0	0.929	0.920	129,139	23,750	18	37	15	38
case300-1-4	12	9	1.33	0	0.929	0.920	133,574	23,750	79	129	159	186
case300-1-5	4	0	0.88	1	0.932	0.940	2	0	1	0	1	0
case300-1-6	7	1	1.07	0	0.929	0.920	120,234	23,159	37	47	36	70
case300-1-7	6	2	1.14	0	0.929	0.920	118,771	23,750	866	421	384	113
case300-1-8	14	1	1.07	0	0.923	0.920	128,390	23,750	92	45	78	39
case300-1-9	5	0	0.91	1	0.939	0.940	1	0	0	0	0	0
case300-1-10	7	0	0.9	1	0.938	0.940	4	0	3	0	3	0
case300-2-1	7	1	1.04	0	0.929	0.920	287	0	7	1	7	1
case300-2-2	11	1	1.28	0	0.844	0.840	32	0	262	40	605	145
case300-2-3	6	0	0.97	0	0.929	0.920	0	0	0	0	0	0
case300-2-4	8	2	1.01	3	0.933	0.940	33	0	31	21	42	6
case300-2-5	10	2	1.19	1	0.928	0.940	66	0	44	114	133	214
case300-2-6	11	20	1.63	15	0.879	0.940	151,757	23,442	326	410	2,681	1,666
case300-2-7	6	0	0.94	0	0.929	0.920	11	0	11	0	11	0
case300-2-8	6	1	1.05	0	0.929	0.920	128,281	23,442	16	7	17	7
case300-2-9	4	1	1.01	0	0.929	0.920	4	0	3	6	3	6
case300-2-10	9	3	1.31	0	0.929	0.920	154,597	23,442	248	172	247	166
case300-3-1	6	3	1.39	0	0.929	0.920	152	0	441	544	77	129
case300-3-2	7	0	0.98	1	0.938	0.940	2	0	1	0	1	0
case300-3-3	6	1	1	0	0.929	0.920	14	0	14	1	14	0
case300-3-4	3	1	1.06	0	0.929	0.920	133,097	23,471	143	124	146	192
case300-3-5	9	0	0.9	1	0.938	0.940	4	0	3	0	3	0
case300-3-6	5	1	1.22	1	0.785	0.940	39	53	18	19	18	19
case300-3-7	7	1	1.19	0	0.941	0.940	11	0	24	35	18	26
case300-3-8	6	1	1.6	2	0.910	0.920	32	0	229	146	590	203
case300-3-9	5	1	1.05	0	0.901	0.900	130,083	23,471	19	63	20	58
case300-3-10	7	4	1.3	1	0.880	0.890	136,670	22,717	222	216	215	240
case300-4-1	4	1	1.85	0	0.929	0.920	283	0	131	521	139	521
case300-4-2	6	0	0.98	1	0.896	0.910	5	0	6	16	6	11
case300-4-3	7	1	1.19	0	0.929	0.920	1	0	51	44	22	42
case300-4-4	6	0	1	1	0.892	0.900	16	0	15	0	27	27
case300-4-5	7	0	0.97	1	0.933	0.940	2	0	1	0	1	0
case300-4-6	6	1	1.04	0	0.929	0.920	3	0	4	14	7	9
case300-4-7	11	0	0.91	1	0.000	0.870	328	34	328	34	328	34
case300-4-8	8	2	1.09	0	0.929	0.920	874	0	106	146	16	2
case300-4-9	7	2	1.09	1	0.909	0.910	138,045	23,783	10	47	10	39
case300-4-10	4	0	0.9	1	0.929	0.930	2	0	1	0	1	0
case300-5-1	8	3	1.07	0	0.939	0.930	131,252	23,584	37	13	31	29
case300-5-2	7	3	1.1	0	0.929	0.920	142,132	23,727	194	80	194	86
case300-5-3	8	1	1.17	2	0.771	0.780	125,512	22,945	31	22	32	63
case300-5-4	6	3	1.1	0	0.929	0.920	142,132	23,727	192	80	193	86
case300-5-5	5	0	1	1	0.937	0.940	4	0	3	0	3	1
case300-5-6	7	1	1.07	0	0.929	0.920	7	0	4	18	4	19
case300-5-7	7	0	0.98	1	0.936	0.940	3	0	2	0	7	0
case300-5-8	9	1	1.13	0	0.929	0.920	36	0	87	51	79	46
case300-5-9	12	0	0.95	0	0.941	0.940	5	0	5	0	5	0
case300-5-10	9	1	1.1	0	0.929	0.920	11	0	16	38	14	33
case300-6-1	5	1	1.02	0	0.929	0.920	3	0	10	14	8	10
case300-6-2	11	4	1.77	0	0.929	0.920	166	0	259	296	259	246
case300-6-3	7	1	1.13	0	0.945	0.940	130,457	23,641	157	81	143	81
case300-6-4	7	0	0.92	0	0.929	0.920	40	0	40	0	40	0
case300-6-5	7	17	2.76	2	0.733	0.840	134,551	23,245	114,262	23,641	112,051	23,245
case300-6-6	4	1	1.05	0	0.929	0.920	6	0	9	13	8	12
case300-6-7	7	1	1.03	0	0.929	0.920	6	0	11	23	11	15
case300-6-8	12	0	0.93	1	0.000	0.940	248	112	248	112	248	112
case300-6-9	10	0	0.93	1	0.935	0.940	3	0	2	0	2	0
case300-6-10	13	0	0.94	1	0.808	0.810	4	0	3	0	3	0
case300-7-1	4	0	0.95	2	0.863	0.870	7	0	5	0	5	0
case300-7-2	9	2	1.1	0	0.929	0.920	9	0	41	47	41	47
case300-7-3	8	11	1.15	2	0.000	0.940	118,136	23,773	99	165	1,708	470
case300-7-4	6	0	1	4	0.872	0.940	8	0	73	78	73	78
case300-7-5	4	0	0.95	1	0.929	0.940	11	0	10	3	10	0
case300-7-6	8	1	1.19	0	0.929	0.920	127,349	23,618	11	54	65	116
case300-7-7	9	3	1.27	0	0.924	0.920	173	0	2,436	2,231	373	245
case300-7-8	7	1	1.19	0	0.929	0.920	109,860	23,263	28	52	17	11
case300-7-9	13	1	1.17	0	0.920	0.920	905	421	47	69	14	43
case300-7-10	11	7	1.42	0	0.929	0.920	119,878	22,648	45	69	413	313
case300-8-1	10	2	1.03	1	0.000	0.940	880	103	884	119	105,670	23,711
case300-8-2	3	4	1.21	0	0.948	0.940	133,729	23,711	44	116	52	129
case300-8-3	9	3	1.09	0	0.929	0.920	-191	15	35	57	35	48
case300-8-4	6	1	1.19	0	0.929	0.920	57,112	12,007	80	119	79	152
case300-8-5	8	1	1.15	2	0.882	0.920	558	0	12	13	14	14

Cascading failure simulation results for all 100 test cases

Case	No. of branch outages	No. of over-currents	Worst $ I / I _{max}$	No. of under-voltages	Worst $ V $	$ V _{min}$	Cascading failure sizes					
							No Control		Centralized MPC		Agent-based MPC	
							$\$ \times 1000$	MW	$\$ \times 1000$	MW	$\$ \times 1000$	MW
case300-8-6	6	1	1.11	0	0.929	0.920	1,443	374	112	32	110	31
case300-8-7	10	3	1.08	0	0.929	0.920	95,429	20,992	57	41	45	30
case300-8-8	5	0	0.91	1	0.000	0.940	5	2	5	2	5	2
case300-8-9	5	1	1.14	1	0.926	0.930	44	0	18	33	10	25
case300-8-10	6	0	0.94	3	0.899	0.940	8	0	32	19	31	18
case300-9-1	5	2	1.34	0	0.945	0.940	5,109	1,069	19	127	20	127
case300-9-2	6	0	0.89	1	0.917	0.920	3	0	2	0	2	0
case300-9-3	10	1	1.01	0	0.872	0.870	2	0	3	2	7	3
case300-9-4	8	2	1.21	1	0.000	0.940	128	0	254	180	257	183
case300-9-5	6	0	0.9	1	0.936	0.940	1	0	0	0	0	0
case300-9-6	6	5	1.88	0	0.943	0.940	124,579	22,627	666	158	721	162
case300-9-7	4	2	1.2	0	0.929	0.920	557	0	113	27	113	47
case300-9-8	7	5	1.33	2	0.838	0.890	289	0	176	73	188	85
case300-9-9	5	3	1.09	1	0.927	0.940	122,769	23,563	38	22	36	21
case300-9-10	12	3	1.14	0	0.945	0.940	133,534	23,567	18	54	63	286
case300-10-1	8	5	1.32	0	0.922	0.920	131,294	22,706	1,273	188	1,044	149
case300-10-2	6	0	0.94	1	0.924	0.930	1	0	0	0	0	0
case300-10-3	4	8	1.51	1	0.865	0.940	138,409	21,240	123,478	23,481	122,366	23,481
case300-10-4	9	1	1.23	0	0.929	0.920	125,713	22,990	121,856	23,283	122,451	23,481
case300-10-5	4	3	1.32	0	0.929	0.920	3,070	436	22	88	228	90
case300-10-6	8	3	1.32	0	0.929	0.920	545	0	161	416	1,558	1,069
case300-10-7	8	0	0.91	4	0.834	0.840	6	0	2	0	2	0
case300-10-8	10	0	0.94	1	0.000	0.930	6	0	6	0	6	0
case300-10-9	5	4	1.81	0	0.929	0.920	234	0	743	401	8,623	2,691
case300-10-10	10	4	1.82	0	0.929	0.920	290	0	644	348	19,220	5,481